Autophagy in Systemic Lupus Erythematosus

Clarke, Alexander James

Awarding institution:
King's College London

Autophagy in Systemic Lupus Erythematosus

Alexander J. Clarke

Submitted for the degree of Doctor of Philosophy,
King's College London

June, 2014

Abstract

Autophagy has emerged as a critical homeostatic mechanism in lymphocytes, influencing proliferation and differentiation.

I sought to explore the role of autophagy in the pathogenesis of human and murine lupus, a disease in which B cells are critical effectors of pathology.

Autophagy was assessed using multiple techniques in NZB/W and control mice, and in patients with SLE compared to healthy controls. I evaluated the phenotype of the B cell compartment in Vav-Atg7$^{-/-}$ mice *in vivo*, and examined human and murine plasmablast formation following inhibition of autophagy.

I found activation of autophagy in early developmental stages of B cell development in a lupus mouse model even before disease-onset, and which progressively increased with age. In human disease, again autophagy was activated compared with healthy controls, principally in naïve B cells. B cells isolated from *Vav-Atg7$^{-/-}$* mice failed to effectively differentiate into plasma cells following stimulation *in vitro*. Similarly, human B cells stimulated in the presence of autophagy inhibition did not differentiate into plasmablasts.

My data suggest activation of autophagy is a mechanism for survival of autoreactive B cells, and also demonstrate that it is required for plasmablast differentiation, processes that induce significant cellular stress. The implication of autophagy in two major pathogenic pathways in SLE suggests the potential to use inhibition of autophagy as a novel treatment target.

Contents

List of Figures

List of Tables

Abbreviations

3-MA	3-methyladenine, page 44
4E-BP1	4E-binding protein 1, page 22
ALPS	autoimmune lymphoproliferative syndrome, page 38
AMBRA1	Activating molecule in beclin-1-regulated autophagy 1, page 17
AMPK	AMP-activated protein kinase, page 17
ANA	anti-nuclear antibodies, page 35
APRIL	A Proliferation Inducing Ligand, page 102
AS	Ankylosing spondylitis, page 52
ATF4	Activating transcription factor 4, page 123
ATF6	Activating transcription factor 6, page 122
ATM	Ataxia telangiectasia mutated, page 118
BAFF	B cell activating factor, page 41
BCA	Bicinchoninic acid, page 64
BCMA	B cell maturation antigen, page 102
BCR	B cell receptor, page 35

BDI Bright Detail Intensity, page 63

BDS Bright Detail Similarity, page 64

BIM Bcl-2 like 11, page 36

BM Bone marrow, page 49

BSA Bovine serum albumin, page 57

CDR Complementarity determining region, page 118

CFSE Carboxyfluorescein succinimidyl ester, page 62

CHOP C/EBP homologous protein, page 123

CREM-α cAMP response element modulator-α, page 39

CSF-1 Colony stimulating factor-1, page 46

CSR Class switch recombination, page 30

cTEC cortical thymic epithelial cell, page 38

DAPK Death-associated protein kinase, page 27

DC Dendritic cell, page 30

Deptor DEP-domain containing mTOR-interacting protein, page 22

DFCP-1 Double FYVE-containing protein-1, page 17

DILE Drug-induced lupus erythematosus, page 32

DMSO Dimethyl sulfoxide, page 62

DN Double negative, page 46

DNA-IC DNA-immune complexes, page 44

DSB Double-stranded break, page 118

EAE Experimental allergic encephalitis, page 47

EBF early B cell factor, page 35

EBV Epstein-Barr virus, page 28

eIF-2B Eukaryotic protein synthesis initiation factor-2B, page 26

eIF2α Eukaryotic translation initiator factor 2α, page 122

eIF4E Eukaryotic initiation factor-4E, page 93

ER Endoplasmic reticulum, page 36

ERAD Endoplasmic reticulum-associated decay, page 123

ERK1/2 Extracellular-signal-regulated kinases 1/2 , page 22

FBS Fetal bovine serum, page 56

FcRγ Fc receptor-γ chain, page 39

FITC Fluorescein isothiocyanate, page 63

Flt3 FMS tyrosine kinase 3, page 30

FO Follicular, page 119

Foxp3 Forkhead box protein 3, page 40

FSC Forward scatter, page 75

GATA3 GATA-binding protein 3, page 19

GC Germinal centre, page 33

GFP Green fluorescent protein, page 117

GM-CSF Granulocyte-macrophage colony stimulating factor, page 30

GSK3 Glycogen synthase kinase 3, page 25

GWAS Genome-wide association study, page 29

HEL Hen egg lysozyme, page 49

HIF1α Hypoxia inducible factor 1α, page 22

HRP Horseradish peroxidase, page 67

HSV Herpes simplex virus, page 43

iE-DAP Nucleotide-oligomerization domain 1/2, page 43

IFN Interferon, page 34

IKK IκB kinase, page 25

IPS-1 IFN-β promoter stimulator-1, page 43

IRE1α Inositol-requiring protein 1α, page 122

IRGM Immunity related GTPase M, page 51

ITGAM integrin, α-M, page 33

JNK c-Jun N-terminal kinase, page 46

LAP LC3-associated phagocytosis, page 42

LCL Lymphoblastoid cell line, page 71

LIR LC3 interacting region, page 19

LKB1 Liver kinase B1, page 24

LPS Lipopolysaccharide, page 30

MDA5 Melanoma differentiation associated-5, page 43

mDC Myeloid dendritic cell, page 34

MDP Muramyl dipeptide, page 43

MEF Mouse embryonic fibroblast, page 43

MHC Major histocompatibility complex, page 30

MIFC Multispectral imaging flow cytometry, page 70

mLST8 Mammalian lethal with Sec13 protein-8, page 22

MOG Myelin oligodendrocyte glycoprotein, page 47

mSin1 Mammalian stress-activated MAP kinase-interacting protein-1, page 22

mTEC medullary thymic epithelial cells, page 38

mTOR Mechanistic target of rapamycin, page 40

mTORC1 Mechanistic target of rapamycin complex-1, page 17

MZ Marginal zone, page 119

Nbr1 Neighbour of BRCA1, page 19

NFATc1 Nuclear factor of activated T cells, cytoplasmic 1, page 19

NOD1/2 Nucleotide-oligomerization domain 1/2, page 42

NZB/W New Zealand Black × White F1, page 109

PAD Peptidylarginine deiminase, page 45

Pax5 paired box protein-5, page 35

PBMC Peripheral blood mononuclear cells, page 57

PBS Phosphate buffered saline, page 57

pDC Plasmacytoid dendritic cell, page 33

PERK Protein kinase RNA-like endoplasmic reticulum kinase, page 122

PI3K Phosphoinosite 3-kinase, page 17

PI3P Phosphatidylinositol-3-phosphate, page 17

PINK1 PTEN-induced kinase-1, page 21

PMA Phorbol myristate acetate, page 25

PRAS40 Proline-rich Akt substrate 40kDa, page 22

PRDM1 PR-domain zinc finger protein 1, page 36

Protor1/2 Protein observed with Rictor 1/2, page 22

PTEN phosphatase and tensin homologue deleted on chromosome 10, page 39

PTM Post-translational modification, page 26

RA Rheumatoid arthritis, page 27

Raptor Regulatory-associated protein of mTOR, page 22

REDD1 Regulation of DNA damage response-1, page 22

Rheb Ras homologue enriched in brain, page 22

Rictor Rapamycin-insensitive companion of mTOR, page 22

RIG-I Retinoic acid inducible gene-I, page 43

RIPA Radioimmunoprecipitation, page 64

RIPK2 Receptor-interacting serine/threonine-protein kinase 2, page 43

RLRs RIG-like receptors , page 43

RNP Ribonucleoprotein, page 34

RPMI-1640 Roswell Park Memorial Institute-1640, page 56

RT Room temperature, page 61

S6K1 S6 kinase-1, page 22

SCID Severe combined immunodeficiency, page 110

SHIP-1 SH2 domain-containing phosphatidylinositol 5-phosphatases, page 39

SHM Somatic hypermutation, page 40

shRNA short-hairpin RNA, page 49

SILAC Stable isotope labeling in cell culture, page 133

siRNA Short-interfering RNA, page 46

SLE Systemic lupus erythematosus, page 28

SNARE Soluble N-ethylmaleimide-sensitive factor attachment protein receptor, page 19

SNP Single nucleotide polymorphism, page 29

ssRNA Single-stranded RNA, page 34

STING Stimulator of interferon genes, page 43

Syk Spleen tyrosine kinase, page 39

TACI Transmembrane activator and calcium modulator ligand interactor, page 102

TASCC TOR-autophagy spatial coupling compartment, page 104

TBK1 TANK1-binding kinase, page 21

TBS-T Tris buffered saline with 0.05, page 65

TCR T cell receptor, page 38

TD T-dependent, page 49

TFEB Transcription factor transcription factor EB, page 19

TFH T follicular helper, page 40

TGF-β Transforming growth factor-β, page 37

TI T-independent, page 49

TIP60 Tat interactive protein, 60kD, page 26

TLR Toll-like receptor, page 33

TRAF6 TNF receptor associated factor-6, page 22

Treg Regulatory T cell, page 40

TSC1/2 Tuberous sclerosis 1/2 complex, page 22

ULK1 Unc-51-like kinase 1, page 15

UPR Unfolded protein response, page 36

UVRAG UV radiation resistance-associated gene, page 17

VSV Vesicular stomatitis virus, page 43

WIPI WD-repeat domain phosphatidylinosite interacting , page 17

XBP1 X-box binding protein-1, page 123

ZAP-70 Zeta-chain-associated protein kinase-70, page 39

$\Delta\psi m$ Mitochondrial transmembrane potential, page 40

Acknowledgments

I would like to thank Tim and everyone in the Vyse lab for all their help and support during my time there. In particular, Ulla Ellinghaus, Ben Rhodes, and Andrea Cortini for their patience (most of the time!) in putting up with my constant hopeless medic questions, and for showing me how to do pretty much everything. I'd also like to thank Myles Lewis and Amy Roberts for all our interesting discussions over the years, albeit on rather different subject matter. In the BRC Flow Core, I am grateful for the help and expertise of Pj Chana and Susanne Heck.

I would like to thank Prof. David D'Cruz and Dr Patrick Gordon at St. Thomas' and King's College Hospitals for their clinical support, which was vital during this project.

I am extremely grateful to Prof. Marina Botto at Imperial College, and to Dr Katja Simon at Oxford University for their generous collaboration, which greatly strengthened my research.

I would like to thank all the patients and healthy controls who participated in this project.

Finally, I am very grateful to the Wellcome Trust for providing a Research Training Fellowship which was the major funding source of this work, and to the NIHR BRC for funding supporting services.

This thesis is dedicated to Zoë, Freddie, and Arthur.

Associated publications

Peer reviewed

Clarke AJ, Ellinghaus U, Cortini A, Stranks A, Simon AK, Botto M, Vyse TJ. Autophagy is activated in SLE and required for plasmablast development. 2014, Jan 14, *Annals of the Rheumatic Diseases* (ePub ahead of print)

Abstract

Clarke AJ, Ellinghaus U, Vyse TJ. Autophagy is activated in the B cells of patients with SLE and is correlated with disease activity. 2012, *Immunology* 137:S1 185-6

1 Introduction

1.1 Autophagy

1.1.1 The machinery and process of autophagy

Autophagy is a highly conserved mechanism whose key function is the recycling of intracellular constituents for the provision of energy during times of metabolic stress. It also degrades long-lived macromolecules, defective organelles, and is capable of selective function. The genetic network governing autophagy was first established in the model organism *S. cerevisiae*, and a marked degree of conservation exists in mammalian homologous genes[1]. The process of autophagy consists of three major stages: initiation, elongation and enclosure of cytoplasmic contents to form a double-membraned autophagosome, and subsequent maturation and lysosomal fusion with degradation of its contents (figure 1.1).

1.1.1.1 Initiation of autophagy

The majority of experimental evidence suggests that the birthplace of nascent autophagosomes is the ER, which is the major of several identified sources of membrane[2]. The earliest pre-autophagosomal structure is the isolation membrane, which forms at points of contact between the ER and mitochondria[3]. Two complexes have been identified to be required for initiation of autophagy, and localize to the isolation membrane: the unc-51-like kinase 1 (ULK1) complex, and the Vps34/Beclin-1

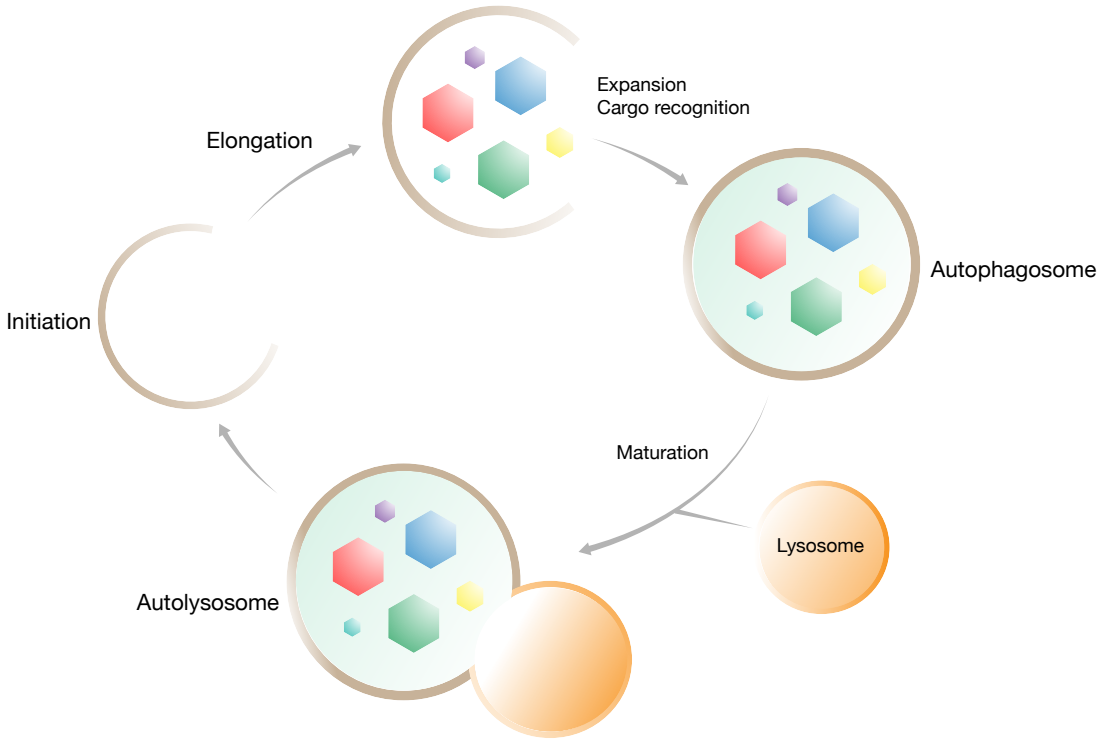

Figure 1.1: **Overview of autophagy**. Autophagosome nucleation occurs at the endoplasmic reticulum, followed by expansion and elongation, then closure of the double membraned autophagosome. Completion and recycling of the constituents of the autophagosome occur after lysosomal fusion.

class III phosphoinosite 3-kinase (PI3K) complex.

The ULK1 complex consists of ULK1 (the mammalian homologue of yeast Atg1), mAtg13, FIP200, and Atg101[4]. It is of importance as it integrates signals from the metabolic master regulatory complex mechanistic target of rapamycin complex-1 (mTORC1), and the energy sensor AMP-activated protein kinase (AMPK)[5]. AMPK activation in response to glucose starvation phosphorylates ULK1 at Ser317/777, which initiates autophagosome formation. The function of the ULK1 complex in initiating autophagy is understood to a limited degree, but FIP200 directs Atg16L1 to the isolation membrane and therefore recruits the two ubiquitin-like systems (discussed in 1.1.1.2) required for elongation[6]. In mammals there appears to be a degree of functional redundancy between ULK1 and its homologue ULK2[7].

The second major complex involved in initiation of autophagosome formation is the class III PI(3)K complex, which consists of Vps34, p150, beclin-1, and variable beclin-1 binding partners including Atg14L, activating molecule in beclin-1-regulated autophagy 1 (AMBRA1), rubicon, Bif-1, and UV radiation resistance-associated gene (UVRAG)[8]. Beclin-1 provides an interface between autophagy and cell death by binding via its BH3 domain to Bcl-2 or Bcl_{XL}, or through its caspase-dependent cleavage. Vps34 phosphorylates phosphatidylinositol on the 3'position of its ring, to generate phosphatidylinositol-3-phosphate (PI3P), which localizes to regions of the ER upon induction of autophagy[9], and acts as a docking site for FYVE- and PX- domains[10]. As with the ULK1 complex, there is limited understanding of how PI3P formation at nucleation sites engages the ubiquitin-like systems required for elongation of the isolation membrane. It appears PI3P binds the double FYVE-containing protein-1 (DFCP-1)[9] and WD-repeat domain phosphatidylinosite interacting (WIPI) complexes, which are also required for autophagosome formation[11].

1.1.1.2 Elongation

In the Atg12 system, Atg12 is covalently conjugated to Atg5. Atg12 is ubiquitin-like and is first activated by Atg7 (E1-like) then transferred to Atg5 by Atg10 (E2-like)[12;13]. The Atg5-12 conjugate then associates with Atg16L1, to form a multimeric complex[14]. Atg16L1 is responsible for targeting Atg5-12 to the developing autophagosome, and subsequently specifies the site of lipidation[15]. The Atg16L1 complex diffuses from the isolation membrane as it matures, and it is therefore an early marker of autophagosome formation.

The second system lipidates LC3 (the mammalian homologue of yeast Atg8) by attachment of phosphatidylethanolamine (PE)[16]. This conjugation system shares the same E1-like enzyme, Atg7, but uses an alternative E2-like enzyme - Atg3. The Atg5-12 conjugate fulfills an E3-like role in transferring LC3 from Atg3 to PE[17]. Following fusion with the lysosome, the protease Atg4, which initially processes LC3 by removing the terminal arginine residue, also delipidates LC3 for subsequent reuse[18;19]. Once conjugated to PE, LC3 (denoted LC3-PE or LC3-II) becomes membrane associated, and mediates membrane tethering and hemifusion during the elongation process[20].

Detection of autophagosome-associated LC3 has emerged as a preferred tool for the quantification of autophagy, as it remains the only identified protein specific for mature autophagosomes[21].

1.1.1.3 Maturation and fusion

Autophagosomes form randomly in the cytoplasm, but move along microtubules[22]. The initial fusion step with endosomes requires Rab7, ESCRTSs, C-Vps, and UVRAG1; following this, a structure called an amiphisome is formed[23–25].

Autophagosome-lysosome fusion[26] appears to be regulated in part by physical

proximity; activation of autophagy by mTORC1 inhibition leads to lysosome trafficking towards the nucleus, where encounter with autophagosomes is more likely[27]. Similarly, the lysosomal master transcription factor transcription factor EB (TFEB) co-regulates autophagosome and lysosome biogenesis in response to nutrient starvation[28].

Directed fusion with lysosomes requires syntaxin 17, a soluble N-ethylmaleimide-sensitive factor attachment protein receptor (SNARE) complex[29].

Finally, lysosomal pH must be appropriate for fusion to occur, and inhibition of lysosomal H^+ATPase with agents such as chloroquine or bafilomycin A_1 provides a key target for pharmacological inhibition of autophagy[30].

1.1.2 Selective autophagy

Autophagy may function as a non-specific bulk process, but also exhibit selectivity, achieved by adapter proteins, that target the substrate to nascent autophagosomes.

The best-characterized adapter protein is p62, also known as sequestosome-1. p62 contains both ubiquitin and LC3-binding domains (UBA and LIR), and therefore targets ubiquitinated substrates to the autophagosome for degradation[31;32]. Interestingly, p62 has homeostatic functions distinct from autophagy, and its accumulation in autophagy deficient cells is cytotoxic and leads to tumorigenesis, in part at least due to NF-κB activation[33;34]. p62 has been demonstrated to be necessary for clearance of protein aggregates, mitochondria, and bacteria[34;35].

The protein neighbour of BRCA1 (Nbr1) has also been identified as an autophagy adapter protein[36]. Nbr1 is structurally homologous to p62, containing UBA and LIR domains, and as with p62 is cleared principally via autophagy. Nbr1 is induced in stimulated $CD4^+$ T cells, and is required for T_H2 differentiation, via regulation of GATA-binding protein 3 (GATA3) and nuclear factor of activated T cells, cytoplasmic 1 (NFATc1)[37].

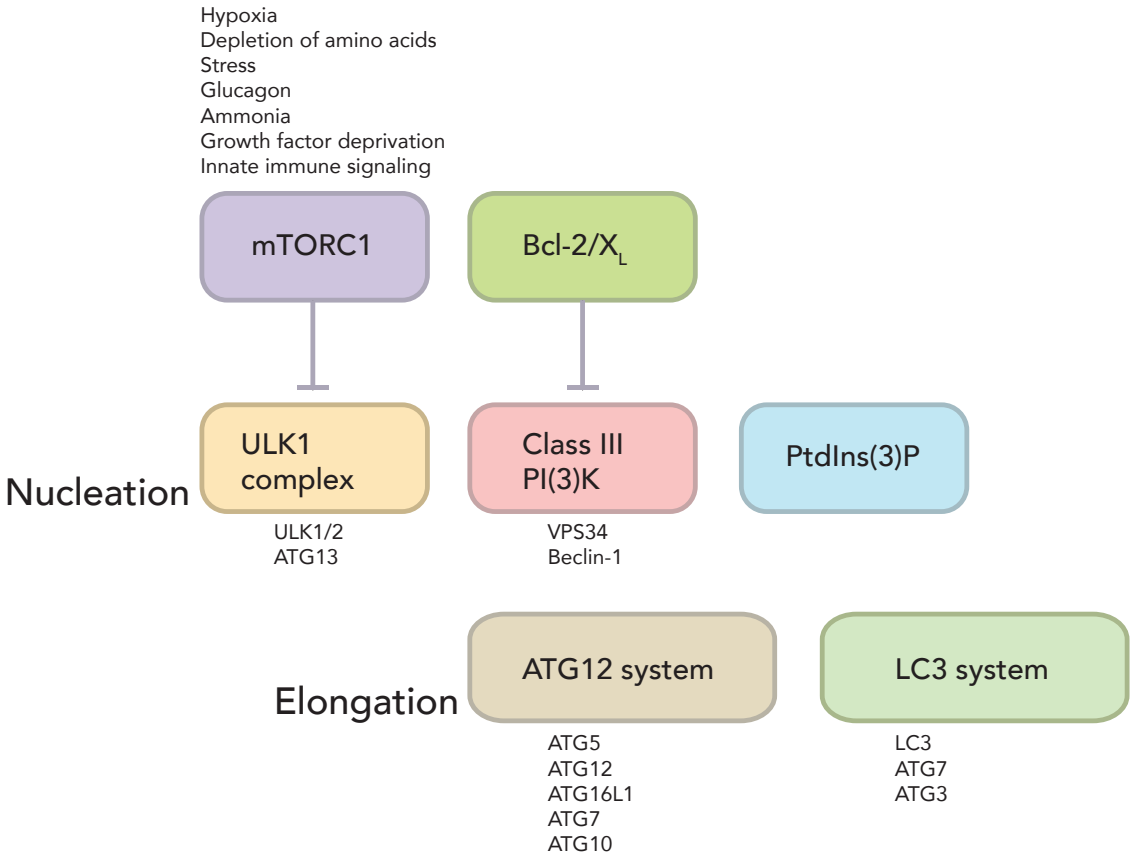

Figure 1.2: **Summary of the process and regulation of autophagy**. Autophagy is broadly activated by cellular stress stimuli, leading to autophagosome nucleation in the ER, a process requiring the ULK1 and class III PI3K complexes. The elongation of the isolation membrane to form an autophagosome requires two ubiquitin-like conjugation systems: the Atg12 system and the Atg8/LC3 system. Upon reaching maturity, autophagosomes fuse first with endosomes, and then with lysosomes, where their contents are degraded.

Structurally dissimilar to p62 and Nbr1 is NDP52, identified as a ubiquitin-binding adapter for TANK1-binding kinase (TBK1) and a selective autophagy receptor. NDP52 is required for restriction of *Salmonella typhimurium*, and contains UBA, galectin-8, and LIR binding domains[38;39].

The selective degradation of mitochondria ('mitophagy'), plays a critical role in the maintenance of cellular homeostasis, as accumulation of defective mitochondria that have undergone outer membrane permeabilization will activate apoptosis[40]. Loss of mitochondrial outer membrane integrity leads to the release of cytochrome *c* into the cytosol, where it induces oligomerization between apaf-1 and caspase-9, forming the apoptosome and activating the 'executioner' caspases -3 and -7, which are the terminal effectors of apoptosis[41].

Mitophagy is also important in erythrocyte maturation, and in clearance of male mitochondria following oocyte fertilization[42;43]. Mitophagy in reticulocytes, which mature into erythrocytes, occurs via the adapter protein NIX, whose expression is markedly increased in the latter stages of red cell development[42;44;45]. NIX, which binds to the mitochondrial outer membrane, contains an LIR, and may therefore recruit mitochondria into autophagosomes[46]. Defective mitochondria are cleared by recruitment of the E3 ligase parkin by PTEN-induced kinase-1 (PINK1). Parkin and PINK1 are mutated in some familial cases of Parkinson's disease[47;48].

1.1.3 Regulation of autophagy: signaling pathways

1.1.3.1 mTOR

mTOR is a serine/threonine kinase identified following the search for the target of the immunosuppressant anti-fungal agent rapamycin, derived from *Streptomyces hygroscopicus*, found on Easter Island (known locally as 'Rapa nui'). mTOR forms two complexes; mTORC1 and mTORC2. mTORC1 consists of mTOR, regulatory-

associated protein of mTOR (raptor), mammalian lethal with Sec13 protein-8 (mLST8), proline-rich Akt substrate 40kDa (PRAS40), and DEP-domain containing mTOR-interacting protein (Deptor). mTORC2 comprises mTOR, rapamycin-insensitive companion of mTOR (rictor), mammalian stress-activated MAP kinase-interacting protein-1 (mSin1), protein observed with rictor 1/2 (protor 1/2), and mLST8[49].

mTORC1 acts to integrate signals from a variety of upstream environmental sensors, including amino acid availability, cell stress, hypoxia, and growth factors. Many of these signals regulate mTOR through the heterodimeric tuberous sclerosis 1/2 complex (TSC1/2). TSC1/2 is a GTPase activating protein for ras homologue enriched in brain (Rheb). Rheb, in its GTP-associated form, phosphorylates and thus activates mTORC1; TSC1/2 therefore negatively regulates mTORC1. The inputs into TSC1/2 include those that are inhibitory, and therefore activate mTORC1 signaling, *e.g.* class I PI3K via Akt, and extracellular-signal-regulated kinases 1/2 (ERK1/2), and those that activate TSC1/2, and therefore inhibit mTORC1, *e.g.* the energy sensor AMPK, and the hypoxia sensor regulation of DNA damage response-1 (REDD1). mTOR is also regulated by amino acids[50] in a TSC1/2 independent manner, through the Rag GTPases. Rag GTPases cause translocation of mTOR to the lysosomal surface, where it is in proximity to Rheb and may thus be activated[51].

Activated mTORC1 phosphorylates the translational regulators S6 kinase-1 (S6K1) and eukaryotic translation factor 4E-binding protein-1 (4E-BP1), resulting in promotion of protein synthesis. It also enhances lipid synthesis, and increases ATP production through positive regulation of hypoxia inducible factor 1α (HIF1α)[49].

mTORC1 inhibits autophagy by several mechanisms. A major mode of action is by association with and phosphorylation of the ULK1-Atg13-FIP200 complex involved in initiation of autophagy[5;52–54]. AMBRA1 is also phosphorylated by mTOR, and once dephosphorylated interacts with TNF receptor associated factor-6 (TRAF6).

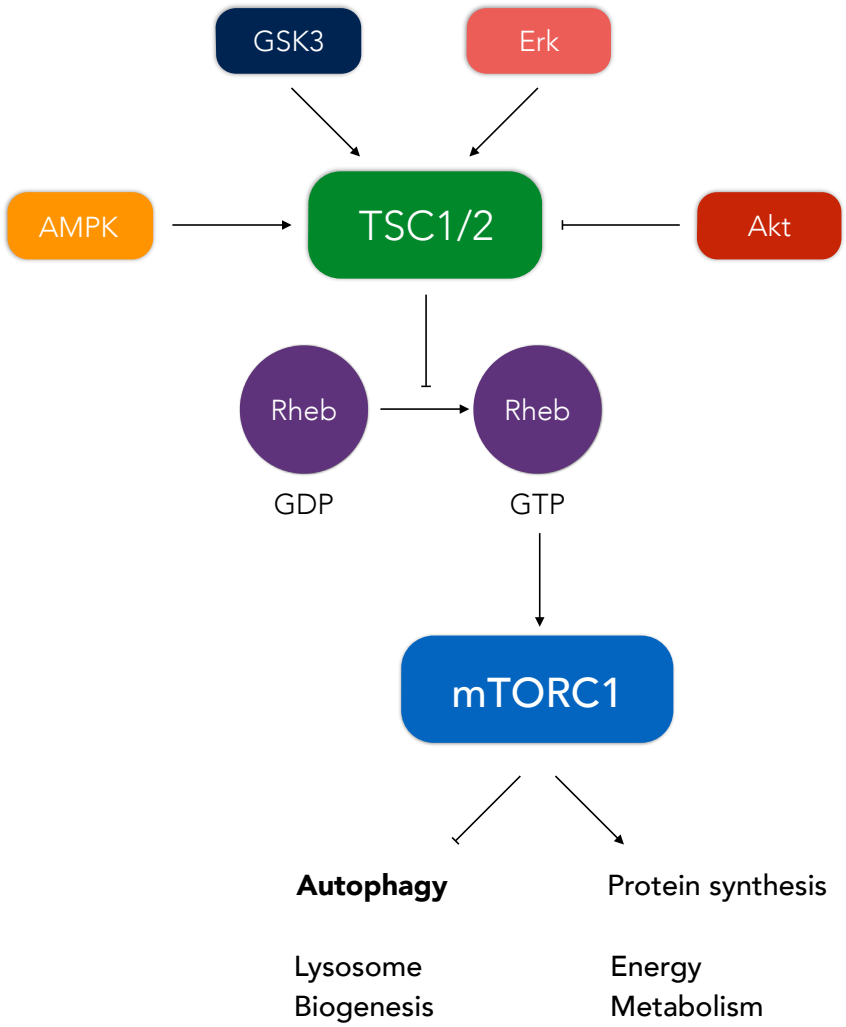

Figure 1.3: **The mTOR signaling pathway**. Regulatory inputs are integrated by the TSC1/2 complex. TSC1/2 is a heterodimeric activating protein for Rheb, which phosphorylates and activated mTORC1 in its GTP associated state. Phosphorylated mTORC1 inhibits autophagy and lysosome biogenesis, whilst stimulating protein synthesis and cell growth.

This results in the ubiquitination and subsequent self-association and activation of ULK1[55].

mTOR signaling is an important determinant of T cell fate[56], as it is required for the metabolic demands of cell proliferation, *i.e.* the switch from catabolism to anabolism. Naïve T cells genetically deficient in mTOR do not differentiate into effector subsets under polarizing conditions[57]. Instead, the formation of T_{regs} is favored. A similar phenomenon is observed using rapamycin[58].

The role of mTOR in B cell homeostasis has been much less explored, with no phenotypic reports of mice deficient in essential mTOR signaling components. However, mTOR is activated upon BCR ligation[59], and treatment of B cells *in vitro* with rapamycin inhibits their proliferation following stimulation[60].

1.1.3.2 AMPK

AMPK is a heterotrimeric kinase, constitutively phosphorylated by liver kinase B1 (LKB1) at Thr172 on its α-subunit. AMPK is allosterically regulated by the binding of adenine nucleotides to its γ-subunit; AMP enhancing its activity and ATP suppressing it[61]. AMPK therefore senses energy depletion, and its downstream effects act in opposition to those of mTOR, by promoting efficient ATP generation through oxidative phosphorylation, inhibiting cell cycle progression, and inducing catabolic processes such as autophagy. AMPK regulates autophagy both by opposing mTOR, through dephosphorylation of the mTORC1 component raptor[62] and TSC2[63], and also, as mentioned above, by phosphorylation of ULK1 at Ser 317/777[5] , leading to its activation.

As with mTOR, AMPK has important roles in immune homeostasis[64]. AMPK activation is associated with a switch away from aerobic glycolysis (the 'Warburg effect'), the preferential energy source for activated macrophages and effector T cell subsets, *e.g.* T_H17, towards mitochondrial oxidative phosphorylation and regula-

tory *e.g.* T_{reg} cell differentiation[65;66].

1.1.3.3 Reactive Oxygen Species

ROS are small, unstable, highly reactive molecules formed from incomplete reduction of oxygen. ROS may act as multifunctional signaling molecules, and are produced at times of cellular stress. It has been shown that ROS activate autophagy, at least in part by oxidizing Atg4, the protease responsible for delipidation of LC3-PE[67]. Autophagy plays a key role in removal of defective and senescent mitochondria ('mitophagy'), and ROS accumulation may therefore activate this process[68].

1.1.3.4 NF-kappa B

It has been reported that beclin-1 contains a binding site for the NF-κB subunit p65, which results in its positive regulation following p65 translocation, subsequently inducing autophagy in the Jurkat T cell line following stimulation with phorbol myristate acetate (PMA) and ionomycin[69]. However, other groups have demonstrated that p65 is dispensable for activation of autophagy in response to multiple stimuli[70;71], but instead IκB kinase (IKK), a component of the NF- κB signaling pathway, plays a distinct and independent role in the regulation of autophagy, at least in part by modulating Akt signaling[72]. Autophagy has been described as suppressed in Ewing sarcoma cells stimulated with TNF-α, a process dependent on NF-κB, with evidence of mediation through mTOR activation[73]. However, contrary findings have been reported in HeLa cells in response to heat shock, with failure to induce autophagy with p65 deficiency, leading to increased cell death[74].

1.1.3.5 Glycogen synthase kinase 3

Glycogen synthase kinase 3 (GSK3) is a serine/threonine kinase, initially identified as phosphorylating and therefore inhibiting glycogen synthase, but which also has

a broad range of targets across cell growth and metabolism. GSK3 exists in two isoforms, α- and β-, which are ≈95% homologous, but exhibit differing substrate specificities[75]. GSK3 is constitutively active in the resting state, and broadly inhibits its transcription factor targets by phosphorylating serine/threonine residues at consensus sites. GSK3 is regulated by phosphorylation (GSK3β at Ser9, -α at Ser21) which leads to its inactivation[76]. Inactive GSK3 is permissive for glycogen synthase and eukaryotic protein synthesis initiation factor-2B (eIF-2B) dephosphorylation and therefore glycogen and protein synthesis. GSK3 is phosphorylated by many growth-associated stimuli, including Akt, S6K1, and p38 mitogen-activated protein kinases (p38 MAPK)[77]. Activation of GSK3 has been found to be required for serum-starvation induced autophagy, via acetylation of HIV-1 Tat interactive protein, 60kD (TIP60), which directly phosphorylates ULK1[78]. However, it has also been demonstrated that pharmacological inhibition of GSK3 may lead to up-regulation of autophagy, through increased lysosomal biogenesis caused by TFEB translocation[79].

1.1.3.6 FoxO transcription factors

The FoxO family of forkhead transcription factors regulates the expression of a genetic network controlling cellular stress response, metabolism, and longevity[80]. FoxO members also modulate autophagy, with binding sites identified on Bnip3, LC3, and Atg12[81–83]. FoxOs are subject to post-translational modification (PTM) including phosphorylation and acetylation, which modify their subcellular localization (nuclear or cytoplasmic), and therefore their ability to act on their target genes. Regulatory phosphorylation is enacted by several growth factor associated kinases, *e.g.* Akt, which phosphorylates FoxO3 at Thr32 and Ser253, causing binding of chaperone proteins such as 14-3-3, and leading to its nuclear export[84]. However, phosphorylation at other sites by AMPK may not result in FoxO3 translocation, but

instead change the target gene specificity and alter the resulting transcriptional program[85]. FoxO3 has been determined to be required for autophagy in cardiac and skeletal muscle myocytes, and in haematopoietic stem cells[81;82;86]. Recently, variants in *FOXO3* have been associated with the severity of Crohn's disease, malaria, and rheumatoid arthritis (RA)[87].

1.1.4 Regulation of autophagy: Beclin-1, Bcl-2 and BH3 proteins

Beclin-1, introduced above, is fundamentally important for the initiation of autophagy[88], and beclin-1$^{-/-}$ mice die at an early stage of embryonic development (E7.5 or earlier)[89]. Beclin-1 contains three structural domains: an N-terminus BH3 domain, which governs its interactions with Bcl-2 family members, a central coiled coil domain (CCD), and an evolutionarily conserved domain, which is critical for induction of autophagy[90].

Autophagy is suppressed by binding of Bcl-2 or Bcl_{XL} to beclin-1[91;92]. However, Bcl-2 may be displaced from Beclin-1 by competitive inhibition from diverse pro-apoptotic proteins including Bnip3, Bad, Noxa, Puma, and BimEL[93;94]. Beclin-1 self-oligomerizes via its CCD, and this association is stabilized by Bcl-2, which may inhibit the interaction between monomeric beclin-1 and class III PI3K[95;96]. Similarly, UVRAG disrupts beclin-1 self-oligomerization and promotes autophagy.

Beclin-1 may also be subject to PTM, by either phosphorylation or ubiquitination. Death-associated protein kinase (DAPK), a tumour suppressor protein, phosphorylates beclin-1 at Thr119, which leads to its dissociation from Bcl_{XL} and activation of autophagy[97]. Beclin-1 is K63 ubiquitinated, principally at Lys117, through TRAF6, which promotes autophagy[98]. The mechanism by which autophagy is stimulated is unclear, but may be due to altered oligomerization.

1.2 Systemic lupus erythematosus

1.2.1 Summary

Systemic lupus erythematosus (SLE) is a multi-system autoimmune disease characterized by engagement of multiple arms of the innate and adaptive immune systems against nuclear auto-antigens. Specifically, there is prominent type I interferon production, B cell hyperactivation, and the production of high-affinity autoantibodies which cause immune complex deposition and trigger the complement cascade resulting in tissue injury. Its clinical manifestations are variable and subject to evolution, and include arthralgia, arthritis, malaise and fever, rash, glomerulonephritis, and neuropsychiatric disease. It is significantly more prevalent in women (9:1), and in those with African, South Asian, or South East Asian ancestry. An environmental trigger for SLE is rarely ascertained, although there is not infrequently an antecedent viral infection, and links have been drawn to Epstein-Barr virus (EBV).

Despite the frequently severe disease phenotype, in the vast majority of cases no aetiological factor is indentified, and the clinical outcome is often unsatisfactory. Over recent years there has been increasing interest in and understanding of the importance of autophagy in multiple aspects of immunity, which potentially intersect with the pathogenesis of SLE. In this introduction, I will first outline the functional mechanism of autophagy, and then consider, in the context of the current understanding of SLE, how it may allow breach of the checkpoints which exist to prevent development of autoimmunity.

1.2.2 Epidemiology

There are considerable variations in estimates of the prevalence of SLE, and difficulties surrounding comparison of populations and geographical regions due to differences in diagnostic accuracy and awareness. However, the range for incidence esti-

mates is 1-10 per 100000 per year. Prevalence estimates range from 0.2-2 per 1000[99]. There is a dramatic difference in incidence between the sexes, with the female:male ratio *c.* 9:1; reasons for this are discussed below[100;101]. SLE is considerably more common in non-European populations, occurring >5 times more frequently in Afro-Caribbeans and twice as frequently in Asians. The peak age of onset in women is 40-49[100;101].

1.2.3 The genetics of SLE

SLE represents a complex trait with a heritability (λS) of 29 assuming a population prevalence of 0.001)[102]. The advent of genome-wide association studies (GWAS) has dramatically increased the number of identified susceptibility loci (table 1.2.3), which had previously been restricted to rare but penetrant Mendelian variants (*e.g.* deficiency in classical complement pathway components)[103]or large intervals mapped through linkage analysis. The whole-genome coverage provided by contemporary genotyping platforms allows freedom from a preconceived candidate gene approach and facilitates discovery of unsuspected mechanistic associations.

Broad insights from GWAS into the genetic architecture of the SLE include the observation that a significant number of risk loci are shared in common with other autoimmune diseases, and that there are considerable differences in associated (SNPs) between racial groups, in so far as it is possible to say given the relative lack of GWAS in Afro-Caribbean and Asian populations. As is observed in other complex diseases (*e.g.* type II diabetes), the effect size of risk SNPs is small, with typical odds ratios of between 1.15-2, and they usually occur in non-coding regions of DNA, whose functional significance is only starting to be appreciated[104;105].

Finally, to date only a small fraction (≈10%) of the heritability of SLE is explained by identified common variants, and this so-called 'missing heritability' may be due to as yet un-genotyped rare variants, copy number variation, or gene-gene interac-

tion.

1.2.4 The female gender bias in SLE

There is a striking difference in the prevalence of SLE between men and women, with similar findings in murine lupus models. Sex hormones have pleiotropic and profound effects on most aspects of immunity. In the innate immune system, oestradiol promotes granulocyte-macrophage colony stimulating factor (GM-CSF) induced differentiation of dendritic cells (DCs), and DCs treated with oestrogen inhibitors express less CD86 and major histocompatibility complex class II (MHC-II) following stimulation with lipopolysaccharide (LPS)[109]. However, oestrogens may also exert negative regulatory effects, particularly following FMS tyrosine kinase 3 (Flt3) ligand stimulation, on DC maturation[110]. As with dendritic cells, the role of oestrogens in T cell homeostasis is nuanced, with differential effects seen as levels increase. Lower levels of estrogen promote T_H1 polarization, whereas high levels promote a T_H2 response. Very high levels of oestrogens, associated with pregnancy, can in fact cause a dramatic reduction in thymocyte numbers and lead to thymic atrophy[111]. Similarly, B cell lymphopoiesis is also inhibited by oestrogens during pregnancy[112]. However, lower concentrations of oestrogen promote humoral immunity, enhancing processes that may lead to autoimmunity, *e.g.* modulation of clonal deletion and class switch recombination (CSR)[113].

Whilst oestrogen has pleiotropic roles in multiple immune cell types[114], there is not a clear correlation between either oestrogen levels or exogenous administration, and SLE disease activity[115].

The complement of X chromosomes acts as an additional, independent risk factor for disease. The X chromosome contains a pseudoautosomal region that encodes multiple genes with important functions in immunity (*e.g. CD40L*, *MECP2*), variants in some of which are associated with SLE[116]. The risk of SLE is substantially

Gene	SNP	p-value	OR (95% CI)	Function
HLA-DRB1	rs3135394	2×10^{-50}	1.98 (1.84-2.14)	MHC region
STAT4	rs7574865	1.4×10^{-41}	1.57 (1.49-1.69)	IL-12, T_H differentiation
IRF5	rs2070197	5.8×10^{-24}	1.88 (1.78-1.95)	Interferon transcription
ITGAM	rs11860650	1.9×10^{-20}	1.43 (1.32-1.54)	Phagocytosis, complement regulation
BLK	rs2736340	7.9×10^{-17}	1.35 (1.27-1.43)	B cell signaling and development
TNFAIP3	rs5029937	1.37×10^{-17}	1.72 (1.52-1.94)	Inhibits NF-κB signaling
PTPN22	rs2476601	3.4×10^{-12}	1.35 (1.24-1.47)	T cell receptor signaling
TNFSF4	rs2205960	2.3×10^{-26}	1.22 (1.15-1.30)	T cell co-stimulation
PRDM1-ATG5	rs4134466	5.8×10^{-12}	1.25 (1.17-1.33)	Lymphocyte differentiation, autophagy
UBE2L3	rs131654	2.99×10^{-16}	0.78 (0.74-0.83)	Ubiquitination

Table 1.1: **Selected genetic associations with SLE. Best *p*-value from referenced GWAS shown**[106–108]

increased in males with Klinefelter's syndrome (XXY), and in murine models with *Sry* deletion on a lupus-prone background, the disease is more severe in XX mice compared with XY-[117;118].

1.2.5 The environment and SLE

The most robust evidence for environmental factors influencing the onset of SLE is for EBV infection, and drug-induced lupus erythematosus (DILE). Antibodies against EBV components are seen more frequently in patients with SLE than in healthy controls, an association not observed with other common viruses[119;120]. This finding is supported by experiments suggesting that molecular mimicry occurs between Epstein-Barr virus nuclear antigen-1 (EBNA-1) and the nucleoprotein Ro, which is frequently the target of antibodies in SLE[121]. Defective anti-EBV immunity is also seen in SLE patients, *e.g.* higher EBV viral loads associated with $CD8^+$ T cell exhaustion[122]. DILE is a well-recognized phenomenon reported with the use of at least 50 different pharmaceuticals, classically including hydralazine, procainamide, and methyldopa. Whilst it has many clinical features in common with SLE, it is very rarely causes hypocomplementaemia or renal disease. Its characteristic autoantibody is anti-histone, seen in the vast majority of cases[123].

Other potential environment risks are less clearly established. There is likely a weak effect for smoking at time of diagnosis ($OR \approx 1.5$)[124]. There is some evidence that exposure to crystalline silica may predispose towards SLE[125]. Associations with environmental pesticides and cosmetic product use have not been substantiated[126].

1.3 Checkpoints in immunity and the development of autoimmune disease

One of the striking properties of the human immune system is the ability to respond and adapt to an essentially unlimited variety of antigenic structures, achieved by the production of highly variable immunoglobulin molecules and T-cell receptors (TCRs) by the recombination of variable (V), diversity (D), and joining (J) genes during lymphocyte development. An inevitable consequence of this random process is the formation of self-reactive receptors which have the potential to cause autoimmune disease. However, in healthy individuals, these lymphocytes are deleted or inactivated and do not proliferate and cause tissue damage. In this section I will consider the checkpoints which exist to prevent the development of autoimmune disease

1.3.1 Clearance of apoptotic cells

A key paradigm in the pathogenesis of SLE is that failure of the clearance of apoptotic or necrotic cells leads to the release of nuclear constituents which subsequently incite a pro-inflammatory immune response; the so called 'waste disposal' hypothesis[127]. Evidence for this comes from disease associated genetic variation, animal models, and clinical findings. Deficiency of components of the classical pathway of complement activation (*e.g.* C1q, C4) impairs opsonization and phagocytosis of nucleic acid-containing immune complexes through complement receptors[103]. These immune complexes are instead hypothesized to stimulate toll-like receptors (TLRs) in, notably, plasmacytoid dendritic cells (pDC), or activate Fc-receptors. Similarly, defects in phagocytosis through complement receptor-3 (CR3) caused by coding variants in integrin, α-M (ITGAM) may also be associated with SLE[128]. Germinal centre (GC) macrophages in patients with SLE display impaired uptake of apoptotic

cells, which may lead to their excessive presentation of auto-antigens to B cells undergoing the GC reaction[129]. Mouse models with macrophages lacking the Tyro3 tyrosine kinase Mer and thus unable to phagocytose apoptotic cells develop anti-dsDNA autoantibodies, but not overt clinical disease; however a full SLE-like phenotype may be induced by constitutive activation of monocytes by additional deletion of the other Tyro3 members *Tyro3* and *Axl*[130;131].

1.3.2 Type I interferon

A hallmark of SLE is overproduction of type I interferon, and the major source of this appears to be from pDCs. pDCs are specialized in the production of type I interferons (IFN) and other pro-inflammatory cytokines upon stimulation of, most relevantly, TLR -7 and -8 by single-stranded RNA (ssRNA), and 9 by unmethylated CpG motifs[132]. Type I IFN serves to activate an antiviral state in multiple components of the immune system. This includes maturation of immature myeloid dendritic cells (mDC) to allow stimulation of $CD4^+$ T cells and the subsequent expansion of B cells[133]. The type I interferon pathway is a central driving force in SLE. This is underscored by the induction of autoimmunity as a side effect of administration of IFN-α, the correlation between serum IFN-α levels and disease activity in many patients[134], the presence of an interferon-inducible gene signature in SLE peripheral blood mononuclear cells, and the amelioration of disease by anti-IFN-α antibodies[135;136]. pDC secrete large quantities of type I IFN after internalizing immune complexes containing DNA or ribonucleoprotein (RNP)[137], or DNA in association with the antimicrobial peptide LL37 (cathelicidin)[138]. Not only does self-nucleic acid stimulation of TLRs drive SLE, but it also accounts for the relative corticosteroid resistance seen in many patients[139].

1.3.3 B cell receptor formation and testing

B cells develop in the bone marrow from the common lymphoid progenitor, which is one of the fates of the multipotent progenitor cell (the other being the common myeloid progenitor)[140]. Commitment to the B cell lineage is determined at the earliest stage by the transcription factors E2A, early B cell factor (EBF) , and (Pax5)[141]. Pro-B cells start to express the B220 marker, recombination activating gene-1/2 (Rag1/2), and *Igh* D_H-to-J_H recombination has concluded as they enter the Pre-B(I) stage, associated with CD19 expression. The *Igh* locus then undergoes $V_H(D_H)J$ recombination until pre-B cell receptor (BCR) formation is possible (composed of IgH, the surrogate immunoglobulin light chains VpreB and $\lambda 5$, Igα, and Igβ).

During normal B cell development, *Igh* locus recombination frequently (up to 75% of immature B cells in humans)[142] results in the production of autoreactive BCRs, which are tested for binding to self-antigen at the transition from pre-B to immature B stage, through pre-BCR signaling. This represents an initial tolerance checkpoint, illustrated when deficiency of surrogate light chains results in the escape of self-reactive B cells and the subsequent development of anti-nuclear antibodies (ANA)[143]. Pre-BCR signaling results in allelic exclusion, so that each B cell utilizes only one heavy and light chain allele during its lifetime.

A second central tolerance checkpoint is through receptor editing. Secondary rearrangement of the V regions of *Igl* or *Igh* occurs, which may result in loss of autoreactivity[144]. However, receptor editing may be only partial, or may even cause *de novo* self reactivity[145;146]. Failure of these early central checkpoints may occur in SLE; newly emigrant B cells from patients are more likely to be autoimmune than those from healthy controls, even when in clinical remission[147;148].

Following encounter with their cognate antigen, B cells migrate to the lymphoid tissue and form germinal centres, structures in which somatic hypermutation (SHM) occurs to hone the affinity of the antibody response and produce either plasma cells

or memory B cells. The germinal center reaction is abnormal in SLE, because autoreactive B cells do not undergo deletion but develop into plasma cells secreting autoantibodies marked by signs of somatic mutation[149]. The mechanisms by which self-reactive B cells generated by SHM are deleted are poorly understood, but it is clear that autoimmunity may arise following dysregulation of many components of the GC. A further tolerance checkpoint is observed to occur in humans as newly emigrant B cells become mature naïve B cells. There is a substantial reduction in the frequency of self-reactive B cells following this transition[142]. Mechanisms that may account for this attrition include internalization of the self-antigen bound BCR, leading in the absence of T cell help to decreased B cell activating factor receptor (BAFF-R) expression and thus deprivation of survival signals[150], and an increase in levels of the pro-apoptotic molecule Bcl-2 like 11 (BIM)[151]. Once mature, B cells become either follicular, or marginal zone subsets. Follicular B cells are resident in the follicles of the lymph nodes or spleen, and recirculate. Marginal zone B cells are an innate-like population resident in the splenic marginal zone.

As B cells undergo terminal differentiation into plasmablasts and then plasma cells, they begin to secrete very large quantities of immunoglobulin, which imposes significant metabolic stress on the cell. In particular, accumulation of defectively folded proteins in the endoplasmic reticulum (ER) can lead to cell death. The adaptive mechanism activated by cells to mitigate this ER stress is known as the unfolded protein response (UPR)[152]. Plasma cells are dependent on the UPR for immunoglobulin secretion, but it is dispensable for normal B cell activation, class switching, and cytokine production[153]. Plasma cell differentiation is associated with up-regulation of genes promoting the UPR, notably PR-domain zinc finger protein 1 (*PRDM1*), also known as Blimp-1, and suppression of cell cycle and growth promotion genes, *e.g. PAX5*[154]. There is evidence that the UPR is also required at an early stage of B cell development, during *Igh* locus rearrangement and

production of the BCR[155]. *Ig* gene rearrangement by necessity induces DNA damage, and it is possible that the UPR is required to control the associated cellular stress.

There is disturbed B cell subset balance in SLE. There is an overall reduction in total B cell numbers, but the number of circulating plasmablasts ($CD27^{++}$) may be markedly increased in active disease[156;157], and these can populate extra-medullary sites such as the kidney, in which inflammation has lead to up-regulation of survival factors such as CXCR12, transforming growth factor-β (TGF-β), and BAFF, forming disorganized ectopic follicular structures[158]. Long-lived plasma cells in the bone marrow enjoy resistance to many standard agents used in the treatment of SLE, including rituximab (due of loss of the targeted antigen CD20), cyclophosphamide, and corticosteroids[159;160]. There is also an increase in the novel $CD5^{+}$ pre-naïve population, which represents an intermediate stage between transitional and naïve B cells[161]. The characteristics of this population are an impaired response to BAFF and increased apoptosis, but a retained capacity to differentiate into plasma cells, and perform anretigen presentation. There is evidence for the existence of regulatory subsets of B cells 'B_{regs}', which suppress immunity by provision of IL-10, thereby promoting T_{reg} rather than T effector polarization of T cells[162]. This regulatory function has been ascribed to a number of B cell subsets, but in humans a $CD19^{+}CD24^{hi}CD38^{hi}$ transitional population was shown to produce IL-10 and inhibit TNF-α and IFN-γ production by T cells[163]. In SLE however, this population, although not reduced in numbers, is dysfunctional and lacks suppressive effect.

1.3.4 T cell receptor formation and testing

T cell development in the thymus proceeds through positive and negative selection stages, and in common with B cell development, strongly autoreactive cells may be deleted at a number of checkpoints. The initial positive selection stage occurs

when the newly formed T cell receptor (TCR) is tested for recognition of MHC associated with bound peptide, presented on cortical thymic epithelial cells (cTECs). Should the thymocyte weakly recognize this self-peptide in the context of MHC, it is selected to survive and undergo further development, whilst *Rag* expression is suppressed, ending receptor gene rearrangement. Following positive selection of those T cells with self-MHC restricted receptors in the thymic cortex, thymocytes proceed to the medulla, where negative selection of those with TCRs strongly reactive against self-antigens expressed on medullary cortical epithelial cells (mTEC) occurs. Notably, TECs require autophagy for efficient presentation of self-antigens on MHC-II, and engraftment of *Atg5*$^{-/-}$ thymi into athymic *Nude* mice results in severe autoimmune disease due to failure of negative selection[164]. Similarly other mechanisms that result in failure of negative selection also lead to systemic autoimmunity[165]. An example of such a defect is the rare disease autoimmune lymphoproliferative syndrome (ALPS), also known as Canale-Smith syndrome, which is associated with splenomegaly, lymphadenopathy, and autoimmune cytopenia. ALPS is caused by defects in Fas signaling, which results in failure of apoptosis induced by negative selection[166].

1.3.5 Anergy

Should a self-reactive receptor escape central selection processes, further mechanisms exist to prevent cell activation and autoimmunity. Collectively, and in normal homeostasis, the processes which limit the proliferation of these cells lead to either apoptosis, or a state of inertia known as anergy[167]. Autoreactive B cells have substantially diminished levels of surface IgM, caused by blockade of transport of the immunoglobulin molecules from the endoplasmic reticulum[168]. Another process especially relevant to the pathogenesis of SLE is the impairment of intracellular trafficking of the endocytosed BCR and endosomal TLR9, inhibiting the synergis-

tic signaling that results from co-stimulation of these receptors[169]. An alternative inhibitory mechanism to limit the response to TLR9 and BCR co-signaling is the induction of ERK by the BCR, which prevents TLR-induced plasma cell differentiation[170]. Signaling pathways downstream of the BCR are also subject to inhibitory feedback through the molecules SH2 domain-containing phosphatidylinositol 5-phosphatases (SHIP-1), and phosphatase and tensin homologue deleted on chromosome 10 (PTEN). SHIP-1 mediates the inhibitory action of the receptor FcγRIIB, and knockout of either of these molecules leads to a systemic autoimmune disease resembling SLE[171]. PTEN dephosphorylates PI3P and therefore antagonizes PI3K signaling. PTEN is upregulated in anergic B cells, and loss of PTEN results in a murine hyper-IgM syndrome[172]. PTEN is downregulated in human SLE, and may contribute to B cell hyperresponsiveness[173].

T cells also possess similar inhibitory receptor systems, for example CTLA-4 competes for binding to B7 and B7.1 with CD28, and also induces T_{reg} formation[174]. CTLA-4 function is defective in SLE, and genetic variants in the CTLA-4 locus predispose to SLE[175]; CTLA-4 knockout leads to severe autoimmune disease in mice[176]. Multiple abnormalities exist in T cell homeostasis in SLE, including in signaling, metabolism, and effector subset balance.

In the TCR signaling complex, there is loss of the CD3ζ chain, which is replaced by the Fc receptor-γ chain (FcRγ) with the effect that the more potent spleen tyrosine kinase (Syk) is activated rather than the canonical zeta-chain-associated protein kinase-70 (ZAP-70) pathway, thereby amplifying the downstream response[177]. Levels of the transcription factor cAMP response element modulator-α (CREM-α) are increased, leading to decreased expression of IL-2, but elevated IL-17A production[178]. Additional effects of abnormal signaling include elevated expression of the surface adhesion molecule CD44, and the co-signaling molecule CD154[179;180].

T cells in SLE exhibit features of disordered metabolism. These include mito-

chondrial hyperpolarization, excessive production of ROS, and relative depletion of ATP[181;182]. Elevation in mitochondrial transmembrane potential ($\Delta\psi$m) may be a prelude to release of cytochrome *c* and induction of apoptosis, but this is not inevitable and the increase in $\Delta\psi$m recapitulated by CD3/28 stimulation is reversible. Cytokine stimulation with *e.g.* IL-3 and interferon-γ also increase $\Delta\psi$m, but interestingly IL-10 increases ROS production and cell death in SLE T cells but not in healthy controls[182].

Mechanistic target of rapamycin (mTOR), a serine-threonine protein kinase that integrates information on amino acid availability, cellular energy status, and immune receptor binding, is activated in SLE[183]. mTOR is of great importance in the regulation of autophagy and in this capacity will be considered separately. Activation of mTOR is associated with differentiation of T cells to effector subsets; T cell specific mTOR deficiency leads to an increase in Foxp3$^+$ (forkhead box protein 3) regulatory T cells, which is also the case when mTOR is pharmacologically inhibited by rapamycin[57;58].

Whilst there has been some question whether regulatory T cells (T_{reg}) are deficient or dysfunctional in SLE[184], there is clear evidence that the T_H17 CD4$^+$ T cell subset is increased, corresponding to elevated levels of the pro-inflammatory IL-17 cytokine family in active disease[185]. The IL-17 family cytokines are necessary for severe glomerulonephritis in murine lupus, and promote survival of autoreactive B cells[186;187].

Another T cell subset dysregulated in lupus is the T follicular helper (T_{FH}) cell class, whose function is to provide support to GC B cells undergoing somatic hypermutation (SHM) and CSR, principally through the provision of IL-21. T_{FH} cells are required for systemic autoimmunity[188], and are increased in severe disease[189]. This may potentially increase the development of plasma cells producing high affinity IgG autoantibodies, which are a hallmark of SLE.

1.3.6 Competition for survival factors

A regulatory mechanism distinct from suppressive receptor signaling is competition for survival factors, exemplified by the B cell activating factor (BAFF) pathway in B cells. BAFF is produced by innate immune cells, *e.g.* macrophages and dendritic cells, and its secretion is upregulated by pro-inflammatory stimuli such as type I interferon signaling and TLR ligation. The BAFF receptor signals cell survival by activation of NF-κB2 and Akt, which leads to downregulation of BIM and stimulation of cell growth through mTOR. Strong BCR ligation by auto-antigens increases levels of BIM, and therefore increases the dependency of the autoreactive cell on BAFF; these cells are therefore less well able than those without autoreactive receptors to compete for limiting quantities of BAFF[190]. In addition to an anti-apoptotic effect, BAFF also increases the metabolic fitness of B cells through Akt, preparing them for proliferation. BAFF overexpression leads to the production of pathogenic autoantibodies, and the development of a lupus-like disease[191]. In human SLE, levels of BAFF are elevated, and this observation, along with the supporting data provides a rationale for the inhibition of this pathway for clinical benefit. To this end, the drug belimumab, an anti-BAFF monoclonal antibody, has been developed and used in clinical practice to ameliorate lupus disease activity[190].

1.4 Autophagy and immunity

1.4.1 Autophagy and the innate immune system

1.4.1.1 Restriction of invasive pathogens

The innate immune system has harnessed autophagy for defense against invasive microorganisms, in both a direct capacity through selective degradation, and also in a supportive subsidiary role. One of the main mechanisms for survival of in-

vasive intracellular bacteria *e.g.* group A *Streptococcus* or *Mycobacterium tuberculosis*, is interference with endosomal maturation following phagocytosis, leading to either escape into the cytosol or proliferation within vesicles. Autophagy is utilized to recapture escaped bacteria, and deliver them to the lysosome for digestion. The double-membraned autophagosome securely incarcerates the bacteria, and provides resistance to evasion strategies[192]. Bacteria are targeted for selective autophagy by deposition of ubiquitin, or galectin-8 on their surface[38;193]. However, the identity of the E3 ubiquitin ligase responsible remains unclear. Next, autophagy adapter molecules, including p62, Nbr1, and NDP52, target the bacterium to the autophagosome via their LIR domains.

An alternative, non-canonical autophagy known as LC3-associated phagocytosis (LAP) may also be important for pathogen restriction. LAP, distinct from canonical autophagy, results in the formation of single-membraned vesicles, unlike the double-membraned classical autophagosomes[194]. Decoration of phagosomes with LC3 promotes their maturation by fusion with the lysosomal compartment. LAP requires some, but not all of the canonical autophagy machinery[195].

1.4.1.2 Innate immune signaling

The role of autophagy in innate immune signaling is complex, and it is likely to have both inhibitory and stimulatory effects. Autophagy is generally up-regulated by PRR engagement.

Stimulation of TLRs activates LAP in the case of TLR2[194], or canonical autophagy (TLRs 4, 7, and 9)[194;196]. With the exception of TLR2, autophagy induction is MyD88-dependent[196], and promotes phagosome-lysosome fusion, resulting in enhanced microbial killing. Autophagy may also be directly induced by cytosolic DNA, either transfected or as the result of TB infection[197].

Similarly, the PRRs nucleotide-oligomerization domain 1/2 (NOD1/2), which

recognize intracellular γ-D-glutamyl-meso-diaminopimelic acid (iE-DAP) and muramyl dipeptide (MDP) respectively, also induce autophagy upon stimulation with their ligands[198;199]. A consequence of this is enhanced antigen presentation on MHC class II, as autophagosomes fuse with MHC-II loading compartments[200]. The mechanism by which NOD ligands stimulate autophagy may be through direct interaction with ATG16L1, as there is co-localization between NOD1/2 and ATG16L1, and autophagy induction is independent of the downstream signaling molecules receptor-interacting serine/threonine-protein kinase 2 (RIPK2) and NF-κB[199].

Autophagy also plays an important role in antiviral immunity, and therefore potentially autoimmunity. Autophagy has been identified as functional both in cytoplasmic and endosomal nucleic acid sensing. Cells sense cytoplasmic nucleic acids through receptors signaling via IFN-β promoter stimulator-1 (IPS-1), localized on the mitochondria, or stimulator of interferon genes (STING), which is ER-bound. The principal RNA receptors, transduced by IPS-1, are melanoma differentiation associated-5 (MDA-5) and retinoic acid inducible gene-I (RIG-I), CARD-domain helicases that sense long dsRNA and short RNA with 5'ppp respectively[201]; so called RIG-like receptors (RLRs). *Atg5*$^{-/-}$ mouse embryonic fibroblasts (MEFs), exposed to immunostimulatory RNA, produce more type I IFN than wild type cells, and have higher resistance to infection with vesicular stomatitis virus (VSV)[202;203]. Interestingly, infection with the dsDNA virus herpes simplex (HSV) resulted in decreased interferon production in the autophagy deficient cells. The Atg5-12 conjugate was seen to co-localize with IPS-1, and it may therefore act as a repressor of signaling downstream of RLRs[202]. Alternatively, the accumulation of mitochondria in autophagy deficient cells may enhance RLR signaling through increased production of ROS[203].

Autophagy is also important for delivery of nucleic acids into signaling compartments. In pDC, the response to infection with VSV was inhibited by pharmacologic

or genetic inhibition of autophagy *in vitro* and *vivo.* Accordingly, *Atg5*$^{-/-}$ chimeric mice were significantly more susceptible to mortality following infection[204]. Autophagy in human pDC is also important for production of IFN-α in response to *in vitro* infection with HIV-1[205]. A role for LAP in response to phagocytosis of DNA-immune complexes (DNA-IC) in pDC has also recently been demonstrated[206]. It was shown that engagement of Fc-γ-receptors by immune complexes leads to decoration of the phagosome with LC3, which co-localized with TLR9. Interestingly, CpG alone does not induce LAP, highlighting a requirement for Fc-γ signaling via an as yet undetermined pathway. Abrogation of LAP by the class III PI3K inhibitor 3-methyladenine (3-MA) or *Atg5* or -7 knockdown inhibited IFN-α production in response to DNA-IC, but NF-κB translocation induced by TNF-α is intact.

Autophagy has an important role in regulation of the inflammasome, which as discussed above, is a mediator of pathology in SLE. Inhibition of autophagy has a potentiating effect on IL-1β and IL-18 secretion in response to a variety of stimuli. For example, macrophages deficient in Atg16L1 or Atg7 produce markedly more IL-1β following stimulation with LPS or oxidized ATP, a P2X7 receptor agonist, but normal amounts of IL-6[207]. Conversely, induction of autophagy reduces IL-1β secretion[208;209]. Several mechanisms have been proposed for this finding. Firstly, pro-IL-1β, which is cleaved into its active form by caspase-1, is targeted to the autophagosome for degradation[208]. Secondly, inflammasomes have been observed to co-localize with autophagosomes, and are targeted for degradation by ubiquitination via the adapter protein p62[209]. Finally, autophagy deficiency leads to the accumulation of defective mitochondria and ROS, which themselves stimulate inflammasome signaling[210;211].

1.4.1.3 Antigen presentation

Recognition of antigens by T cells in the context of MHC proteins is integral to the functioning of the adaptive immune system. The classically held model is that MHC class I presents endogenous antigens to $CD8^+$ T cells, whereas MHC class II presents exogenous antigens to $CD4^+$ T cells. To this end, the mechanisms for processing and loading of antigens differ accordingly; MHC-I receives input from the proteasome, MHC-II from the endosome-lysosome system. However, this demarcation is not absolute, and a proportion of endogenous antigens may be presented on MHC-II, and exogenous on MHC-I, a phenomenon known as cross-presentation[212]. Autophagy has been recognized as a mechanism for the entry of cytoplasmic and nuclear contents into MHC-II loading compartments, with subsequent presentation to $CD4^+$ T cells[200;213–216].

Constitutive autophagy in antigen-presenting cells leads to autophagosome input to MHC-II loading compartments, and fusion of experimental antigens to LC3 leads to a marked increase in presentation on MHC-II[200]. Activation of autophagy has effects on the MHC-II 'ligandome', leading to preferential presentation of intracellular and nuclear antigens[213;216]. One functional consequence of increased MHC-II cross presentation is enhanced immunity against intracellular microorganisms, *e.g.* TB or HSV[200;217]. Autophagy may also post-translationally modify antigens – citrullination of proteins has been noted to be promoted by peptidylarginine deiminase (PAD) activity in the autophagosome, which may lead to a source of novel self-antigens, and autoimmune disease (as is seen in rheumatoid arthritis)[218].

Interestingly, autophagy in thymic epithelial cells has been co-opted to display self-antigen to developing T cells, and is therefore necessary for induction of anergy; mice with $Atg5^{-/-}$ thymus allografts develop severe colitis[164;215].

1.4.1.4 Monocyte differentiation

Autophagy is activated in monocytes following *ex vivo* stimulation with colony stimulating factor-1 (CSF-1)[219] or GM-CSF[220], which induce differentiation into macrophages. Inhibition of autophagy, either *in vitro* with the pharmacological autophagy inhibitor 3-MA, siRNA (short-interfering RNA), or in *Atg7*$^{-/-}$-Vav-Cre conditional knockout mice, restricts differentiation of human and murine monocytes. GM-CSF was demonstrated to activate c-Jun N-terminal kinase (JNK) signaling, and to cause dissociation of beclin-1 from Bcl-2[220].

1.4.2 Autophagy and the adaptive immune system

1.4.2.1 Autophagy and T cells

Murine models deficient in critical autophagy genes have demonstrated an important role for this pathway during T cell development. *Atg5*$^{-/-}$, *Beclin-1*$^{-/-}$ and *Atg7*$^{-/-}$-*Rag* chimeras and *Atg3*$^{F/F}$ *Lck*-Cre, *Atg5*$^{F/F}$-*CD4*-Cre, and *Atg7*$^{F/F}$-*CD4*-Cre conditional knockouts have decreased thymic cellularity, and with the exception of the *Atg3*$^{F/F}$ *Lck*-Cre model, there is a proportional increase in frequency of cells at the CD4^{-}CD8^{-} double negative (DN) stage[221–224]. Expression of autophagy genes is maximal in DN thymocytes, as are levels of LC3-II[222], and beclin-1[225]. This observation suggests that autophagy may be required for transition from this stage.

In the periphery, deficiency of Atg5, Atg7, and Atg3, but not Beclin-1, leads to a significant reduction in total T cell numbers, most pronounced in the CD8^{+} population. There is an increased proportion of T cells with the CD44^{hi}CD62^{lo} phenotype, which suggests homeostatic proliferation in response to lymphopenia[226]. Autophagy is activated following T cell stimulation through the TCR, and further enhanced by CD28 co-ligation[225;227;228]. Deficiency of Atg3 or Atg7 does not affect stimulation-induced expression of the activation markers CD69 and CD25[224;226], al-

though a reduction in IL-2 production has been observed[229]. However, autophagy is required for efficient T cell proliferation[222–224;229]. Autophagy deficient T cells cultured in T_H2 conditions are more susceptible to cell death during proliferation than T_H1 or T_H17[227;230].

A number of mechanisms are potentially responsible for this phenotype. Mitochondrial mass is increased in Atg5 and Atg7-deficient T cells due to impaired mitophagy, sensitizing them to apoptosis[222;224;231], although mitochondrial accumulation has not been observed in beclin-1 deficient T cells. Autophagy is also required for control of ER quantity ('ERphagy'), and the resulting expansion of ER seen in autophagy deficiency increases intracellular calcium stores, and impairs calcium influx in response to TCR cross-linking[226]. Whilst the defect in calcium flux is marked, it is probable that compensatory mechanisms exist, since calcium associated signaling is relatively intact.

Autophagy may be required to provide for the metabolic needs of rapid cell division, as ATP levels are markedly depleted in stimulated *Atg7*$^{-/-}$ T cells, with some restoration of cell viability upon addition of exogenous methylpyruvate[229]. Autophagy may also promote T cell survival through degradation of proteins involved in apoptosis, such as caspase-8[230].

The potential importance of autophagy in the pathogenesis of autoimmune disease is illustrated by the observation that *Beclin1*$^{F/F}$*-CD4*$^{+}$-cre mice are completely resistant to experimental allergic encephalitis (EAE) induced by myelin oligodendrocyte glycoprotein (MOG) immunization[230].

1.4.2.2 Autophagy and B cells

In the bone marrow of an *Atg5*$^{-/-}$ *Rag*$^{-/-}$ chimeric mouse model, whilst there are normal numbers of pro- and pre-B-I cells, there is a substantial decrease in the proportion of B cells at the pre-B-II and immature stages of development)[232]. A *beclin-1*$^{-/-}$

Rag$^{-/-}$ chimera displays similar abnormalities[221]. As described **??**, the pro- and pre-B stages are when *Igh* locus recombination occurs. However, whilst total peripheral B cell numbers are decreased in these models, in a similar *Atg5*$^{-/-}$ chimera[223], and in an *Atg7*$^{F/F}$-*Vav*-Cre conditional knockout[233], there are normal proportions of transitional, follicular, and marginal zone B cells[232]. An *Atg5*$^{F/F}$-*CD19*-Cre conditional knockout has a subtler phenotype, with reductions only in mature B cells ($B220^{+}CD43^{-}IgM^{+}IgD^{+}$) (2-fold) and peritoneal B1a cells (5-fold) with otherwise normal peripheral B cell populations[232].

Examination of a beclin-1-GFP reporter mouse demonstrates a biphasic pattern of beclin-1 expression, with levels highest in pro-B cells, falling on transition to the pre-B stage[225]. Interestingly however, beclin-1-GFP levels were also higher in mature than transitional B cells. This pattern is similar to Bcl-2 expression[234], and may reflect the interaction between these proteins[91]. The dependency on autophagy for B1a survival is interesting, as these innate-like cells have unique properties, such as a long lifespan, the ability to self-renew, and constitutive production of 'natural' IgM[235]. They are also selected for self-reactivity, as natural IgM is important for clearance of apoptotic cells and other debris[236]. It is possible that autophagy is required for clearance of defective organelles or proteins that accumulate during the lifetime of these cells, or that it is important in survival during the positive selection events they undergo during their development.

TLR4 stimulation with LPS, or BCR ligation with anti-IgM induces autophagy in cultured and primary murine B cells[218;237;238], an effect attenuated by co-ligation of CD40. The signaling events that lead to activation of autophagy are unknown.

Beclin-1$^{-/-}$ B cells appear to proliferate normally in response to LPS and IL-4 stimulation[221]. However, this may not reflect a general phenotype of autophagy deficiency, as whilst *beclin-1*$^{-/-}$ T cells also proliferate normally, this is not the case for *Atg3*$^{-/-}$, *Atg5*$^{-/-}$, or *Atg7*$^{-/-}$ T cells.

Recently, autophagy has been demonstrated to be required for plasma cell development[238;239]. In both reports, *CD19*-Cre-*Atg5*$^{F/F}$ conditional knockout mice were studied. Autophagy was found to be activated following LPS stimulation of B cells *in vitro*, with a peak in LC3 turnover and GFP-LC3 fluorescence following 2 days of stimulation, with a decrease to basal levels by day 4[238]. *In vivo*, following immunization with NP-Ficoll, there were more GFP-LC3 punctae in plasmablasts and plasma cells than resting B cells. This is somewhat in opposition to the *in vit*SLE*ro* results, but may reflect differences in response to LPS compared with NP-Ficoll. Pengo *et al.* also found enhanced ER stress and UPR activation, and unexpectedly, increased antibody secretion from autophagy deficient plasma cells, which were, however, more prone to apoptosis than wild-type controls. They, as with Conway *et al.*, noted fewer bone marrow (BM) plasma cells in the *CD19*-Cre-*Atg5*$^{F/F}$ mice, and an attenuated response to immunization with both T-dependent (TD) and independent (TI) antigens. Autophagy deficiency in B cells was determined to be protective against experimental colitis. Neither group reported impairment of class switching or GC formation.

Autophagy is also important in antigen processing in B cells. Autophagosomes form constitutively in B cells[200], and induction of autophagy in B cell lines by serum starvation or in primary B cells by BCR ligation facilitates presentation of citrullinated hen egg lysozyme (HEL) to cognate T cells, which does not occur if autophagy is inhibited pharmacologically with 3-MA or by shRNA (short-hairpin RNA) antisense to *Atg5*[218].

Following BCR ligation, autophagy acts to recruit endosome localized-TLR9 to a larger signaling compartment where hyperactivation of p38 MAPK occurs[240]. This mechanism may account for the synergy observed with simultaneous BCR ligation and TLR9 activation[241] and is of potential significance in the pathogenesis of SLE.

1.5 Autophagy and its potential significance in the pathogenesis of SLE

1.5.1 Genetic association

GWAS of SLE have repeatedly highlighted variation at the *Atg5-PRDM1* locus as contributing towards disease risk. The *Atg5-PRDM1* locus on chromosome 6 includes the genes *Atg5*, which as discussed above is a critical component of the Atg5-Atg12-Atg16L1 complex, and *PRDM1*, which encodes Blimp-1, the master transcription factor of plasma cell development. Both genes therefore, are relevant candidates. The two genes are in linkage disequilibrium (LD), and whilst an initial study identified a risk SNP in an intron of *ATG5*, subsequent GWAS refine the association to the intergenic region, within a block of LD primarily encompassing *PRDM1*. Two studies have attempted to clarify which of the two genes is affected by the disease-associated variants. In the first, $CD4^+$ T cells and B cells were isolated from Chinese controls and patients based on their genotype for rs6937876, an intergenic SNP[242]. They found that in B cells, rs693SLE7876 was an expression quantitative trait locus (eQTL) for *Atg5* but not *PRDM1* mRNA. There was no effect in $CD4^+$ T cells. A second study examined monocytes, and conventional and plasmacytoid dendritic cells[243]. In this case, the intergenic risk SNP rs548234 reduced expression of *PRDM1*. However, *Atg5* expression was not quantified. The effects of variation in the *Atg5-PRDM1* locus are therefore complex and appear to be cell type specific.

Other autophagy-associated genes that have shown disease association in SLE GWAS include vesicle-associated membrane protein-7 (*VAMP7*), a protein involved in homotypic fusion of autophagosomes[244], and with a lesser degree of certainty *PIKFYVE*, which encodes phosphoinositide 5-kinase[245]. A candidate gene-based study in a Chinese population identified disease association with variants in *Atg7*

and *IRGM* (immunity related GTPase M)[242], the latter promoting autophagy through as yet not fully defined mechanisms[246].

1.5.2 Existing experimental work

1.5.2.1 Autophagy in SLE

To date, autophagy in SLE has been examined in two studies. In the first, Gros *et al.* quantified autophagy using western blotting of LC3 and electron microscopic imaging of autophagosomes in the $MRL_{lpr/lpr}$ and NZB/W $_{F1}$ mouse models[247]. They found activation of autophagy in thymocytes and peripheral T cells of disease model mice, but were unable to detect a difference in unstimulated B cells. They also found an increase in autophagy following stimulation of T cells with PMA and ionomycin, which was more pronounced in the NZB/W mice than controls. Intraperitoneal injection of LPS did, however, induce autophagy in the B cells of control mice. They also examined peripheral T cells ($CD4^+$ and $CD8^+$) from patients with SLE using electron microscopy, and found an increased number of autophagosomes in the disease patients compared with controls. Autophagic flux was not assessed.

The second study looked at larger cohort of SLE patients, and divided T cells by subset[248]. Using quantitative LC3 western blotting, they found no difference in autophagy in the total T cell pool, but autophagy was enhanced in the naïve $CD4^+$ population. B cells were not examined. They also found that treatment of healthy donor $CD4^+$ T cells with serum IgG from SLE patients induced autophagy, but that SLE patient cells were resistant to this phenomenon.

1.5.2.2 Autophagy and other autoimmune diseases

The most fully characterized role for autophagy in autoimmunity is in the pathogenesis of Crohn's disease. One of the major findings from GWAS in Crohn's disease

was an associated coding variant in *Atg16L1* (T300A)[249]. Mice deficient in Atg16L1 were demonstrated to have exaggerated macrophage production of IL-1β and IL-18 following LPS stimulation, to be more susceptible to dextran-induced colitis, and to have Paneth cell functional abnormalities[207;250]. In patients with the T300A risk allele, corresponding Paneth cell granule abnormalities were also noted[250].

Autophagy has also been implicated in rheumatoid arthritis, as a mediator of TNF-α induced cartilage damage[251]. Autophagy is activated in osteoclasts from mice with experimental arthritis, and joint damage is abrogated in TNF-α transgenic mice reconstituted with *Atg7*$^{-/-}$ bone marrow. Similarly, TNF-α treatment of synovial fibroblasts activates autophagy, and those cells from RA patients have increased basal autophagy[252]. As described above, peptide citrullination may occur as a consequence of autophagy in antigen presenting cells[218]. Anti-citrullinated peptide antibodies are a hallmark of RA, and it is therefore possible that autophagy may be a source of post-translationally modified novel auto-antigens that drive this disease[253].

In ankylosing spondylitis (AS), possession of the HLA-B27 allele is seen in the great majority of patients (90%)[254], but its role in disease pathogenesis is largely unknown[255]. One hypothesis is that HLA-B27 misfolding occurs in the ER, leading to UPR activation and cytokine release[256]. However, it has been demonstrated that in the gut of patient with AS, HLA-B27 misfolding leads to autophagy rather than UPR activation, and that inhibition of autophagy with 3-MA in isolated lamina propria cells reduces IL-23 secretion in response to LPS stimulation[257].

1.5.3 Rationale for investigating autophagy in SLE

As has been outlined above, there is considerable overlap between the functions identified for autophagy in immunity, and the pathogenesis of SLE (figure 1.4).

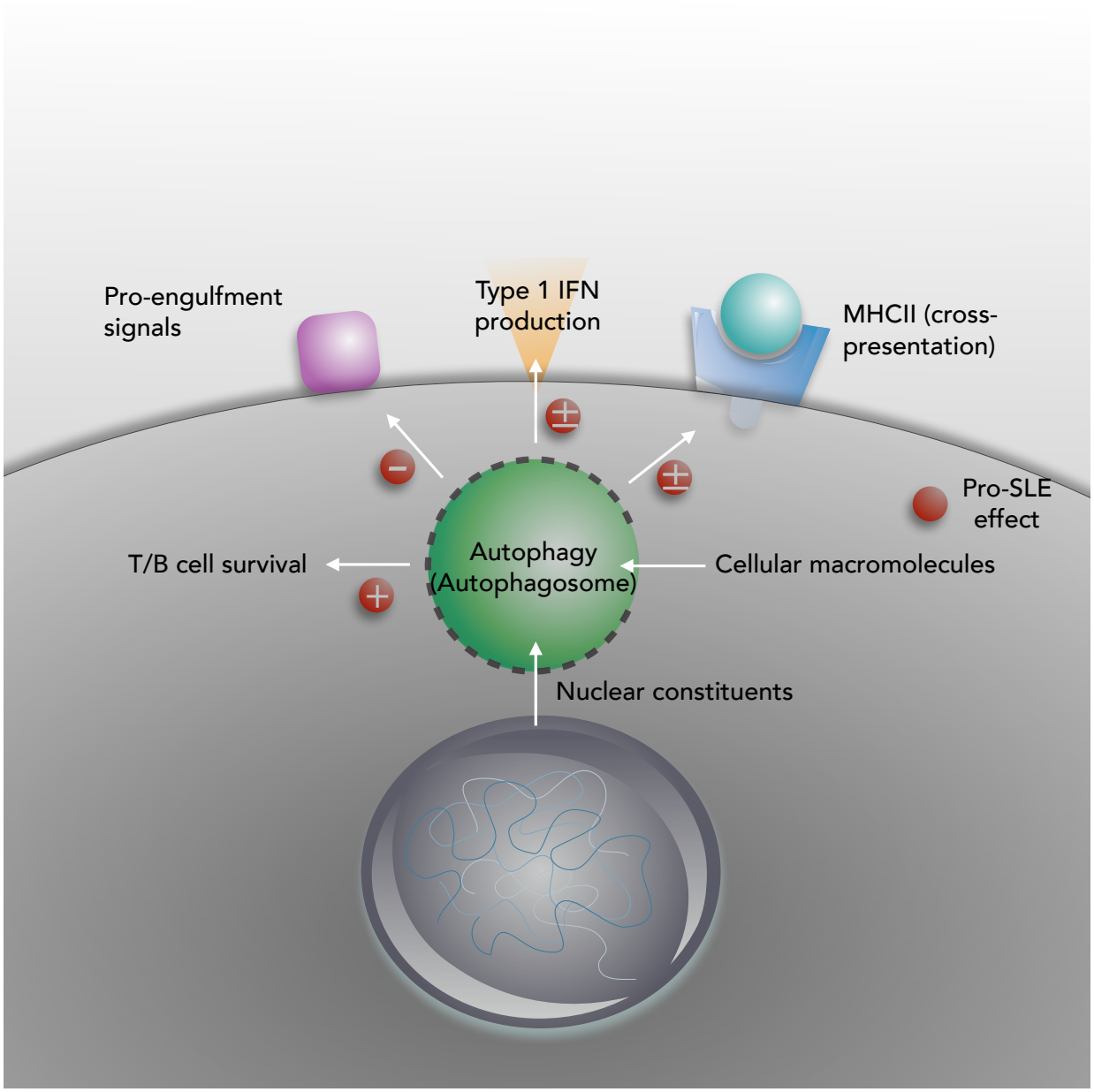

Figure 1.4: **Hypothesized role of autophagy in the pathogenesis of SLE**. Autophagy may lead to presentation of endogenous molecules on MHC-II, modulate type I IFN production, and enhance the survival of autoreactive immune cells. It may also influence the phagocytosis of apoptotic cells, leading to their recognition as foreign.

Innate immune signaling Autophagy has key roles in both the detection of nucleic acids, and also modulation of the subsequent response. Canonical autophagy has been demonstrated to be required for TLR7 signaling in pDC[204], and of particular note is that LAP is activated following Fc-γ receptor binding by immune complexes, with subsequent TLR9 signaling[206]. SLE is a type I IFN mediated disease, and autophagy may contribute to the excessive production and dysregulation of this key group of cytokines.

Survival of autoreactive cells SLE is characterised by a failure of immune tolerance mechanisms associated with the elimination of autoreactive immune cells. Given the role autophagy is known to play in cell survival, it may be enlisted as a mechanism to avoid homeostatic deletion of lymphocytes with self-reactive receptors.

Recognition of self As outlined above (1.4.1.3), autophagy is important in the presentation of endogenous molecules on MHC-II (cross presentation). This process may enhance the repertoire and density of self-antigens displayed, with the potential to incite autoimmunity.

1.5.4 Potential therapeutic considerations

Autophagy is modifiable by many existing pharmacologic agents, a significant number of which are approved in the US and EU for other indications. Table 1.5.4 lists some examples. One point of interest is that hydroxychloroquine, a standard medication for SLE, inhibits autophagy by pH neutralization of the lysosome, which therefore blocks autophagosome-lysosome fusion. Whilst it certainly has other modes of action, *e.g.* inhibition of endosomal TLR signaling, autophagy inhibition may a further important function. However, there are few drugs that modify autophagy

Activators	Inhibitors
Rapamycin	Hydroxychloroquine
Carbamazepine	3-Methyladenine
Lithium	Bafilomycin
Tamoxifen	Wortmannin

Table 1.2: **Pharmacological modifiers of autophagy**

without significant off-target effects. For example, whilst the autophagy-activator rapamycin is in clinical use as an immunosuppressant, mTOR inhibition has many other profound effects on protein synthesis and cell proliferation.

2 Methods

2.1 Cell culture

2.1.1 Cell lines

The following cell lines were used:

- GM12752 (EBV-transformed human lymphoblastoid cell line), (Coriell Institute for Medical Research, NJ, USA)
- Ramos RA-1 (human Burkitt's cell lymphoma line, CRL1596), (American Tissue Culture Collection, VA, USA)

Cells were passaged when a concentration of 1×10^6cells/ml was achieved.

2.1.2 Culture media and conditions

Cells were cultured in Roswell Park Memorial Institute-1640 media (RPMI-1640), (Invitrogen, UK) supplemented with 10% fetal bovine serum (FBS), 2mM L-glutamine, and 100U/ml penicillin/streptomycin (Invitrogen, UK), at 37°C and in 5% carbon dioxide.

2.1.3 Human peripheral blood mononuclear cell preparation

Blood was collected into tubes containing 1:10 sterile acid-citrate-dextrose anticoagulant (0.073g citric acid, 2.45g dextrose, 2.2g sodium citrate in 100ml water). Follow-

ing 1:1 dilution with phosphate buffered saline (PBS), blood was layered onto ficoll (Histopaque HybriMax-1077, Sigma, UK), and density gradient centrifugation was performed at 1600×g for 20 minutes at 21°C. Platelets were removed by centrifugation at 200×g in PBS supplemented with 0.5% bovine serum albumin (BSA), (Sigma, UK). Following separation, peripheral blood mononuclear cells (PBMC) were enumerated with a haemocytometer.

2.1.4 Murine splenocyte preparation

Spleens were mechanically dissociated by passage through a 70μm cell strainer (BD Biosciences, UK). Erythrocytes were lysed using hypotonic buffer (RBC lysis buffer, eBioscience, UK), and splenocytes were enumerated with a haemocytometer.

2.1.5 Magnetic cell separation

Human $CD19^+$ B cells were separated using negative selection (Human Untouched B Cell Kit, Invitrogen, UK). Briefly, PBMC were incubated with biotinylated antibodies against non-B cells, and then with streptavidin-conjugated magnetic microbeads. Magnetically labeled cells were subsequently separated in a magnetic field then discarded, and unlabeled B cells collected. Cell purity was checked using flow cytometry and found to be routinely >98%.

Murine B cells were also isolated using negative selection (Mouse Pan B Cell Kit, Miltenyi, Germany), using a protocol similar to that described above. Cell purity was routinely >98%.

2.1.6 Human cell stimulation

$CD19^+$ B cells were cultured at a density of 3×10^5/well in a 48-well cluster plate (BD Falcon, UK). For human plasmablast differentiation, B cells were stimulated with ODN2006 (5μM) (Invivogen, San Diego, USA), IL-10 (50ng/ml) and IL-15

(10ng/ml), (PeproTech, USA), and monoclonal mouse anti-CD40L (1µg/ml) (clone 82111, R&D Systems). Alternatively, human B cells were stimulated with goat anti-IgM F(ab´)2 fragment (5µg/ml) (Stratech, USA) and monoclonal mouse anti-CD40L (1µg/ml) (R&D Systems, USA).

2.1.7 Murine cell stimulation

Murine B cells were stimulated with lipopolysaccharide 10µg/ml (0111:B4) (Sigma, UK) and IL-4 (10ng/ml) (PeproTech, USA).

2.1.8 Inhibition of autophagy

Autophagy was inhibited by 3-methyladenine (5mM), bafilomycin A_1 (100nM), or chloroquine (10µM), all from Sigma, UK.

2.2 Patients

Patients were recruited at sites of King's Health Partners (St. Thomas' and King's College Hospitals) following informed consent and with London Multi-centre Ethics Committee approval (MREC 07/H0718/49). The mean age of the patients was 36, with a male:female (M:F) ratio of 0.12. Patients were excluded if they had received rituximab therapy within the last year, or intravenous methylprednisolone within the preceding month. SELENA-SLEDAI scores were calculated[258]. Healthy controls were recruited from King's College London. The mean age of the controls was 33 years, with a M:F ratio of 0.18. I found no statistical association between age or sex and autophagy measures in the control group. Patient characteristics are reported in table 8.1.

2.3 Mice

Female NZB/W F_1 (NZB/W) and C57BL/6 (B6) mice were obtained from Charles River, UK. *Atg7*$^{Flox/Flox}$ mice (a kind gift from Maasaki Komatsu, Tokyo Metropolitan Institute of Medical Science, Japan) were crossed with Vav-iCre mice (a kind gift from D. Kioussis, Medical Research Council National Institute for Medical Research, London, UK) to obtain Vav-iCre; Atg7$^{Flox/Flox}$. Male and female mice were used equally, and Vav-iCre-; Atg7$^{Flox/Flox}$ and Vav-iCre+; Atg7$^{Flox/WT}$ littermates were used as controls in comparative experiments. All mice were housed according to local institutional care policies and under license.

2.4 Flow cytometry

Flow cytometry was performed on Canto II or Fortessa instruments (BD). In longitudinal experiments, cytometer settings were standardized using Cytometer Setup and Tracking Beads (BD Biosciences), run before each acquisition.

2.4.1 Viability and surface immunophenotyping

Cell viability was assessed by staining either using either 1µl/ml Live/Dead Green (Invitrogen, UK), or Fixable Viability Dye 780 (eBioscience, UK), in 1ml PBS for 30 minutes at RT. Up to 1×10^6 cells were stained in 150µl buffer (PBS with 0.5% BSA). Fc receptors were first blocked for 10 minutes at 4°C with either Human Fc Receptor Inhibitor (eBioscience, UK), or anti-mouse CD16/32 ([clone 9], eBioscience, UK). Fluorochrome conjugated antibodies were then added, and the cells incubated for 20 minutes at 4°C, washed in 3ml PBS-BSA, and then resuspended in 250µl PBS-BSA for analysis.

Antibody target	Clone
CD19	HIB19
CD4	OKT4
CD27	O323
CD38	HIT2
IgD	IA6-2
CD14	M5E2

Table 2.1: **Antibodies used in surface immunophenotyping of human cells by flow cytometry**

Antibody target	Clone
CD19	6D5
CD4	RM4-5
CD23	B3B4
CD21	7E9
CD138	281-2
IgD	11-26c.2a
IgM	RMM-4
GL-7	GL-7

Table 2.2: **Antibodies used in surface immunophenotyping of murine cells by flow cytometry**

2.4.2 Annexin V staining

Annexin V staining was performed following surface staining, using recombinant annexin V-phycoerythrin (eBioscience, UK), in calcium and magnesium containing buffer (Annexin V staining buffer, [eBioscience, UK]), for 10 minutes at room temperature.

2.4.3 Intracellular staining for p62

$1{\times}10^6$ cells were Fc-blocked and surface stained as described in 2.4.1, then fixed in 4% paraformaldehyde (BD CytoFix, BD Biosciences) for 15 minutes at room tem-

Antibody target	Clone
Phospho-S6 (Ser235/6)	N7-548
Phospho-Akt (Ser473)	M89-61
Phospho-ERK1/2(Tyr204)	20-A
Phospho-IRS-1 (Tyr896)	K9-211
Phospho-p38 MAPK (Thr108/Tyr182)	36/p38
Phospho-Bcl-2 (Ser70)	N46-467
Isotype Control Mouse IgG1	MOPC-21

Table 2.3: **Antibodies used in phospho-epitope specific flow cytometry (PhosFlow)**

perature (RT). Cells were then washed in PBS, and then permeabilized and non-specific binding blocked by incubation in the saponin-containing BD Perm/Wash I (BD Biosciences, UK) for 15 minutes at RT. If secondary antibody staining was to be performed, cells were also blocked in 10% normal goat serum (eBioscience, UK) in Perm/Wash buffer for 30mins at RT.

Human cells were stained with mouse monoclonal anti-p62-Alexa Fluor 647 (1µg/ml) (MBL, Japan) for 1 hour at room temperature, in Perm/Wash buffer I. Mouse cells were incubated with monoclonal rabbit anti-p62 1:500 (clone D10E10, [Cell Signaling Technology, USA]), washed twice in Perm/Wash buffer, and then with DyLight 649-goat anti-rabbit secondary antibody (Abcam, UK).

Isotype controls used for intracellular staining were monoclonal mouse IgG1κ Alexa Fluor 647 (BioLegend) and monoclonal rabbit IgG XP® (clone DA1E, [Cell Signaling Technology, USA]), for human and murine samples respectively.

2.4.4 PhosFlow staining

Cells were prepared and stained as described in section 2.4.1. Following overnight storage at 4ºC in PBS, intracellular staining was performed. The anti-phospho-epitope antibodies used are listed in table 2.4.4 (all from BD Biosciences, UK).

2.4.5 CytoID staining

Up to 1×10^6 cells were incubated in complete RPMI medium at 37°C for 30 minutes in the presence of 0.25µl/ml Cyto-ID Green Autophagy Detection Reagent (Enzo, UK). Cells were subsequently analyzed by flow cytometry, with excitation using the 488nm laser. In some experiments, cells were fixed with 4% paraformaldehyde (BD CytoFix, BD Biosciences) for 15 minutes at room temperature following staining.

2.4.6 LysoID staining

Up to 1×10^6 cells were incubated in 500µL complete RPMI medium with 1µl/ml LysoID Red (Enzo, UK), at 37°C for 30 minutes. The cells were washed once in complete RPMI medium and then surface and intracellular staining was performed as described in 2.4.1 and 2.5. Laser excitation for flow cytometry was at 650nm.

2.4.7 MitoTracker staining

To prepare stock solutions of MitoTracker Green and Deep Red (both Invitrogen, UK) vials of lyophilized dye were diluted with 74 and 92µL of dimethyl sulfoxide (DMSO) respectively, to yield a 1mM concentration. For staining of cells, the stock solutions were diluted to 100nM in complete RPMI medium. 1×10^5 cells were incubated at 37°C in 500µl of the staining solution for 10 minutes, then washed twice in PBS-BSA, before analysis by flow cytometry, exciting MitoTracker Green using a 488nm laser, and MitoTracker Deep Red with a 650nm laser.

2.4.8 CFSE staining

A 5mM stock solution of carboxyfluorescein succinimidyl ester (CFSE) (eBioscience, UK) was prepared in DMSO. 1×10^5 cells were washed twice in PBS (without BSA) and stained with 500µL of a 10µM concentration solution of CFSE in PBS at room

temperature, in the dark, for 10 minutes. Labeling was then stopped by adding 3ml of cold full RPMI media (at 4°C), with incubation on ice for 5 minutes. Cells were then washed twice in PBS-BSA, and plated out for culture as appropriate.

2.5 Multispectral imaging flow cytometry

Up to 5×10^6 cells were used per sample. Cells were stained for viability with Fixable Viability Dye (eBioscience, UK), and then Fc receptors were blocked (mouse: anti-CD16/CD32 [clone 9]; human: Fc Receptor Binding Inhibitor, both from eBioscience, UK). Cells were surface stained using antibodies listed in tables 2.4.1 and 2.4.1, then fixed and permeabilized with the BD Fix/Perm kit I (BD Biosciences). For mouse cells, samples were blocked with 10% goat serum and then incubated with rabbit polyclonal anti-LC3 (Novus Bio, USA) diluted 1:400 in Perm/Wash I for 1 hour at 4°C, washed, and then with Alexa Fluor 488-goat anti-rabbit secondary antibody 1:500 (Invitrogen, UK).

For human cells, samples were incubated with mouse monoclonal anti-LC3-fluorescein isothiocyanate (FITC) 1:400 (Enzo Life Sciences, clone 2E6) and mouse monoclonal anti-active capase-3-PE (BD, clone C92-605) for 1 hour at 4°C, then washed twice. In all cases, cells were resuspended in 100µl PBS for analysis.

MIFC was performed on an Amnis ImageStream^X instrument.

Up to 1×10^5 images were acquired per sample. The 488nM laser was used at 120mW. Using the Bright Field channel, cells were gated on aspect ratio to include only singlets, and then the gradient root-mean-square feature to include focused cells. The cell surface was excluded using a mask (definition: erode 3) based on the bright field image. Alternatively, the Bright Detail Intensity (BDI) R3 algorithm was applied to the FITC channel.

For determination of $LC3^+$ punctae numbers, the Spot Count algorithm was used

following application of a Spot isolation mask (definition: bright, spot:background ratio 3, size 3).

For co-localization of organelles, following staining with LysoID (2.4.6) and anti-LC3 as described above, the Bright Detail Similarity (BDS) algorithm was applied. The BDS algorithm uses the log transformed Pearson's correlation co-efficient of bright details 3 pixels or less included in the masked area, from two input images.

All image analysis was using the Amnis IDEAS 6.0 software package.

2.6 Confocal microscopy

$1{\times}10^6$ Ramos cells were stained with 0.25 µl/ml Cyto-ID Green Autophagy Detection Reagent and 1 µl/ml Lyso-ID Red in 1× Assay buffer at 37°C for 15 minutes. Cells were mounted in SlowFade reagent (Invitrogen, UK). Microscopy was performed on a Nikon A1R Confocal microscope.

2.7 Protein analysis

2.7.1 Cell lysis

Cells were lysed in ice-cold radioimmunoprecipitation (RIPA) buffer (150 mM NaCl, 1.0% IGEPAL® CA-630, 0.5% sodium deoxycholate, 0.1% SDS, 50 mM Tris, pH 8.0 [Sigma, UK]), supplemented with protease and phosphatase inhibitors (Complete Mini and PhoSTOP, Roche, UK) for 15 minutes, then clarified by centrifugation at $10000{\times}g$ for 10 minutes

2.7.2 Protein quantification

To quantify protein concentration, the colorimetric bicinchoninic acid (BCA) assay was used (Thermo Scientific, UK). The BCA method quantifies reduction of copper

to the cuprous cation (Cu^+) by protein. A ratio of analyte to working reagent of 1:8 was used in a 96-well flat-bottomed microplate. Protein concentration was quantified by running an albumin standard curve. The plate was incubated at 37°C for 30 minutes, and read in a spectrophotometer at 495nm. Samples were assayed in triplicate, and the mean determined.

2.7.3 Immunoblotting

Twenty-five μg protein per well were heated in sample buffer (2% SDS, 50mM Tris pH 6.8, 10% glycerol, 10% mercaptoethanol) at 95°C for 5 minutes, then loaded into 3-15% Tris-Glycine gels (BioRad, UK). Recombinant Rainbow Marker (GE Amersham, UK) was used to determine protein size. Electrophoresis was performed in running buffer (25mM Tris, 250mM glycine pH 8.3, 0.1% SDS) until sufficient separation of protein bands was achieved. The gel was allowed to equilibrate in transfer buffer for 20 minutes (20% methanol, 25mM Tris, 250mM glycine). The protein contents of the gel were transferred onto PVDF (polyvinylidene fluoride [Immobilon P, Merck Millipore, UK]) membranes by wet electroblotting in transfer buffer. Following transfer, the membrane was briefly washed in methanol and allowed to air dry for 30 minutes before further use.

Membranes were blocked with 5% non-fat milk in Tris buffered saline (150mM NaCl, 50mM Tris) with 0.05% Tween-20 (TBS-T) or 2.5% BSA in TBS-T (for phosphoepitope immunodetection) for 1 hour at room temperature then probed overnight with either polyclonal rabbit anti-p62 1:40000 (MBL, Japan), rabbit polyclonal anti-LC3 1:4000 (Novus, UK), rabbit monoclonal anti-phospho-mTOR [Ser2448] 1:4000, anti-mTOR 1:4000, anti-phospho-4EBP1 [Thr37/46] 1:10000, or anti-β-actin 1:20000 (Cell Signaling Technology), all in blocking buffer. Membranes were then washed for 10 minutes × 3 in TBS-T, and then incubated with 1:40000 HRP-conjugated goat anti-rabbit secondary antibody in 2.5% BSA –TBS-T buffer at room temperature for

1 hour.

Blots were developed with Luminata Forte ECL (Merck Millipore, UK), and Fuji radiographic films.

2.7.4 ELISA

2.7.4.1 Murine immunoglobulin isotyping

Murine immunoglobulin subclasses were determined using the semi-quantitative Mouse Ig Isotyping Ready-Set-Go kit (eBioscience, UK). This assay detects IgM, IgA, IgG1, IgG2a, IgG2b, IgG3, and κ/λ chains. The assay was prepared by coating wells of a 96-well flat bottomed ELISA plate (Nunc, Denmark) with capture antibody diluted in 100µl per well of PBS, and incubating overnight at 4°C. Each well was washed twice with 400µl wash buffer (PBS with 0.05% Tween-20), and then blocked with 250µl blocking buffer (PBS with 1% Tween-20 and 10% BSA) for 2 hours at RT. The wells were washed twice with 400µl wash buffer, and 50µl per well of assay buffer (PBS with 1% Tween-20 and 10% BSA) was added. Fifty-µl of tissue culture supernatant was then added and the plate incubated for 1 hour at RT on a plate shaker. Wells were washed 4 times with 400µl wash buffer, and then 100µl detection antibody was added. The plate was again incubated for 1 hour at RT on a plate shaker, and then washed four times with 400µl wash buffer. One hundred-µl per well of tetramethylbenzidine (TMB) substrate was then added, and the plate incubated at RT for 15 minutes. Following substrate development, 100µl stop solution (2N H_2SO_4) was added, and the plate read at 450nm.

2.7.4.2 Phospho-AMPK

AMPK phosphorylated at Thr172 in B cell lysates was quantified using the Invitrogen AMPK [T172] ELISA kit (Invitrogen, UK). Cells were lysed as described in

2.7.1. Twenty-five μg protein made up to 100μl with diluent buffer was used per well of pre-coated strips. Samples were incubated for 2 hours at RT, then washed 4 times with 400μl wash buffer. Anti-AMPK (Thr172) antibody was then added, and the plate incubated for 1 hour at RT, followed by washing 4 times with 400μl wash buffer. The wells were incubated with anti-rabbit horseradish peroxidase (HRP) detection antibody for 30 minutes at RT, then washed 4 times with 400μl wash buffer. Stabilised chromogen was then added, and the plate incubated in the dark at RT for 30 minutes. One-hundred μl stop solution was added, and the plate read at 450nm. pAMPK concentration was determined using a standard curve calculated with pAMPK standards.

2.7.5 Luminex

Phosphorylated and total proteins were measured using antibody-capture fluorescent microspheres in a suspension array system. This methodology uses microspheres (beads) with individual fluorescent identity labels (addresses) that allows the assay to be multiplexed. The microspheres are conjugated to a capture antibody, and following binding of the target antigen, a secondary biotinylated detection antibody is used, and after the addition of streptavidin-phycoerythrin (SA-PE), the assay is read by a 96-well microplate format flow cytometer.

B cells were isolated and lysed as described in sections 2.1.5 and 2.7.1. Following quantification, 5μg of protein was assayed per well of a 96-well microplate. The following antibodies were used (all Bio-Rad BioPlex, UK):

The following control proteins were used (all Bio-Rad, UK):

The samples were mixed with the multiplexed coupled beads diluted in 50μl wash buffer per well, and incubated overnight at room temperature at 300rpm on a plate shaker, in the dark. The beads were then washed 3 times in 200μl of wash buffer with the aid of a magnetic frame, and 25μl of detection antibody diluted in

Phospho-epitope	Control
Phospho-GSK3-alpha/beta (Ser9/21)	Total GSK3
Phospho-Akt (Thr308)	Total Akt
Phospho-ERK1/2 (Thr202/Tyr204, Thr185/Tyr187)	Total ERK1/2
Phospho-p70-S6K (Thr421/Ser424)	Total p70-S6K
Phospho-p38 MAPK (Thr180/Tyr182)	Total p38 MAPK

Table 2.4: **Antibodies used in suspension array system (Luminex)**

Control protein	Pathway
Epidermal growth factor (EGF)-treated HEK293 cell lysate	Akt, GSK3, ERK1/2
Nerve growth factor-beta (NGF-beta)-treated PC12 cell lysate	p70-S6K
Phosphatase-treated HeLa	Negative control

Table 2.5: **Control proteins used in suspension array system (Luminex)**

its diluent was added to each well. The samples were then incubated at room temperature for 30min on a plate shaker at 300rpm. The plate was washed three times with 200µl wash buffer, and then 50µl of streptavidin-PE was added to each sample. The samples were incubated at room temperature for 10min on a plate shaker at 300rpm. The samples were washed three times with 200µl wash buffer, and then resuspended in 125µl resuspension buffer. Analysis was performed on a Luminex FlexMap 3D instrument (Luminex, US). Each sample was analyzed in duplicate.

2.8 Statistical analysis

Data were analyzed using GraphPad Prism 5.0 (GraphPad Software, US), or R 2.11 (The R Foundation for Statistical Computing, US). Data were tested for normality using the D'Agostino and Pearson omnibus normality test. The selected statistical test is shown in each figure legend.

3 Quantification of autophagy by flow cytometry

3.1 Introduction

Measurement of autophagy has been an area of intense interest over recent years, and has also generated controversy; consensus based guidelines endorsed by leaders in the field have emerged[21;259;260], but their length and breadth reflect the fact that no single methodology is universally applicable.

Most techniques detect autophagosome-associated LC3, either by immunoblotting, based the electrophoretic mobility shift seen when it is conjugated to PE (LC3-II), or by imaging autophagosomes, defined as $LC3^{+}$ punctae, through immunohistochemistry or following LC3-GFP transfection.

However, immunoblotting and conventional microscopy have the disadvantage that they are low-throughput, and cell population subset analysis is challenging. Furthermore, in a cross-sectional study, semi-quantitative immunoblotting typically yields high inter-experimental variability, and with microscopy it may be difficult to achieve statistical power with comparatively small sample sizes.

3.1.1 Multispectral imaging flow cytometry

The development of multispectral imaging flow cytometry (MIFC), which allows high-throughput imaging of single cells in flow, provides a potentially useful platform for quantifying autophagy and has already been utilized and evaluated for this purpose[261–263]. Cells of interest can be identified by conventional immunophenotyping based on fluorochrome-conjugated antibodies. For a longitudinal study of *ex vivo* immune cells, MIFC has notable advantages compared with *e.g.* immunoblotting, in that machine parameters can be standardized and maintained over time, and also dead or apoptotic cells, which may potentially be confounding, can be excluded from analysis by standard assays.

3.1.2 CytoID autophagosomotropic dye

Whilst dyes have been used previously to stain autophagosomes (*e.g.* acridine orange, LysoTracker Red, or monodansylcadaverine)[21], they have the major disadvantage that there is significant off-target staining of lysosomes, and high non-specific background staining[264]. Recently, a novel proprietary amphiphilic tracer dye, CytoID, has been introduced. Uptake of this dye has been shown to have good correlation with LC3-II levels, and there have been reports of negligible lysosomal staining[265–267]. CytoID may therefore provide a complementary methodology for assessing autophagy by flow cytometry.

3.2 Aims

In this chapter, I evaluate and confirm the utility of MIFC and CytoID for the quantification of autophagy.

3.3 Results

3.3.1 MIFC provides a functional, high-throughput means for quantifying autophagy

An Epstein-Barr virus transformed human B lymphoblastoid cell line (LCL) was selected for initial experiments. Following fixation and permeabilization, the cells were stained with monoclonal FITC-conjugated anti-LC3 antibody and data were acquired on an Amnis Imagestream^X instrument. As a positive control, cells were treated with the H^+ ATPase pump inhibitor bafilomycin A_1 for 18 hours to inhibit autophagy by blocking autophagosome-lysosome fusion, but thereby increase the number of $LC3^+$ autophagosomes. To inhibit autophagy, the class III PI3K inhibitor 3-MA was used.

Figures 3.1 and 3.2 show the gating strategy, and example images from this experiment. Two algorithms were evaluated: the Spot Count mask and the Bright Detail Intensity algorithm, both implemented within the platform specific application IDEAS 6.0.

Analysis was performed by selecting focused images of single cells, applying a mask to exclude the cell surface, and then, in the case of the Spot Count algorithm, using a further mask to define and count spots, based on size and threshold. Alternatively, the Bright Detail Intensity algorithm was used, which rather than using a user-defined mask to quantify spots, automatically subtracts the background signal from 'bright details' 3 pixels or less in diameter, and then quantifies their intensity. The final value from the BDI algorithm is the integrated sum of the brightness of all the isolated details in the mask area. Representative distributions from the BDI and Spot Count algorithms are illustrated in figure 3.1. Staining of cells with a FITC-conjugated isotype control antibody is shown in figure 3.3.

The distribution of BDI has a degree of left-skew, and therefore an empirical gate

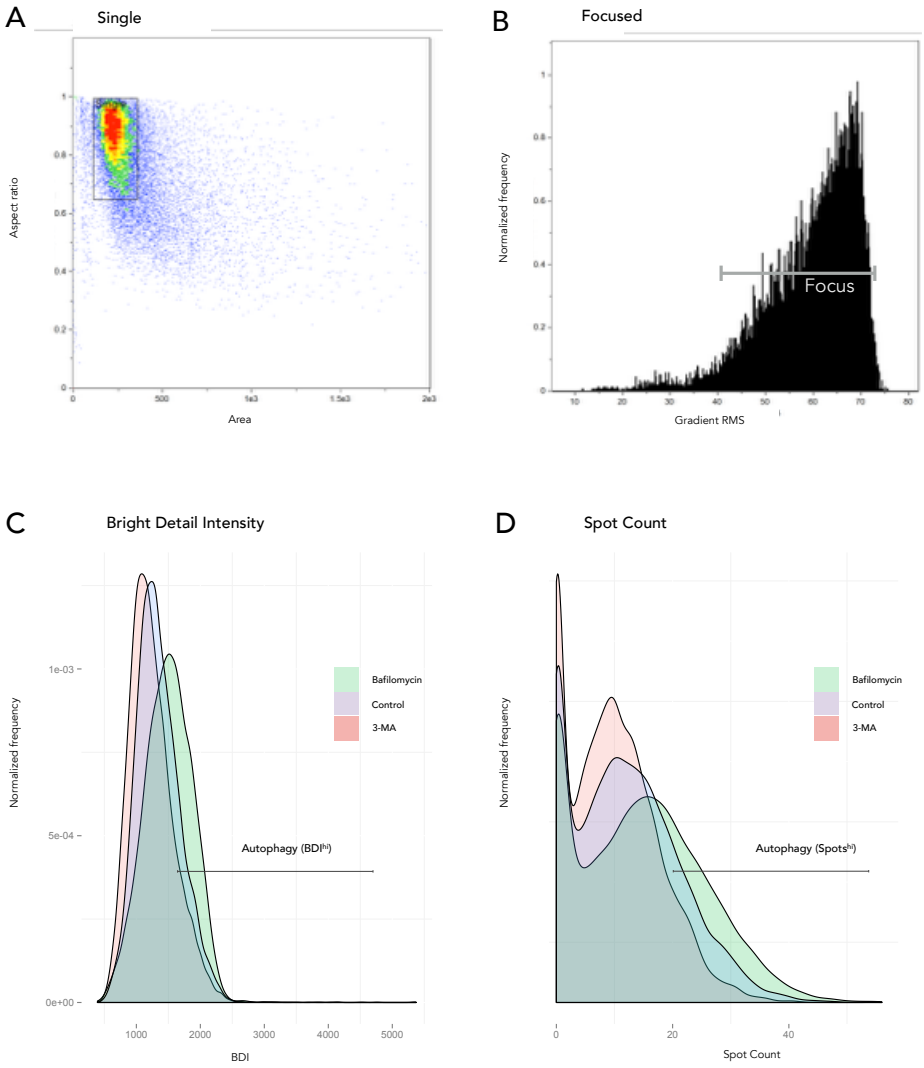

Figure 3.1: **Example MIFC gating and distributions**. **A**. Clumped cells were excluded from analysis by gating on aspect ratio and area. **B.** Focused cells were included based on the gradient root-mean-square feature of the bright field images. **C & D.** Example distributions of the BDI and Spot Count features following treatment of lymphoblastoid cells for 18 hours with 100nM bafilomycin A_1 or 5µM 3-methyladenine. Experiment performed twice with equivalent results.

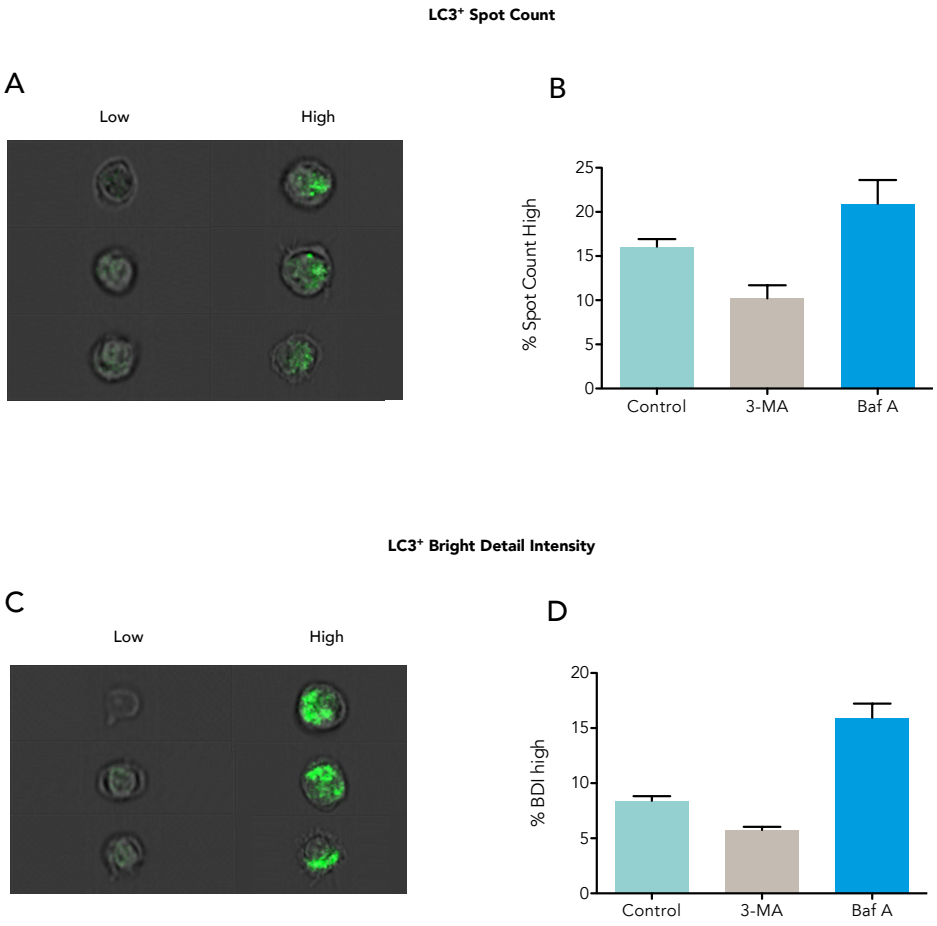

Figure 3.2: **Example MIFC images**. **A**. Representative images of lymphoblastoid cells from high and low quantiles of LC3-FITC Spot Count. **B**. Effect of *in vitro* pharmacologic increase (with bafilomycin 100nM) or decrease (with 3-methyladenine 5μM) of autophagosomes on Spot Count^{HI} population following 18 hours of culture. **C&D**. Equivalent data for Bright Detail Intensity^{HI} population. n=3 per group, $1{\times}10^4$ cells per sample. Images are merged Bright Field and FITC (LC3) channels. Experiment performed twice with equivalent results.

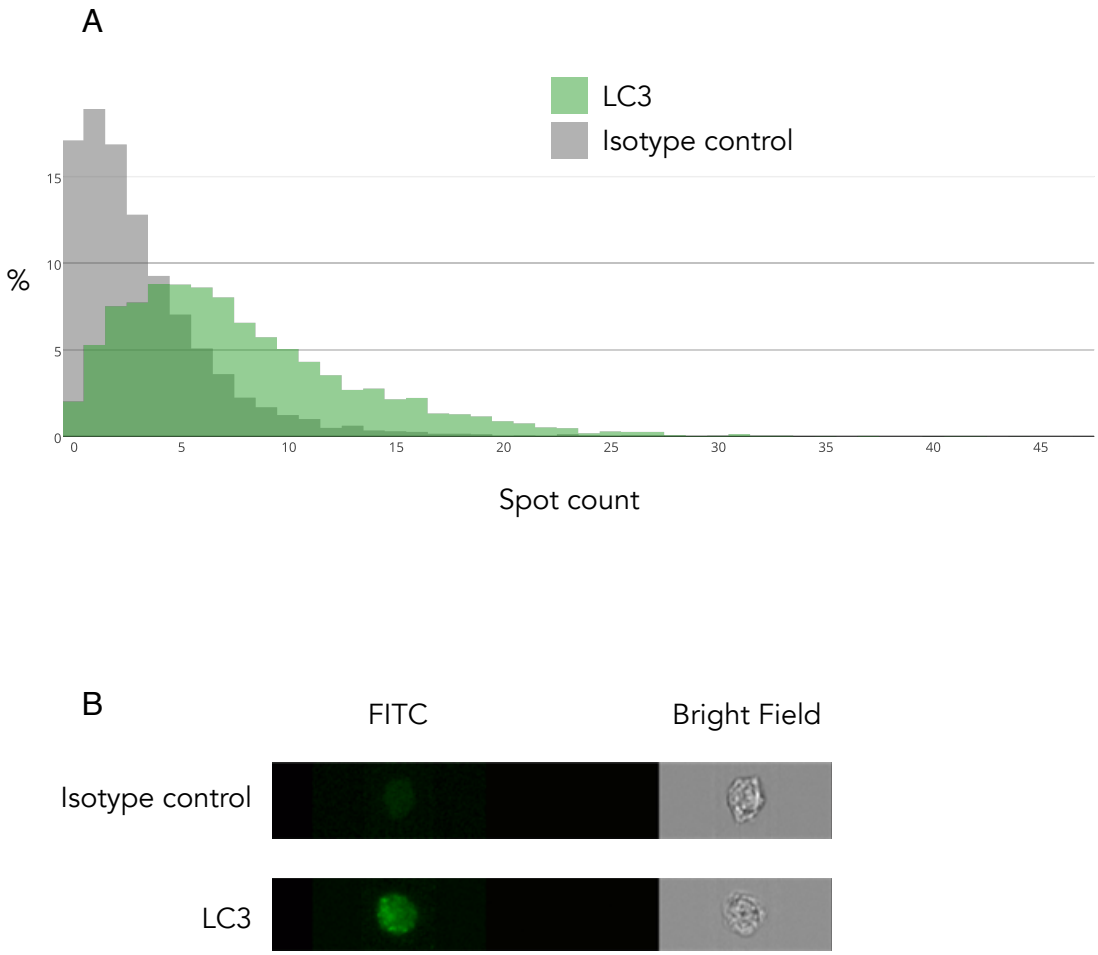

Figure 3.3: **Isotype control staining and distribution**. LCLs were stained with isotype control or FITC conjugated anti-LC3 antibody then analysed using the spot count algorithm. Example distributions (**A**) and images (**B**) are shown.

was placed on a reference control population histogram to include the highest 10% of BDI, which was classified as BDI^{HI}. The Spot Count distribution is bimodal, with a significant number of cells classified as having zero spots, with a secondary left-skewed distribution. Again, a gate was set empirically based on a reference control population to define Spot $Count^{HI}$ cells.

Both analytic modalities discriminated between LCLs treated with bafilomycin or 3-MA compared with untreated control cells.

3.3.2 CytoID has minimal off-target lysosomal staining and is suitable for flow cytometry

Next, to evaluate an alternative method of high-throughput quantification of autophagy, which, as with MIFC shares the inherent advantages of analysis by FACS, I performed experiments to determine the performance of CytoID dye.

Firstly, to confirm staining distinct from the lysosomal compartment – a disadvantage of alternative dyes, I performed confocal microscopy of cells from the Ramos B cell line co-stained with CytoID, and LysoID, a specific and well established lysosome tracer dye (figure 3.4). There was good distinction between autophagosomes and lysosomes. I next performed flow cytometry of LCLs treated with the mTOR inhibitor rapamycin for 18 hours to induce autophagy. There was a higher CytoID MFI in the rapamycin treated cells than in untreated control cells (figure (3.4)).

There was a moderate but statistically significant correlation between CytoID MFI and forward scatter (FSC) ($r=0.4$, $p<0.0001$), a laser deflection pattern in most circumstances proportional to cell size.

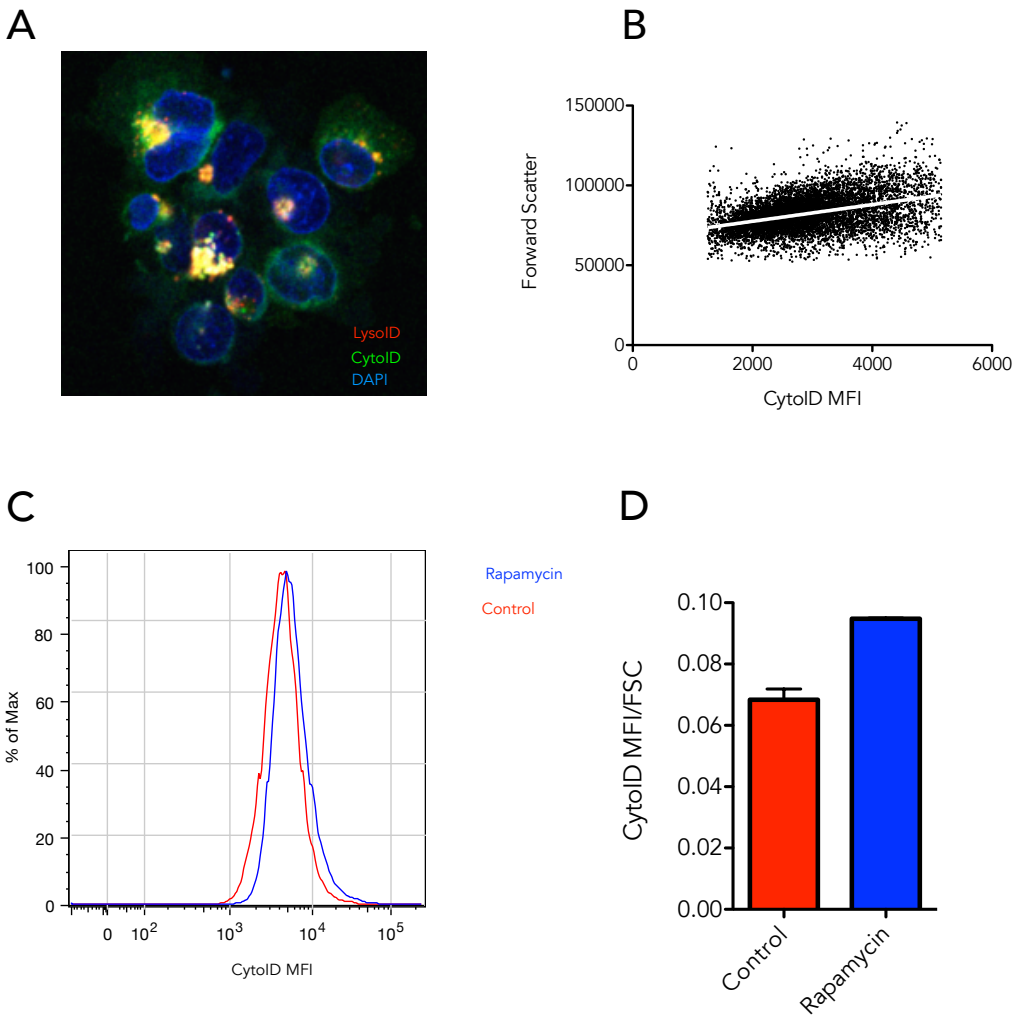

Figure 3.4: **Evaluation of CytoID dye**. **A**. Confocal microscope image of Ramos B cell line stained with LysoID (lysosomotropic) and CytoID (autophagosomotropic) dyes. **B**. Correlation between Forward Scatter and CytoID MFI in human PBMC. **C**. Example histograms of CytoID MFI from control and rapamycin treated LCLs (200nM rapamycin or control for 18 hours). **D**. CytoID MFI/FSC ratio in LCLs treated with 200nM rapamycin or control for 18 hours. n=3 wells per condition.

3.4 Discussion

In this chapter, I have confirmed that MIFC and CytoID represent practical modalities for the quantification of autophagy in further experiments. The utility of MIFC is due to the combination of easy collection of image data from large numbers of individual cells, providing statistical power, with the functional advantages of flow cytometry *e.g.* multiplex parameter measurement. Furthermore, the Amnis Imagestream^X instrument incorporates quality control routines that confirm instrument stability between experiments, making it suited to clinical longitudinal studies. Of the two algorithms assessed for further use, both discriminated well between cells in which autophagy had been induced or inhibited. I elected to use the Spot Count algorithm for further cell analysis, as it reproduced the widely used and reported LC3$^+$ punctum count.

CytoID dye demonstrated limited co-staining with LysoID by confocal microscopy, in keeping with manufacturer data and other reports in the literature[265–267]. Treatment with the autophagy activator rapamycin increased CytoID staining in LCLs, as would be expected. A significant question in the interpretation of CytoID fluorescence is the effect of cell size on non-specific signal. There was a moderate but highly statistically significant correlation between CytoID MFI and FSC (r=0.4). It is somewhat unclear to what extent this relationship can be considered as relevant to the choice of the optimum metric for the dye. However, as there may be significant differences in cell size within *e.g.* B cell subsets, the ratio between CytoID MFI and FSC has been chosen as the reported outcome variable.

CytoID is a particularly convenient method for quantification of autophagy, as staining is rapid and since total fluorescence is the measured parameter, it can be used with conventional FACS, which may allow a wider range of fluorochromes to be incorporated in the experimental design.

4 Assessment of autophagy in human SLE

4.1 Introduction

Whilst there have been studies exploring autophagy in SLE[247;248], they have only examined T cells in human disease. The results have been somewhat conflicting; one group noting activation of autophagy only in naïve $CD4^+$ and $CD8^+$ T cells, but not the whole T cell pool[248], whilst another found up-regulation in all $CD4^+$ T cells[247]. B cells, a major driver of the pathogenesis of SLE, and monocytes, have not been studied. In this chapter, I use the MIFC and autophagosomotropic dye assays described in chapter 4 to study *ex vivo* cells of patients with SLE, with focused attention on the B cell pool. I then explore the effects of varying stimulation on autophagy on human cells *in vitro*, and finally, attempt to determine the mechanism of autophagy activation in SLE.

4.2 Aims

In this series of experiments, I seek to determine if there is a difference in autophagy in B cells, $CD4^+$ T cells, and monocytes in patients with SLE compared to healthy controls, and to explore the potential mechanisms for my findings.

4.3 Results

4.3.1 Autophagy is increased in SLE patient B and CD4+ T cells compared with healthy controls

In the MIFC experiment, PBMCs from cases and controls were isolated and then stained for surface phenotype markers (CD19, CD4, and CD14), viability, and with anti-LC3 and active caspase-3 antibodies following permeabilization. An increase in apoptotic lymphocytes is observed in SLE[268], and so one further advantage of MIFC is that using anti-active caspase-3 antibody, apoptotic cells may be removed from the analysis, removing a potentially confounding variable.

To explore clinical parameters, and in particular to attempt to determine the existence of confounding due to immunosuppressive medication, disease activity (as measured by the SELENA-SLEDAI), C3/4, autoantibody status, and medication were recorded.

Figures 4.1 and 4.2 demonstrate the gating strategies used, example distributions, and images of $CD4^+$ T cells, $CD19^+$ B cells, and $CD14^+$ monocytes.

There were significantly more $CD19^+$ B cells and $CD4^+$ T cells with high numbers of autophagosomes ($LC3^+$ punctae) in the SLE patients compared with healthy controls. There was no difference however, in the $CD14^+$ monocytes (figure 4.3). Differential autophagy in B cells is a novel finding, and I therefore focused further experimental work on investigation of this observation.

The influence of clinical parameters on B cell autophagosome count was determined by univariate linear regression (table 4.3.1). First, correlation between SLEDAI score and autophagosome count was sought; there was a modest but significant association between these two parameters (r^2 0.2, p=0.03) (Table 4.3.1, Figure 4.4). Immunosuppressant medication, in particular corticosteroids and hydroxychloroquine, has the potential to modulate autophagy and therefore confound the re-

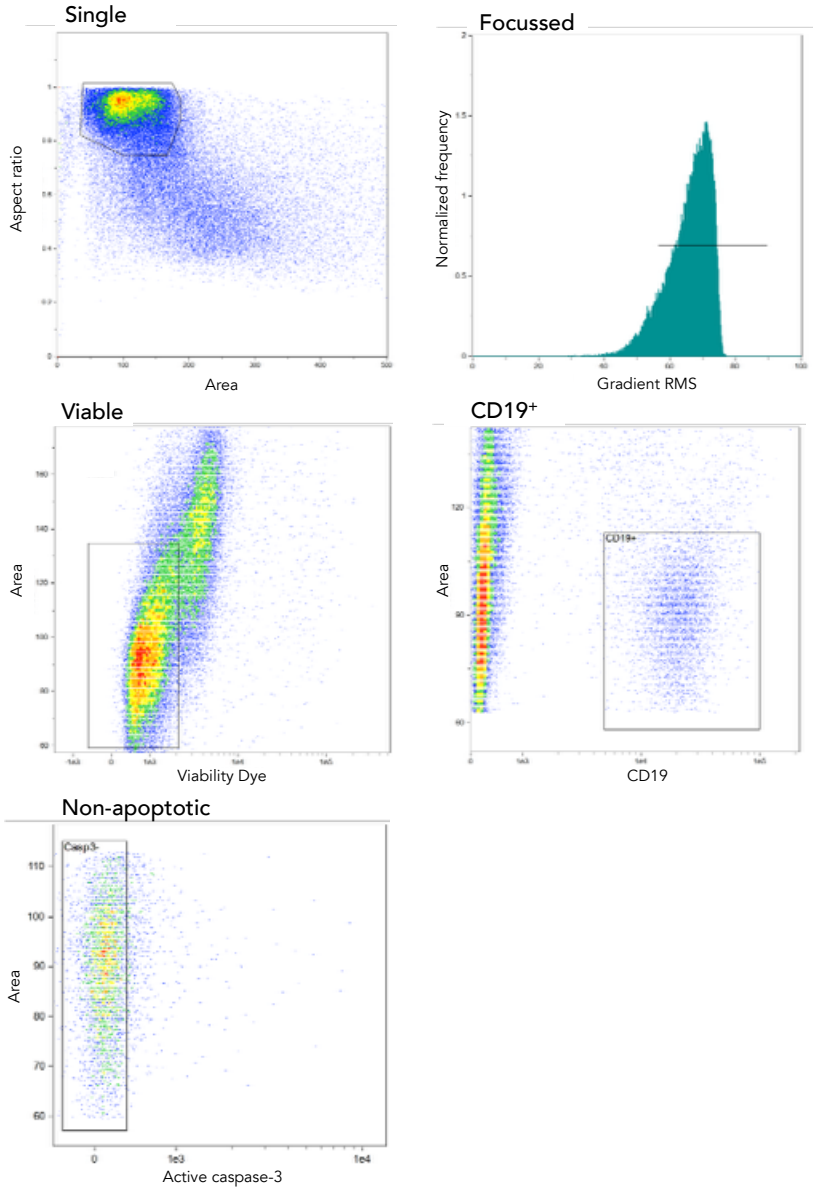

Figure 4.1: **Example MIFC gating strategy for B cells**. MIFC images of isolated human PBMCs were first acquired. Doublets and cell debris were excluded by gating on cell brightfield area and aspect ratio. Next, focused cells were selected by gating on cells exceeding a brightfield root-mean-square threshold. Viable cells were gated on the exclusion of a fixable viability dye, and then $CD19^{+}$, active caspase-3 low gates selected non-apoptotic B cells.

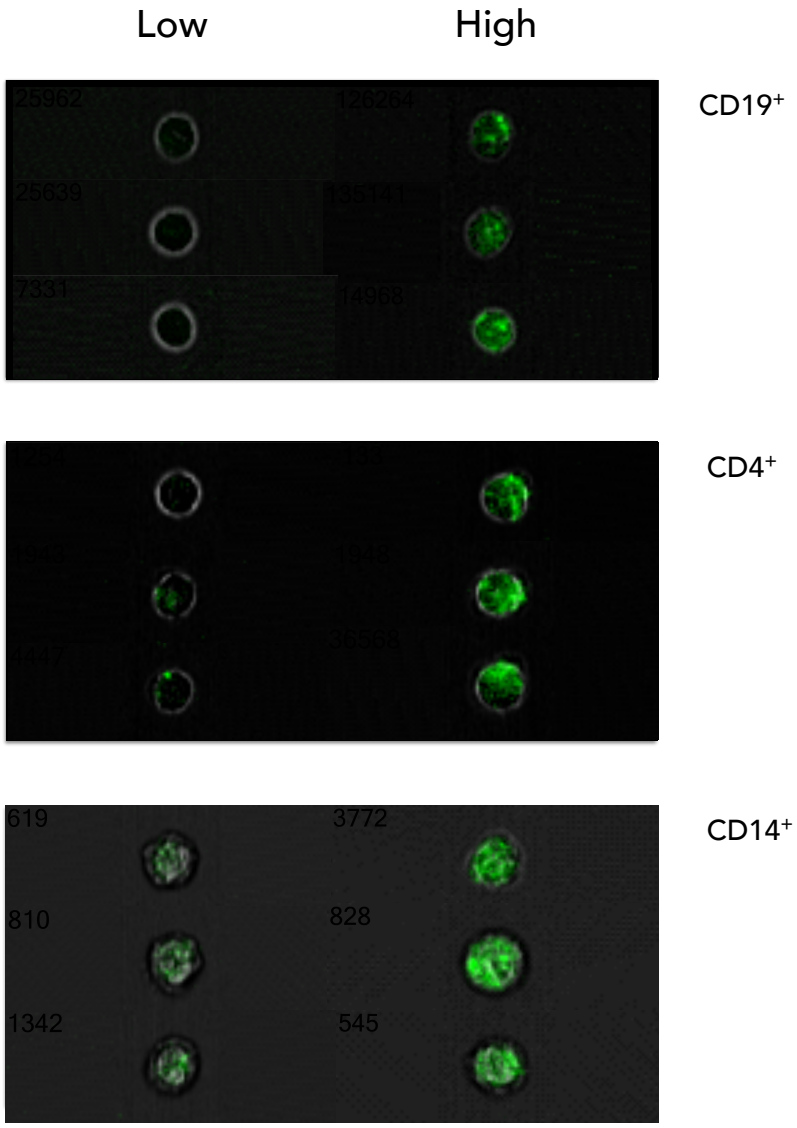

Figure 4.2: **Example images of CD19$^+$ B cells, CD4$^+$ T cells, and CD14$^+$ monocytes with high and low Spot Counts**. PBMCs were surface stained, then intracellular staining with LC3-FITC was performed. Following image acquisition and preliminary analysis as outlined in figure 4.1, the Spot Count algorithm was applied. High and low quantiles of Spot Count are shown.

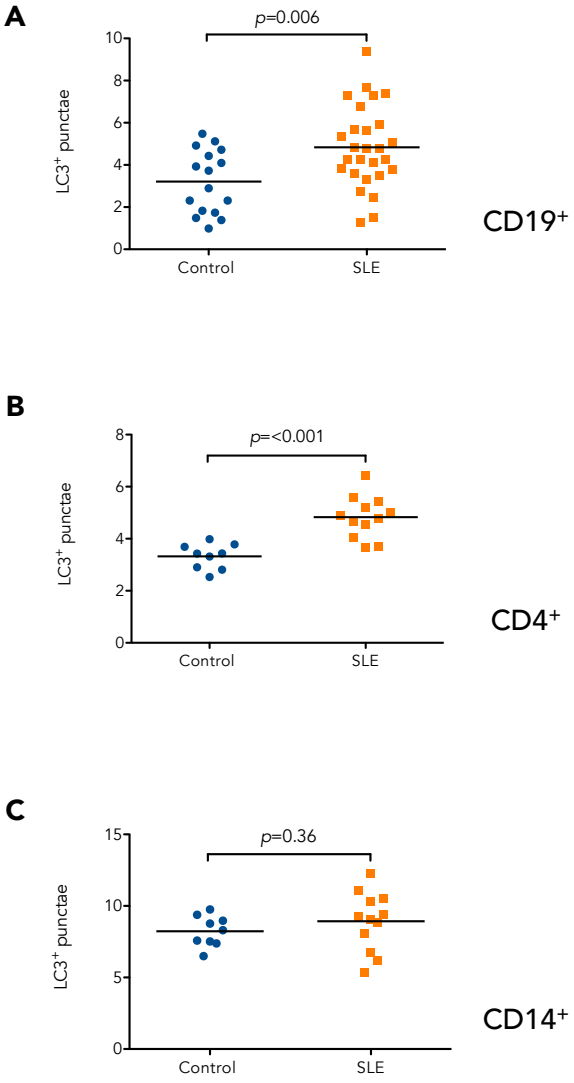

Figure 4.3: **Autophagosome density is increased in CD19$^+$ and CD4$^+$ T cells but not CD14$^+$ monocytes in SLE**. Each point represents one individual patient or control. The Spot Count (LC3$^+$ punctae) in **A**. CD19$^+$ B cells, **B**. CD4$^+$ T cells, **C**. CD14$^+$ monocytes as determined by MIFC is depicted. Student's unpaired *t* test used for comparisons.

Covariate	Beta-coefficient	Std Error	t value	r^2	*p*
SLEDAI score	1.95	0.85	2.30	0.20	**0.03**
Anti-dsDNA (0/1)	-0.26	5.04	-0.052	-	0.96
Anti-Ro (0/1)	6.27	4.749	1.32	-	0.2
Low C3/4 (0/1)	-0.90	4.90	-0.184	-	0.2
Anti-RNP/Sm (0/1)	-1.31	5.30	0.248	-	0.8

Table 4.1: **Univariate linear regression modeling of SLEDAI and laboratory parameters on B cell LC3$^+$ Spot Count**

Covariate	Beta-coefficient	Std Error	t value	r^2	*p*
Hydroxychloroquine (mg)	-0.008	0.014	-0.519	-	0.61
Prednisolone (mg)	0.2	0.3761	0.543	-	0.66
Azathioprine (mg)	0.018	0.047	0.424	-	068
Mycophenolate mofetil (mg)	-0.001	0.0034	-0.47	-	0.64

Table 4.2: **Univariate linear regression modeling of the effect of medication on B cell LC3$^+$ Spot Count**

sults[269;270]. However, there was no statistically significant correlation between medication and autophagy in the sample. There was also no association between anti-Ro, anti-RNP and anti-dsDNA antibodies, or low C3/4 and autophagy. However, these results should be interpreted with some caution, as the small sample size for regression analysis makes type II error likely. There were insufficient sample numbers for multivariate regression.

4.3.1.1 Autophagic flux is increased in SLE B cells

Standard techniques that quantify LC3-II, either by its electrophoretic mobility following SDS-PAGE and immunoblotting, or by visualization of autophagosomes, have the inherent limitation that they cannot quantify autophagic flux. Therefore, it has become accepted practice that cells are examined with and without an inhibitor of autophagosome degradation, typically one that prevents fusion with the lysosome, such as chloroquine or bafilomycin A_1, or inhibits lysosomal proteases,

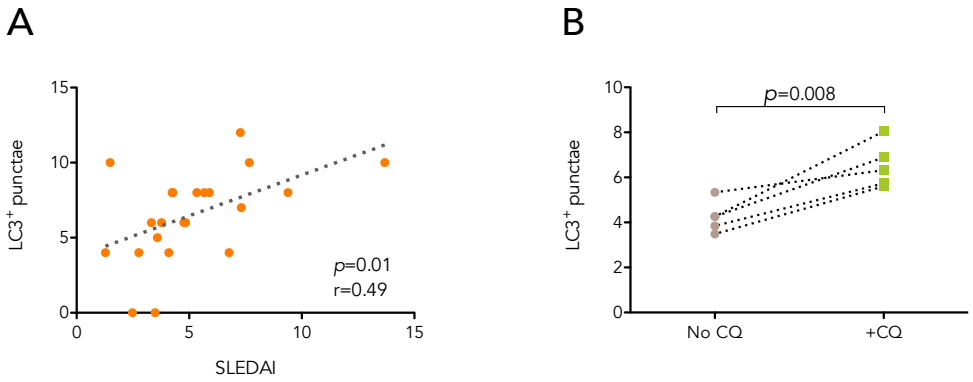

Figure 4.4: **A. Correlation between SLEDAI and B cell autophagy**. **B. Autophagic flux assay**. Isolated CD19$^+$ B cells from patients with SLE were incubated in complete RPMI media with 20μM chloroquine for 4 hours, and then LC3$^+$ Spot Count determined using MIFC. Pearson's correlation coefficient used in A. Paired student's *t* test used in B.

e.g. pepstatin/leupeptin. Accumulation of autophagosomes or LC3-II with the addition of the clearance inhibitor indicates active flux, whereas no increase suggests a clearance defect.

To examine autophagic flux in SLE B cells, CD19$^+$ cells were isolated, and incubated in complete RPMI with and without 20μM chloroquine for 2 hours (figure 4.4). Active flux was confirmed by an increase in the LC3$^+$ Spot Count following this period.

An alternative technique to infer active autophagic flux is to directly observe fusion of autophagosomes with lysosomes by microscopy. Co-localization of autophagosome (typically LC3) and lysosomal markers (*e.g.* lysosomal-associated membrane protein-1 [LAMP-1], or a lysosomotropic dye) is taken to represent flux, whereas lack of spatial association implies a defect in terminal fusion. Recently, it has been demonstrated that MIFC may be used to measure this co-localization in a high-throughput manner[263], and I therefore utilized this established protocol

to examine autophagic flux in the B cells of a group of SLE patients and healthy controls.

To quantify co-localization, the Bright Detail Similarity algorithm implemented in Amnis IDEAS 6.0 was used. The BDS algorithm computes the log-transformed Pearson's correlation co-efficient between 'bright details' 3 pixels or less in diameter from two image channels. To identify autophagosomes, LC3-FITC intracellular staining was used as described above. Lysosomes were marked with the lysosomotropic dye LysoID. Examples of B cells with low and high levels of BDS are shown in figure 4.5. I found no impairment of lysosome-autophagosome fusion in SLE compared with healthy controls in a limited sample size.

4.3.1.2 B cell subset analysis with CytoID

To confirm the observations made using MIFC, I employed CytoID staining to quantify autophagosome density in B cell subsets. In accordance with the results seen using MIFC, there was higher CytoID fluorescence in the SLE patient B cells than the healthy controls. B cells subsets were defined as naïve ($CD27^{+}$, IgD^{+}), memory ($CD27^{+}$, IgD^{-}), and plasmablast ($CD27^{++}$, IgD^{-}), based on their expression of the TNF-superfamily receptor CD27, and IgD. I found that autophagosome density was differentially higher in the naïve subset, compared with the memory and plasmablast subsets in patients with SLE compared with healthy controls (figure 4.6).

4.3.1.3 p62 levels are lower in naïve and memory B cell subsets in SLE

An alternative method for quantifying autophagic flux is to measure the levels of autophagy substrate proteins, whose level decreases with increased autophagic activity. One typically used such protein is p62, which serves as an autophagosome adapter protein, and which is degraded primarily by autophagy. In order to allow

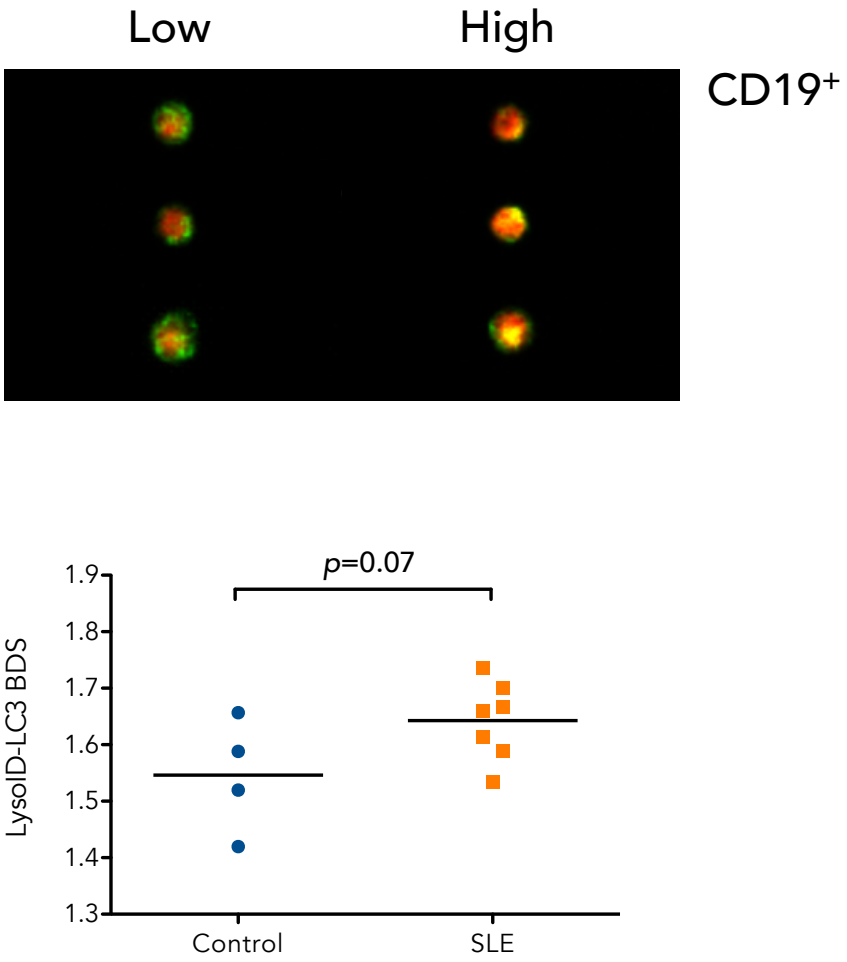

Figure 4.5: **Active autophagosome-lysosome fusion in SLE**. Examples of $CD19^+$ B cells with high and low levels of spatial correlation between LC3 (green) and lysosomes (red). Mann-Whitney U test used.

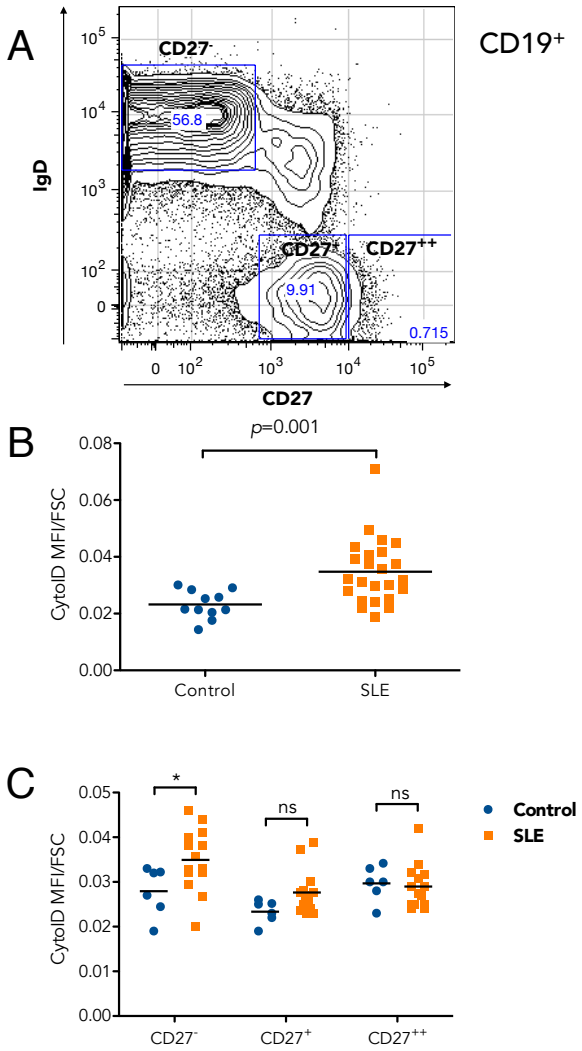

Figure 4.6: **Analysis of autophagy in B cells with CytoID**. **A**. Gating strategy for naive ($CD19^+CD27^-IgD^+$), memory ($CD19^+CD27^+IgD^-$) and plasmablast ($CD19^+CD27^{++}IgD^-$) B cells. **B**. CytoID uptake is significantly increased in SLE *vs.* healthy controls. **C**. Differential autophagy between SLE and controls is maximal in the naive subset. B. Mann-Whitney U test used. C. ANOVA, *p<0.05

convenient longitudinal data collection in B cell subsets, I employed intracellular FACS using a monoclonal, fluorochrome conjugated anti-p62 antibody (figure 4.7). These results mirrored those seen in the CytoID experiment; decreased p62 levels in the naïve and memory B cell subsets in SLE compared with healthy controls (figure 4.8). Notably, whilst p62 levels were lower in B cells, there was no significant difference in $CD4^+$ T cells.

This experiment, in conjunction with the flux inhibitor results described above, is highly indicative of intact autophagic flux in SLE B cells.

4.3.2 Autophagy is downregulated in B cells *in vitro* as stimulatory support is increased

The results presented above indicate that autophagy is activated in SLE, but the relevance of this finding is not clear. It may represent either cell stimulation, or be a means to resist cell death. To start to elucidate this question, I cultured *ex vivo* B cells from healthy donors with additive combinations of stimuli, and assessed activation of autophagy using CytoID uptake.

I found that autophagy substantially increased following 24 hours of culture compared with baseline, but that the activation of autophagy was abrogated in an additive fashion with anti-IgM, anti-CD40, and interferon-α treatment (figure 4.9). This observation mirrors an increase in apoptosis enumerated by annexin V binding, which is suppressed by anti-IgM treatment (figure 4.10).

Interestingly, on a single cell level, there appeared to be a degree of mutual exclusivity between autophagy and apoptosis, with autophagy much diminished in annexin V^+ cells. This may be expected given their reciprocal relationship, mediated at least in part by the interaction between Bcl-2 and beclin-1[91]. The association between activation of autophagy and cell death is highlighted by a strong inverse correlation between the extent of CytoID uptake and cell viability, assessed by the

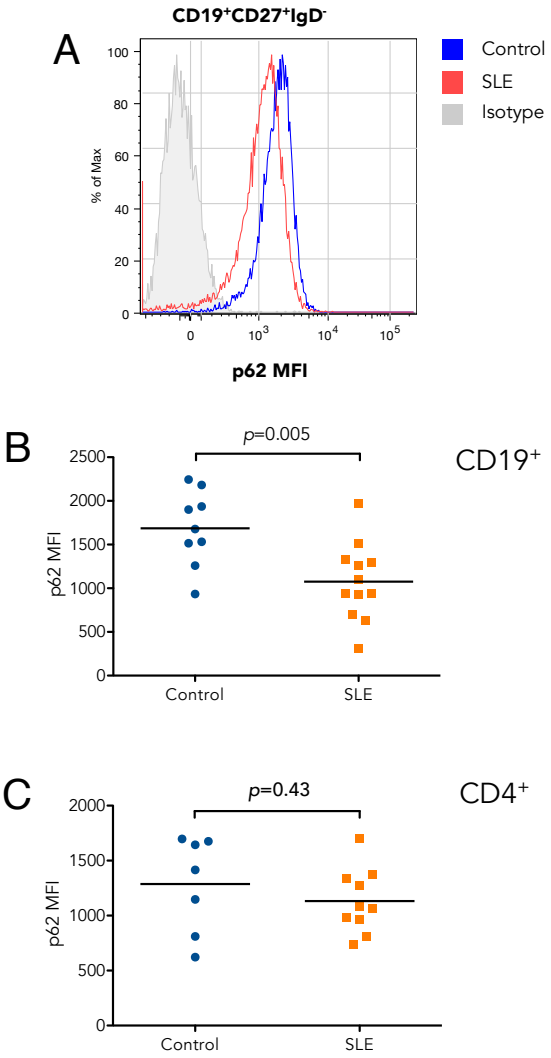

Figure 4.7: **p62 levels in SLE and healthy control lymphocytes**. **A**. Example distributions of p62 MFI in SLE and controls. **B&C**. p62 MFI is lower in $CD19^+$ B cells from patients with SLE compared with controls, but not in $CD4^+$ T cells. B. Unpaired *t* test used, C. Mann-Whitney U test used.

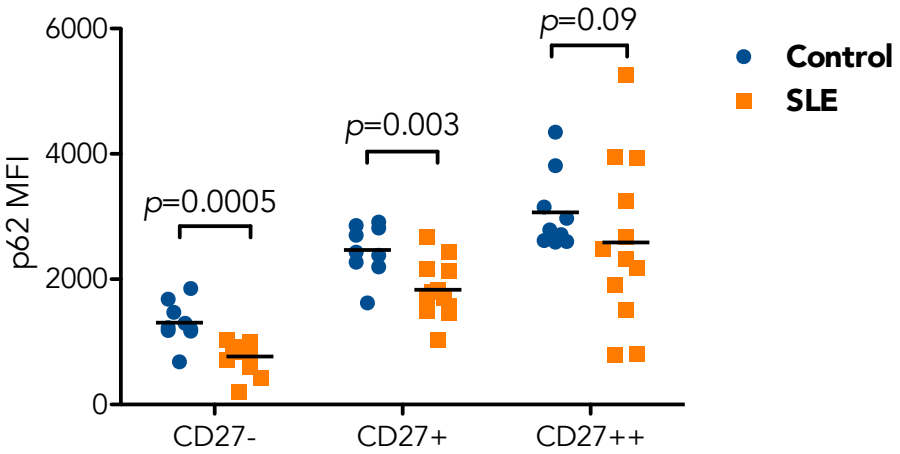

Figure 4.8: **p62 levels in B cell subsets**. p62 levels are lowest in the naïve B cell subset, followed by memory B cells. There was no statistically significant difference observed in plasmablasts. Pairwise comparisons between SLE and controls made by preplanned, unpaired *t* test. Unadjusted *p* value shown.

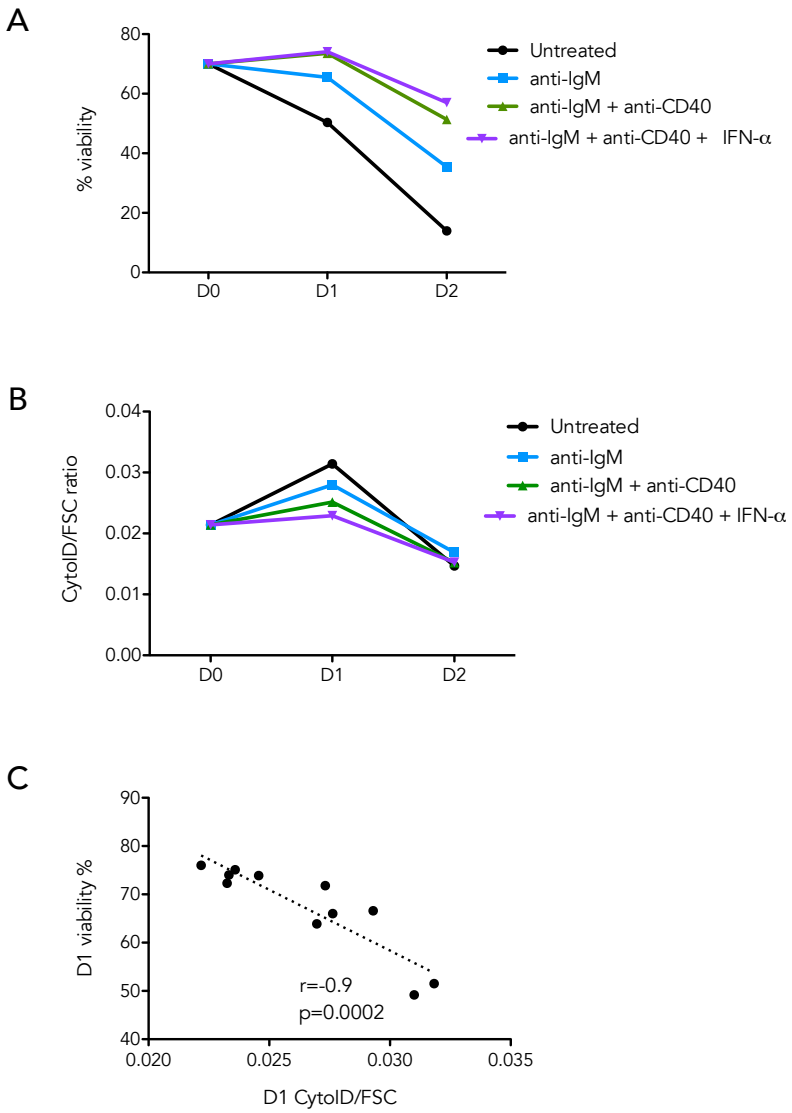

Figure 4.9: **Autophagy *in vitro* following B cell stimulation**. **A**. Human B cells were isolated and stimulated with combinations of anti-IgM, anti-CD40, and interferon-α for up to 48 hours, then viability determined by exclusion of fixable viability dye. **B**. CytoID staining for the experiment described in A. **C**. Correlation between cell viability and CytoID uptake after 24 hours of culture. n=3 per treatment condition, representative experiment shown, repeated in triplicate. C. Pearson's correlation used.

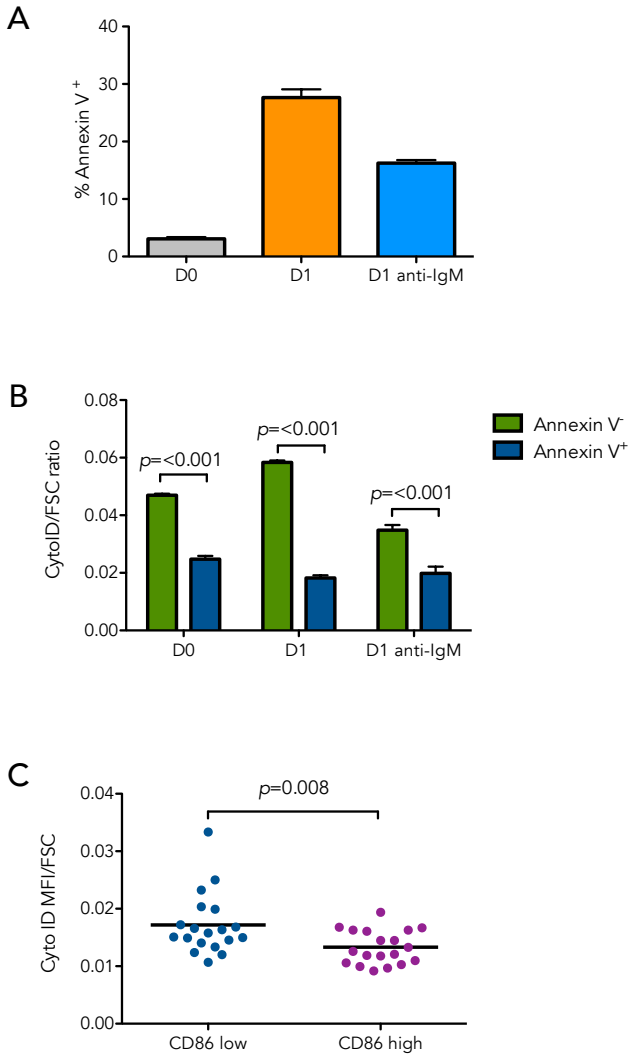

Figure 4.10: ***In vitro* relationship between autophagy, apoptosis, and cell activation in B cells**. **A**. Apoptosis was determined by annexin V-phycoerythrin staining in B cells stimulated with anti-IgM for 24 hours. **B**. Co-staining with CytoID and annexin V-phycoerythrin. **C**. CytoID uptake in CD86 low or high cells. n=3 per treatment condition, representative experiment shown, repeated in triplicate, except C, which includes data from multiple wells in 3 separate experiments. B. Preplanned unpaired *t* test used for pairwise comparisons; C. unpaired *t* test used.

exclusion of a vital dye (figure 4.9). A potentially analogous result is that CytoID uptake was significantly increased in B cells with high levels of the co-stimulatory molecule CD86. CD86 is up-regulated in antigen presenting cells following their activation, and this finding suggests that autophagy is reduced in cells that are likely to have received sufficient survival signaling to avoid cell death.

4.3.2.1 mTOR is activated following B cell stimulation

Using the stimulation and culture conditions described in the preceding experiment, I examined the phosphorylation status of mTOR (at Ser2448) and 4E-BP1 (Thr37/46) in *ex vivo* B cells from healthy donors, using immunoblotting. Phosphorylation of mTOR at Ser2448 by S6K leads to mTOR activation[271]. 4E-BP1 phosphorylation by mTORC1 releases it from the mRNA cap binding protein eukaryotic initiation factor-4E (eIF4E), allowing initiation of protein translation[272]. I found that mTOR and 4E-BP1 were increasingly phosphorylated with anti-IgM and anti-CD40 stimulation, following culture for 24 hours (figure 4.11). Untreated cells had the lowest level of mTOR and 4E-BP1 phosphorylation, commensurate with the observation that autophagy is maximally activated in the absence of survival signals.

4.3.3 Pathways regulating autophagy in human SLE

Finally, to attempt to determine the underlying basis for activation of autophagy in SLE B cells, I analyzed the phosphorylation state of key signaling proteins relevant to the regulation of autophagy using flow cytometry, antibody coated bead array (Luminex), and a phospho-specific AMPK ELISA.

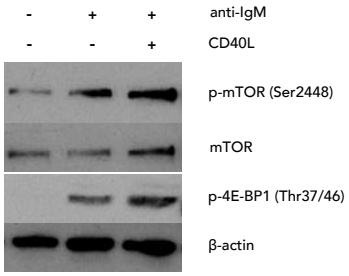

Figure 4.11: **mTOR is activated following B cell stimulation *in vitro***. Healthy B cells were stimulated with goat anti-IgM F(ab´)2 fragment (5µg/ml) and monoclonal mouse anti-CD40 (1µg/ml) for 24 hours, then lysed in the presence of phosphatase inhibitors. Immunoblotting was then performed with the indicated antibodies. Experiment representative of two independent replicates.

4.3.3.1 Phospho-epitope specific flow cytometric analysis of protein phophorylation

For the flow cytometric assay, PBMCs from patients with SLE and healthy controls were isolated, and surface stained to discriminate between naïve, memory, and plasmablast B cell subsets, then intracellular staining using phospho-specific antibodies was performed.

Using the phospho-specific antibodies in table 4.3.3.1, I found no statistically significant difference between the B cells of patients with SLE and healthy controls, in either in the total B cell pool, or by subset (figure 4.12), albeit in small sample sizes.

4.3.3.2 Phospho-AMPK ELISA

Next, I assessed the phosphorylation status of AMPK at Thr172, in total B cell lysates, using a phospho-specific ELISA. AMPK is phosphorylated by LKB1 at Thr172 in response to an increase in intracellular AMP and ADP, with decreasing ATP[61]. Phosphorylation at Thr172 activates AMPK, which may then subsequently phosphorylate ULK1 and thereby induce autophagy[5]. The antibody used in the ELISA is specific for AMPK phosphorylated at Thr172. I found no significant difference in Thr172 phosphorylation in SLE patients compared with controls (figure 4.13). The level of optical density was very low in both groups.

4.3.3.3 Luminex assay of protein phosphorylation

To quantify phosphorylation of proteins with the potential to regulate autophagy in B cell lysates treated with phosphatase inhibitors, I employed a magnetic-bead coupled Luminex panel to measure the phosphoproteins listed in table 4.4. In addition to the phosphorylated protein, the total unphosphorylated protein was also measured, allowing the calculation of a ratio of phosphorylated to total protein. Using

Antibody target	Summary	Effect of phosphorylation on autophagy
Phospho-S6K1 (Ser235/6)	Human ribosomal protein S6 peptide. Phosphorylated by p70-S6K, an effector of cellular growth and a target of mTOR signaling	Downregulates
Phospho-Akt (Ser473)	Phosphorylated under growth conditions following PI3K signaling. Promotes cell survival by phosphorylating and inactivating Bad. A target of mTORC2	Downregulates
Phospho-ERK1/2 (Tyr204)	MAPK family members. Phosphorylated in response to growth stimuli. Inhibits autophagy via TFEB	Downregulates
Phospho-IRS-1 (Tyr896)	Insulin receptor substrate protein-1. Major target of insulin and insulin growth factor (IGF-1) signaling	Downregulates
Phospho-p38 MAPK (Thr108/Tyr182)	Responds to inflammatory cytokine signaling and cell stress. Major signaling kinase	Upregulates
Phospho-Bcl-2 (Ser70)	Phosphorylation of Bcl-2 leads to dissociation of Beclin-1 and activation of autophagy[273]	Upregulates

Table 4.3: **Signaling pathways analyzed using PhosFlow**

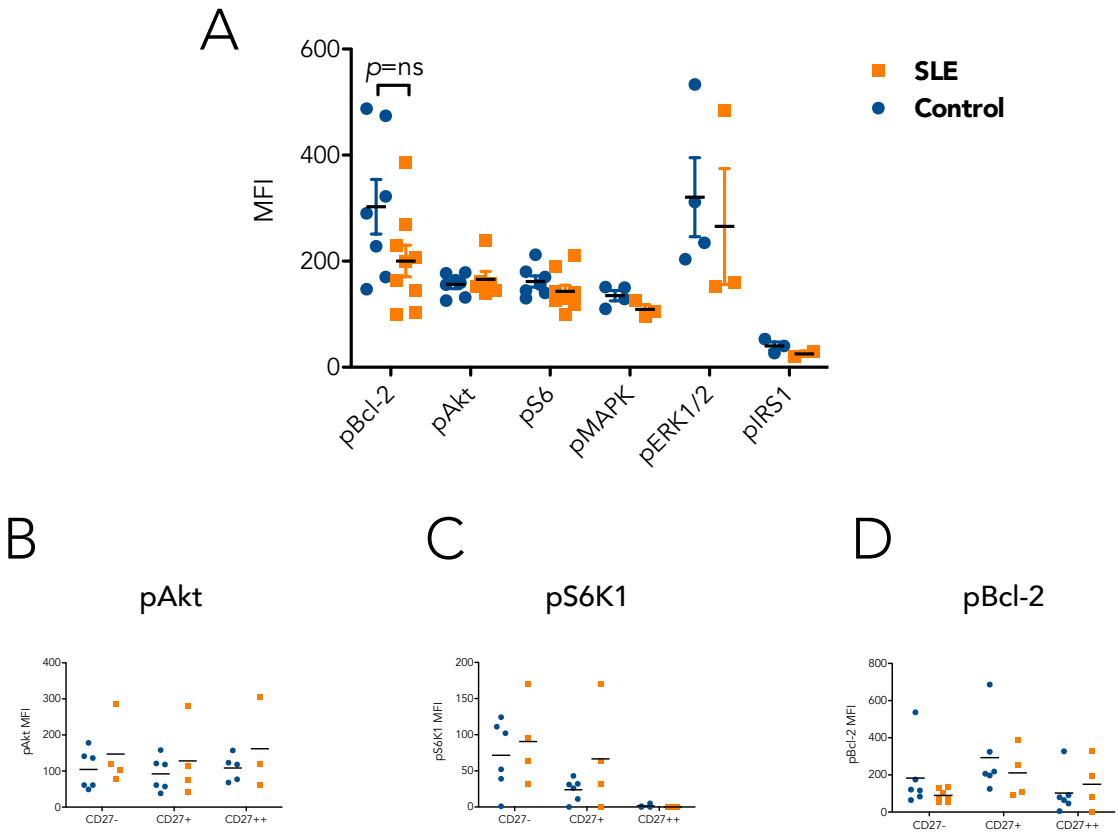

Figure 4.12: **Analysis of signaling in SLE *vs.* healthy control B cells by PhosFlow**. **A**. The total $CD19^+$ B cell pool was analyzed for the phosphorylated proteins listed in table 4.3.3.1. **B-D**. B cell subset specific analysis of phospho-Akt (Ser473) (**B**), phospho-S6K1 (Ser235/6) (**C**), and phospho-Bcl-2 (Ser70) (**D**) in $CD19^+CD27^-$ naïve, $CD19^+CD27^+$ memory, and $CD19^+CD27^{++}$ plasmablast B cells. Each point represent an individual patient or control.

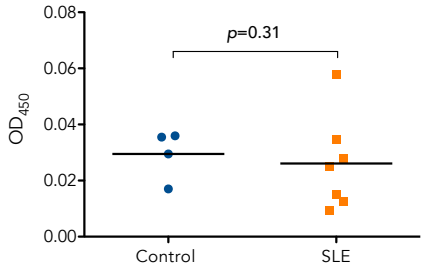

Figure 4.13: **ELISA of phospho-AMPK (Thr172) in SLE B cell lysates compared with healthy controls.** Freshly isolated total $C19^+$ B cells were lysed in the presence of phosphatase inhibitors. Each point represents an individual patient or control. The mean is shown. Mann-Whitney U test used.

Antibody target	Summary	Effect on autophagy
Phospho-GSK3 (Ser9/21)	Phosphorylates and inhibits glycogen synthase, and has broad metabolic effects. Phosphorylated in resting states, which is growth permissive	+/-
Phospho-Akt (Thr308)	Phosphorylated under growth conditions by PDK1 following PI3K signaling. Promotes cell survival by phosphorylating and inactivating Bad.	Downregulates
Phospho-ERK1/2 (Thr202/Tyr204, Thr185/Try187)	MAPK family members. Phosphorylated in response to growth stimuli. Inhibits autophagy via TFEB	Downregulates
Phospho-p70-S6K (Thr421/Ser424)	An effector of cellular growth and a target of mTOR signaling	Downregulates
Phospho-p38 MAPK (Thr180/Tyr182)	Responds to inflammatory cytokine signaling and cell stress. Major signaling kinase	Upregulates

Table 4.4: **Analytes in Luminex assay of protein phosphorylation**

this assay, I found that there was significantly more phosphorylation of GSK3α/β in SLE compared with healthy controls, expressed as a ratio (figure 4.14). If phosphorylated protein alone is compared, there were also statistically significant increases in phospho-Akt and phospho-p70S6K1.

4.4 Discussion

The chapter describes the application of novel tools for the analysis of autophagy in *ex vivo* lymphocytes, for the study of autoimmune disease.

The differential activation of autophagy in SLE B cells is a novel finding. Notably, the largest increase in autophagosomotropic dye uptake and the lowest level of p62

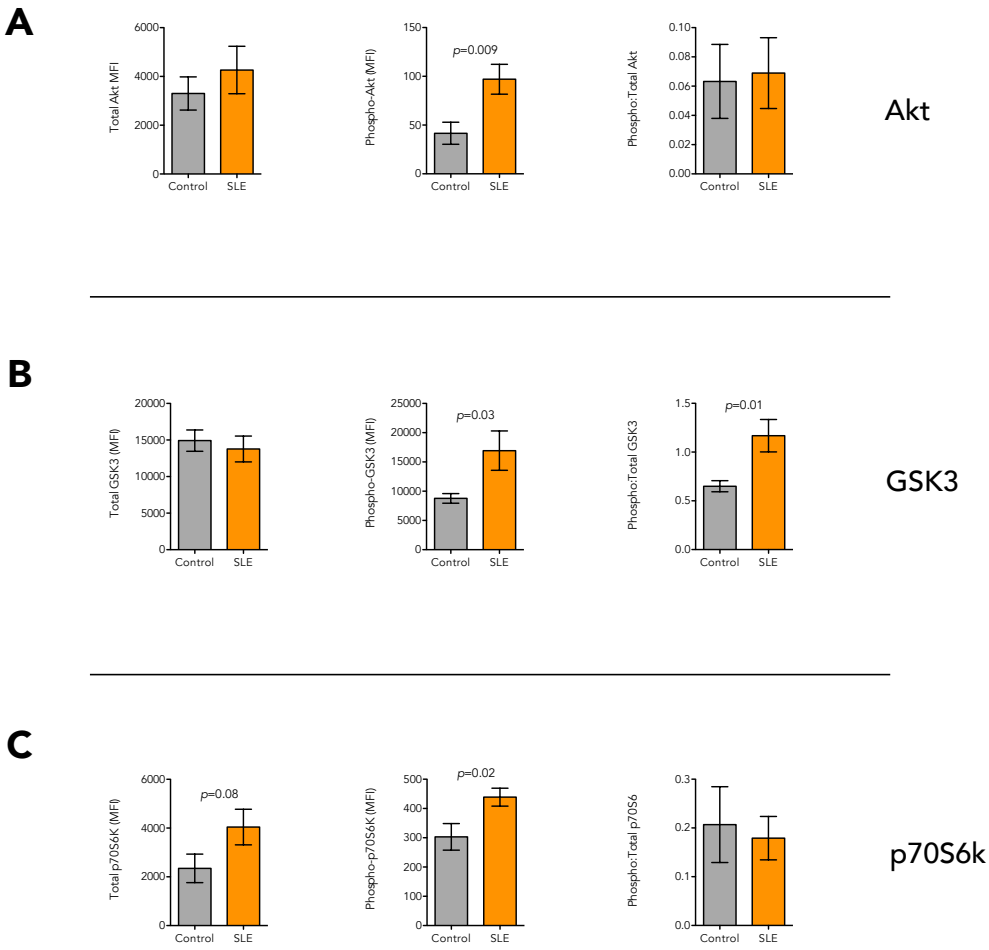

Figure 4.14: **Phosphoprotein assay of A. Akt (Thr308), B. GSK3α/β (Ser9/21), and C. p70S6K (Thr421/Ser424) in SLE B cell lysates**. Freshly isolated total C19$^+$ B cells were lysed in the presence of phosphatase inhibitors. n=10 per group. Error bars denote SEM. Unpaired *t* test used for comparisons.

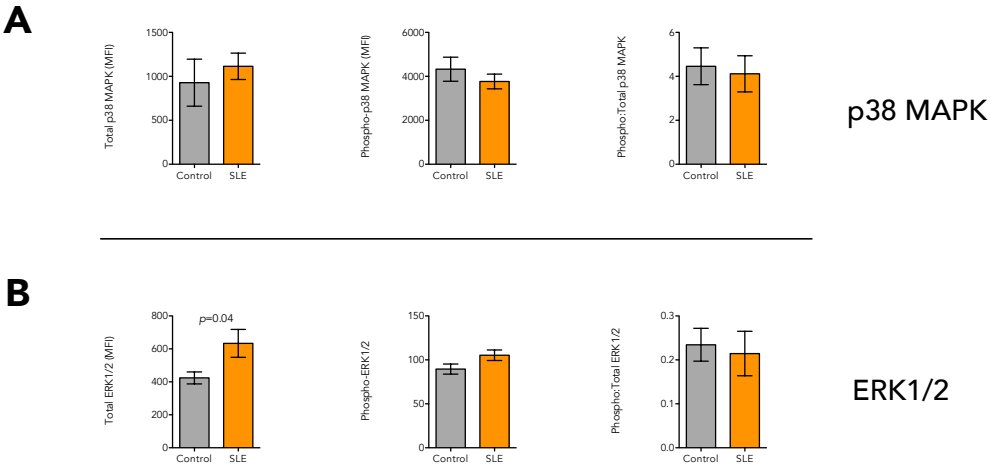

Figure 4.15: **Phosphoprotein assay of A. p38 MAPK (Thr180/Tyr182) and B. ERK1/2 (Thr202/Tyr204, Thr185/Try187)**. n=10 per group. Error bars denote SEM. Unpaired *t* test used for comparisons.

is in the $CD27^{-}IgD^{-}$ subset, with lesser increases in memory B cells ($CD27^{+}$). Interestingly, there was no difference in plasmablasts, if the CytoID MFI was expressed in terms of a ratio to FSC. A difference in autophagy between B cell subsets within the healthy control subjects was also apparent, with relative increases in the $CD27^{-}$ population compared with $CD27^{+}$ and $CD27^{++}$ cells.

The $CD19^{+}CD27^{-}IgD^{+}$ population identified as that with maximal autophagy includes principally naïve, but also transitional B cells, populations with specific and separate survival requirements and characteristics from memory B cells and plasmablasts. In SLE, this population ($CD19^{+}CD27^{-}$) of naïve B cells is reduced, in contrast to a relatively normal memory compartment and an increased number of $CD27^{++}$ plasmablasts[156]. Underlying mechanisms for this naïve B cell lymphopenia have not been established.

Multiple possibilities exist for the finding of activated autophagy in naïve B cells, and may be classified into three broad categories.

4.4.1 Autophagy as a mechanism for the survival of autoreactive B cells

As has been outlined above, a tolerance checkpoint exists as transitional B cells complete their development into naïve B cells, and which has been demonstrated by single cell Ig cloning to be defective in SLE[148]. Whilst there is no significant difference in autoreactivity between newly emigrant B cells from patients with SLE and healthy controls, autoreactive B cells were enriched in the mature naïve B cell pool in disease. In health, peripheral B cell survival is an outcome contingent on appropriate BCR stimulation, and access to survival factors, most notably BAFF. B cells that receive stimulation through their BCR in excess of a threshold are rendered anergic, a state characterized by down-regulation of surface IgM and inhibition of antibody secretion[274]. Alternatively, high levels of BCR stimulation may induce apoptosis, with consequent deletion of the autoreactive B cell[167;275]. This process may be mediated by stimulation of the extrinsic pathway of apoptosis through interaction between B cell CD95 and Fas-ligand on $CD4^+$ T cells[276], but principally depends, as mentioned above, on adequate BAFF exposure[277;278]. BAFF and its homologue A Proliferation Inducing Ligand (APRIL) are members of the TNF family, and are secreted by innate immune and stromal cells, the activation of which leads to the cleavage and secretion of the transmembrane forms of these proteins[191]. BAFF and APRIL have differences in receptor binding; BAFF-R (BAFF receptor) is specific for BAFF, whereas B cell maturation antigen (BCMA) and transmembrane activator and calcium modulator ligand interactor (TACI) may bind both BAFF and APRIL. BAFF-R signals through two major pathways: PI3K-Akt-mTOR, and NF-κB[191]. BAFF stimulation activates mTORC1[279], which as described in **??**, leads to cell anabolism and proliferation, and inhibits autophagy. Furthermore, Akt signaling inhibits the pro-autophagic transcription factor FOXO3a. However, levels of the BH3 family member Bim are reduced, which promotes autophagy as its inhibitory

interaction with beclin-1 is suppressed[280]. Bim appears to play a critical role in the death of autoreactive B cells, as deficiency of this protein leads to autoimmunity[151].

To date, the effect of genetic activation of autophagy on autoimmunity has not been examined. However, *Atg5* and *Atg7*-overexpressing transgenic mice on non-autoimmune backgrounds have enhanced lifespans and are not reported to develop features suggestive of immune-mediated disease[281;282]. These relatively preliminary findings imply that autophagy over-activation is not in itself sufficient to induce autoimmune disease. These data are somewhat surprising given the importance of autophagy throughout the immune system, and further study of the properties of these mice is likely to be of great interest, particularly in the context of infectious disease.

4.4.2 Autophagy as a reflection of B cell activation

Given that SLE is associated with B cell hyperactivation, could this account for the observed up-regulation of autophagy? The extent to which autophagy is activated or suppressed following stimulation in B cells is not entirely clear, and may depend on accompanying survival signaling. It has been observed by Watanabe *et al*. that in murine primary B cells, BCR stimulation activates autophagy, probably as a prelude to apoptosis, but when CD40 is co-ligated, autophagy is suppressed[237]. Signaling through TLR4 or TLR9 has been demonstrated to activate autophagy[238;240]. It seems probable that in SLE, activated B cells that have not yet received co-stimulation and are therefore at risk of apoptosis, may up-regulate autophagy and contribute towards the observed results. The *in vitro* results I have obtained (4.3.2) are contrary to those of Watanabe *et al.*, but support the hypothesis that autophagy may act as a survival mechanism for threatened B cells. Mechanistically, I have demonstrated the activation of mTOR signaling following B cell stimulation, which is agreement with the observed reduction in autophagy following growth signaling. In fact, it is

difficult to reconcile mTOR signaling following differentiation and growth stimuli with autophagy activation, as reported[237;238;283]. One interesting explanation however, might be that mTOR signaling and autophagy regulation become detached, with activation of both pathways serving to support high levels of protein synthesis. Narita *et al.* have demonstrated that this phenomenon may occur in the specific sub-cellular location they termed the TOR-autophagy spatial coupling compartment (TASCC)[284]. It is possible therefore that the TASCC may operate as B cells differentiate to secrete immunoglobulin. My *in vitro* B cell stimulation experiments were over a relatively short time-course (up to 48 hours), and it may be that the TASCC is not yet active. One further issue is that I have only used one assay of autophagy (CytoID), and have not examined flux. Further work is therefore required to allow more conclusive account to be made of the role of autophagy in early B cell activation.

4.4.3 Autophagy as a mechanism for presentation of self-antigens

A remaining hypothetical role for autophagy in the pathogenesis of SLE is that its up-regulation, perhaps in the contexts discussed above, may enhance or lead to the presentation of self-antigens on MHC-II by B cells. Whilst this question has not been addressed by my experimental work, there is supporting literature that is suggestive of this possibility. Autophagy has been demonstrated to be required for antigen presentation on MHC-II by dendritic cells, and has an important function in cross-presentation of endogenous antigens[200;213;216]. Notably, stimulation of autophagy increases the display of nucleus-derived antigens. It also enhances the immune response to intracellular organisms *e.g.* HSV and TB *in vitro* and *in vivo*[200;217]. Finally, in tumour cells, activation of autophagy by chemotherapeutic agent-induced cell stress leads to the release of ATP, thereby enhancing recruitment of T cells[285].

4.4.4 T cells

The increased autophagosome density in the total $CD4^+$ T cell pool is in agreement with the work of Gros *et al.*, who observed increased autophagosome density by electron microscopy in the T cells of SLE patients compared with healthy controls[247], but differs from the results of Alessandri *et al.*, who detected differential autophagy only in the naïve T cell subset[248], rather than the entire $CD4^+$ T cell population. Methodologically, Gros *et al.*, Alessandri *et al.* and I all used differing techniques to quantify autophagy, which may to some extent account for the discrepant results. Due to the relative novelty of my findings in B lymphocytes, further experimental work concentrated on this cell type, and so the findings in T cells is therefore largely preliminary. Specifically, I have not performed a flux assay and so it is possible that the significantly increased autophagosome count may result from impaired autophagosome-lysosome fusion. It is noteworthy that I did not detect a difference in p62 levels in SLE $CD4^+$ T cells.

In common with the clinical experimental data from B cells, the role of T cell autophagy in the pathogenesis of SLE must remain largely speculative, and the extent to which its distinct functions contribute to disease on a differential basis is unknown.

4.4.5 Regulation of autophagy in SLE

Whilst I have outlined hypotheses that might explain the observed activation of autophagy in SLE, how might this be regulated? In the results presented in 4.3.3, I have examined a number of signaling pathways known to influence autophagy, by detecting protein phosphorylation in either intact cells by flow cytometry, or in B cell lysates. Using a Luminex-based suspension array system, I found that the ratio of phosphorylated:total GSK3 was significantly increased in SLE compared with

healthy controls. There were also relative increases in the total and phosphorylated forms of Akt and p70S6K1, but the phosphorylated:total ratio was not significantly different. GSK3 is a serine/threonine protein kinase which is constitutively active in basal conditions, as described in **??**. Phosphorylation of GSK3 at Ser9 for the β-isoform, and at Ser21 for the α-isoform, leads to inactivation of GSK3 and therefore transcription factor dephosphorylation and activation. The function of the GSK3 signaling pathway in the regulation of autophagy is unclear, and the conflicting literature outlined in **??** suggests that a degree of cell type specificity may exist. GSK3 signaling has not been examined in SLE before and this result is therefore a novel finding.

Using an ELISA for the phosphorylated form of AMPK (Thr172), I was unable to detect a difference between SLE and healthy control freshly isolated B cells, in a small sample set. Whilst this negative finding may simply represent a type II error or true result, the degree of phosphorylation was very low in both groups, suggesting the possibility of technical experimental failure, interference during sample processing, or that a significant difference may only be revealed following stimulation.

The data obtained from the PhosFlow experiments is hampered by two potential issues: phosphatase activity, and small sample sizes. Samples were stored overnight at 4°C in PBS before permeabilization with a saponin-containing buffer and intracellular staining the following day. During this time period there is significant potential for intracellular phosphatase activity which would result in loss of target phosphorylation and thus experimental signal. This shortcoming needs to be addressed by the use of a phosphatase inhibitor (as used during cell lysis), and staining before cell storage, or selection of an alternative permeabilizing agent *e.g.* methanol which prevents phosphatase activity.

The pathways assayed are not exhaustive and it is unknown to what extent rela-

tive levels of phosphorylation of key proteins regulate autophagy in sum. Although it is probable that GSK3 signaling may tend to inhibit autophagy, it is possible that this activation is counter-regulatory. The pro- and anti-apoptotic BH3 proteins also require examination, as a potentially important regulator of autophagy in SLE. Similarly, Foxo3 nuclear translocation may be assayed using MIFC.

5 Autophagy in the NZB/W murine model of lupus

5.1 Introduction

In the preceding chapter, I have presented results demonstrating that autophagy is activated in the $CD19^+$ B and $CD4^+$ T cell populations from patients with SLE. Whilst these data are derived from human disease and are therefore of maximal clinical relevance, they are subject to a number of shortcomings inherent in the study of human SLE. These include, in probable order of maximum importance:

Confounding by therapy

The patients I have studied had all been subject to pharmacologic intervention, including agents known to influence autophagy at high dose *in vitro* (*e.g.* prednisolone and hydroxychloroquine). Whilst I found no statistical evidence of correlation between drug use and markers of autophagy (table 4.3.1), the existence of type II error cannot be fully excluded. Ideally, I would only include patients either before, or on no, drug treatment; however in practice it is extremely difficult to recruit such subjects and it is therefore impractical over a reasonable timescale.

Limited access to the B cell compartment I was restricted to the collection of peripheral blood from both patients and healthy controls. Whilst naïve and memory

B and circulating plasmablasts are sampled, B cells in the earlier stages of development, and those undergoing the germinal centre reaction and plasma cells are largely excluded from study. To capture these other populations, lymph node and bone marrow sampling would be required, which again is impractical in the patient pool from which I was able to recruit.

Clinical heterogeneity SLE is a disease that exhibits great clinical and immunologic heterogeneity. Moreover, it is subject in many cases to significant temporal variation and typically follows a relapsing-remitting course. The complex multifactorial aetiology of SLE as discussed in chapter 1, accounts for this.

5.1.1 The NZB/W murine model of SLE

The study of a murine model of SLE largely overcomes these three considerations, but with the major caveat that those available do not necessarily fully or accurately recapitulate the human disease. The principal murine models of lupus are the New Zealand Black × White F_1 hybrid (NZB/W), the MRL/*lpr* mouse, and the BXSB/Yaa[286], all of which develop an ultimately fatal autoimmune disease characterized by ANA and glomerulonephritis[287].

The NZB/W model has more complete disease expression in female mice, with a correspondent earlier mortality. The mean age for 50% and 90% of mice to have succumbed is 8.5 and 12.5 months respectively[287]. NZB/W mice develop severe glomerulonephritis with heavy proteinuria and C3 and IgG deposition. There are not typically ANA until later than 2 months; anti-dsDNA antibodies appear from 5-6 months and progressively accumulate thereafter[287]. NZB/W mice also exhibit lymphadenopathy, vasculitis, hypocomplementæmia, and immune complex formation, notably with antibodies against the murine endogenous retrovirus protein gp70[287].

Immunologically, the NZB/W mouse displays B cell hyperactivity, and this property is intrinsic, as autoimmunity is induced in severe combined immunodeficiency (SCID) mice transplanted with NZB/W pre-B cells[288;289]. The genetic basis for the NZB/W phenotype is unknown, but it behaves as a complex trait with polygenic inheritance[290]. The NZB/W derivative strains NZM2410 and NZM2328 contain the susceptibility loci *Sle1-3,* mapped via linkage analysis. Congenic models containing the *Sle1* locus develop anti-chromatin antibodies, but the genetic interval incorporating this region is wide, and includes several smaller risk loci, influencing T and B cell activation[286;290]. The *Sle2* locus, again studied using congenic strains, is similar structurally, containing many separate risk genes, which lead to lower B cell activation thresholds and increased numbers of B1a B cells[291].

In this chapter, I use the NZB/W model to study autophagy in murine SLE, both before and after the onset of disease.

5.2 Aims

To determine autophagy in the NZB/W murine model of SLE, in pre- and post-disease mice

5.3 Results

5.3.1 Autophagosome density is increased in NZB/W B cells

To determine autophagosome density in splenic lymphocytes, MIFC was employed, using immunofluorescent detection of endogenous LC3. Female NZB/W mice were sacrificed at 13 weeks of age, and compared with sex and age matched C56BL/6 (B6) control mice.

As in the analytic approach performed on *ex vivo* human cells, the Spot Count

algorithm was applied to detect $LC3^+$ punctae, representing autophagosomes, in splenic B cells. Figure 5.1 (A) illustrates examples of B cells with high and low spot counts, and figure 5.1 (B) shows representative distributions of Spot count between NZB/W mice and B6 controls. As in human SLE, the distribution was left-skewed and therefore autophagy was quantified using an empirical defining gate.

Using MIFC, I found more autophagosomes in NZB/W splenic B cells than in B6 controls (figure 5.1).

To confirm this result using an alternative technique, I again utilized the autophagosomotropic dye CytoID, the uptake of which was quantified using conventional FACS (figure 5.2). To gain access to the full B cell compartment, spleen and bone marrow was analyzed (figure 5.3).

The results from this experiment are in agreement with the MIFC data, demonstrating increased autophagosome density in NZB/W splenic B cells, defined broadly as $CD19^+$. In contrast to the results in humans with SLE however, I did not find increased dye uptake in $CD4^+$ T cells, albeit using a different experimental methodology. Extending the analysis across wider B cell phenotyping, there are two major observations.

Firstly, autophagosome density is generally increased in bone marrow B cells, compared with peripheral cells, in both diseased and control mice. Secondly, differential dye uptake was maximal in relatively less mature B cells (*i.e.* bone marrow stages). Specifically, differences were greatest in pre-B, immature B, and mature B cells (defined as $CD19^+IgD^-IgM^-$, $CD19^+$, IgD^-IgM^+, and $CD19^+IgD^+IgM^+$ respectively) in the bone marrow. In the periphery, transitional T1 ($CD19^+IgD^-IgM^+CD23^-CD21^-$) and T2 ($CD19^+IgD^+IgM^+CD23^+CD21^+$) B cells displayed greatest relative autophagosome density. Interestingly, and mirroring human data, there was less autophagy in plasma cells in NZB/W mice compared with B6 controls.

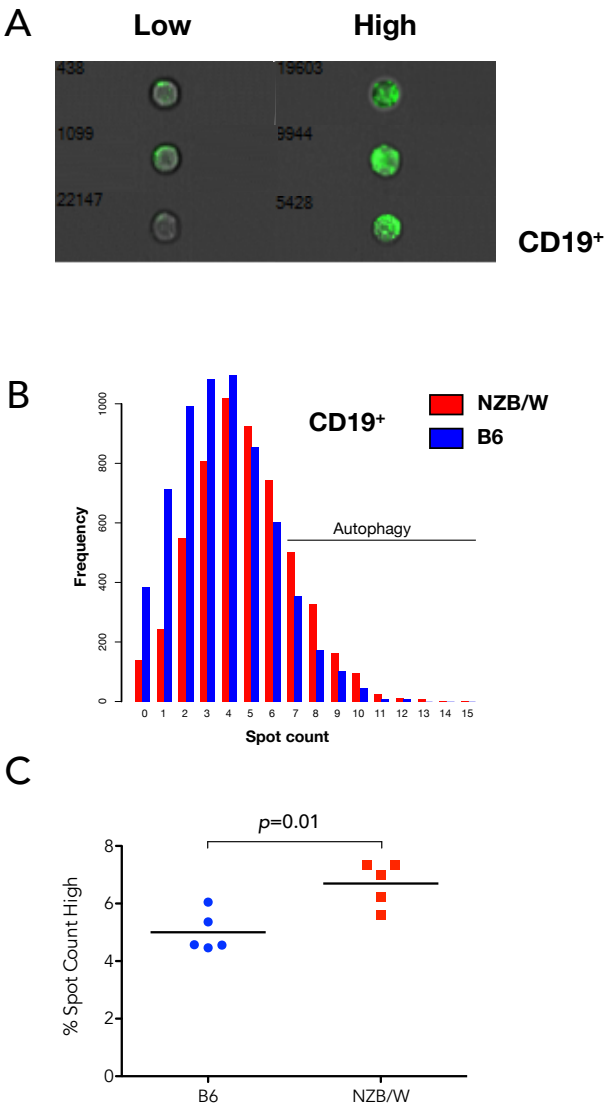

Figure 5.1: **Autophagy in murine lupus quantified by MIFC**. Autophagy in splenic NZB/W CD19$^+$ B cells was compared with control B6 mice. **A**. Representative MIFC images of B cells with high and low numbers of LC3$^+$ autophagosomes. **B**. Example distributions of LC3$^+$ punctae in diseased *vs.* control mice at 13 weeks of age, with gating of autophagy-positive cells (defined as ≥7 spots per cell). **C**. There are increased numbers of LC3$^+$ autophagosomes in the CD19$^+$ B cells of NZB/W compared with control mice at 13 weeks (post-disease onset). Each point represents an individual mouse. C. Mann-Whitney U test used

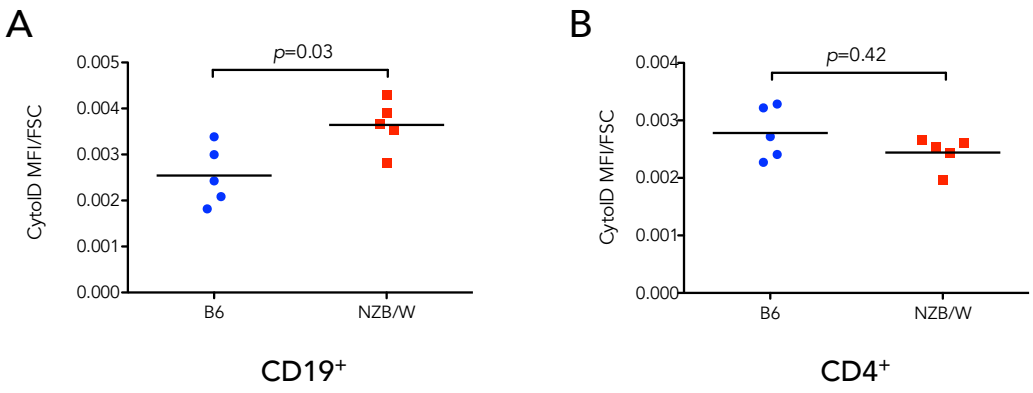

Figure 5.2: **Autophagy in murine lupus quantified by CytoID uptake**. **A**. $CD19^+$ B and **B**. $CD4^+$ T cells. Each point represents an individual mouse. Mann-Whitney U test used.

5.3.2 Autophagic flux is active in NZB/W B cellstrend

As has been described above (4.3.1.1), to exclude a defect in autophagosome-lysosome fusion, it is necessary to employ an assay that reveals autophagic flux. In this experiment, p62 levels were quantified by intracellular FACS following incubation of cells in complete RPMI media supplemented with bafilomycin A_1 for 3 hours. p62 is an autophagosome adapter protein mainly cleared by autophagy, and whose levels are inversely correlated with autophagic activity. Blockade of autophagosome-lysosome fusion would, in the context of active flux, therefore lead to an increase in p62 levels. I found significantly decreased basal p62 levels in both the total peripheral $CD19^+$ pool, and a non-statistically significant trend to a decrease in $CD19^{+/-}CD138^+$ splenic plasma cells (figure 5.4). For the bafilomycin A_1 flux experiment, splenic $CD19^+$ B cells were examined. I found an increase in p62 levels following the incubation period, indicating accumulation of autophagosomes and therefore active autophagic flux.

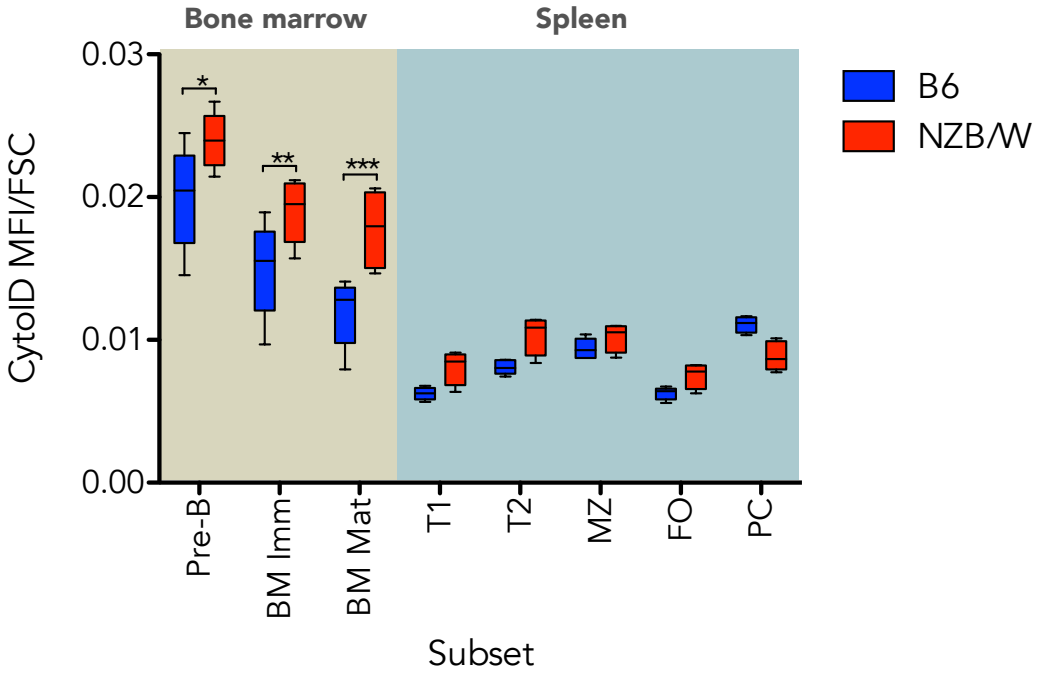

Figure 5.3: **Autophagosome density in mouse B cell subsets**. Distribution of CytoID MFI in B cell subsets from bone marrow and spleens of 13 week-old NZB/W mice and age matched controls. Pre-B ($CD19^+IgD^-IgM^-$), immature B (BM Imm, $CD19^+IgD^-IgM^+$), mature B (BM Mat, $CD19^+IgD^+IgM^+$), T1 ($CD19^+IgD^-$ $IgM^+CD23^-CD21^-$), T2 ($CD19^+IgD^+IgM^+CD23^+CD21^+$), marginal zone (MZ, $CD19^+IgD^-IgM^+CD23^-CD21^{++}$), follicular (FO, $CD19^+IgD^+IgM^-CD23^{++}CD21^+$), and bone marrow plasma cell ($CD19^{+/-}CD138^+$) subsets are illustrated. n=5 mice per group. Box and whisker plots denote maximum and minimum, interquartile range, and median. *p<0.05; **p<0.01; ***p<0.001. ANOVA used for analysis.

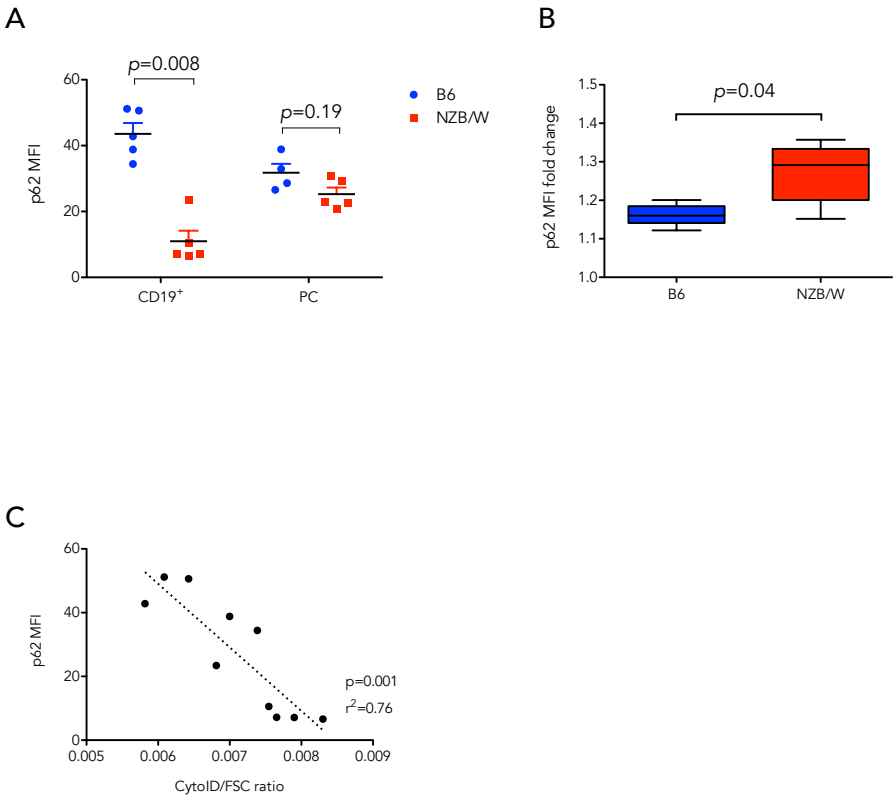

Figure 5.4: **p62 dynamics in *ex vivo* NZB/W and B6 B cells**. **A**. There is decreased basal p62 expression, measured by intracellular FACS in splenic $CD19^+$ B cells, and a trend towards a reduction in $CD19^{+/-}CD138^+$ plasma cells (PC) in 13 week-old NZB/W mice. **B**. To demonstrate accumulation of the autophagic substrate p62, isolated splenocytes were incubated in complete RPMI with 100nM bafilomycin A_1 for 3 hours. n=5 mice per group. Fold change in p62 MFI compared with untreated cells is shown. **C&D**. There is good inverse correlation between p62 levels and CytoID uptake (C). A-B: Mann-Whitney U test used, C: Pearson's correlation.

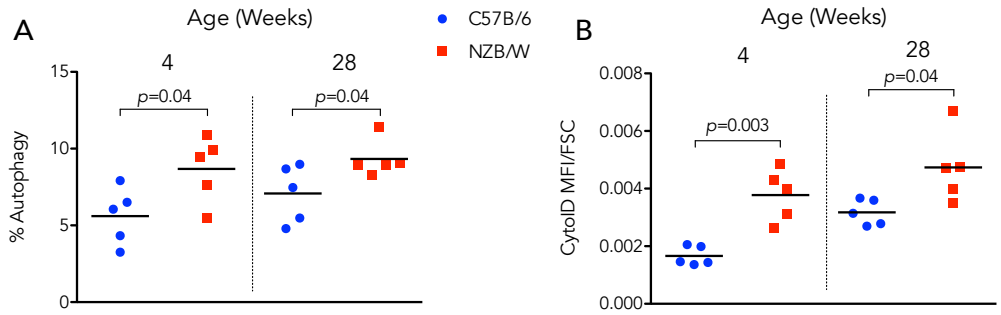

Figure 5.5: **Autophagy before and after the onset of disease in B cells of NZB/W mice**. The number of autophagosomes measured using MIFC (A) or autophagosomotropic dye (B) increases with age, but a difference between the mice is present even at 4 weeks, before disease has developed. Unpaired *t* test used for comparisons.

5.3.3 Autophagy is activated even before the onset of disease in the NZB/W mouse

I next went on to determine the temporal relationship between the onset of disease and the activation of autophagy in the NZB/W mouse. To do this, NZB/W mice were compared with age matched B6 controls at 4 and 28 weeks of age; that is, in pre-disease and established disease. Autophagy was determined in splenic $CD19^{+}$ B cells using MIFC and CytoID assays (figure 5.5). I found that autophagy was differentially enhanced in the NZB/W mouse even at 4 weeks, and remained elevated to a similar degree at 28 weeks. In the B6 mice however, there was an increase in autophagosome density from 4 to 28 weeks of age, more clearly appreciated by the CytoID assay.

5.4 Discussion

The results described in this chapter demonstrate that autophagy is also activated in the B cells of a murine model of SLE, and provide a more detailed assay of the response of individual subpopulations within the broader B cell pool. It also reveals an increase in autophagosome density in the early, bone marrow stages of B cell development compared to more mature peripheral cells, in both healthy and diseased mice. The final key finding is that autophagy is activated at an early stage of development in the NZB/W mouse, before the onset of disease.

5.4.1 Activation of autophagy in the early stages of B cell developmenttrend

The direct observation of activation of autophagy in the early stages of B cell development is a novel finding, but one that is supported by existing data. Beclin-1 expression, detected using a beclin-1-GFP transgenic reporter mouse, is increased in pro-B cells relative to pre-B and immature B stages[225]. Activation of autophagy at this transition is commensurate with the phenotype of B cells deficient in key autophagy genes, *e.g. Atg5* and *beclin-1*, which are characterized by a block in development at the pro- to pre-B stage[221;232]. There are a number of possible explanations for this finding. Firstly, the role of Bcl-2 in B cell development will be considered. Bcl-2 is highly expressed in pro-B cells, but down-regulated at the pre-B and immature B stages[234]. This transition is associated with significant physiological loss of B cells, with approximately 75% of precursors failing to progress from pro-B to pre-B cells[142]. At the pre-B stage, the newly rearranged heavy chain is paired with a surrogate light chain, to form the pre-BCR. Successful formation of a pre-BCR is vital for cell proliferation and the development of a normal B cell compartment[292]. Autoreactive pre-BCRs are eliminated by mechanisms that have not been fully elucidated,

but may include binding of self-antigens to the complementarity determining regions (CDRs) of the newly rearranged heavy chains, or by defective association with surrogate light chains[293]. I hypothesize that one mechanism for the activation of autophagy is this down-regulation of Bcl-2 expression, liberating beclin-1 and thereby initiating autophagosome formation. Autophagy may, in this circumstance, provide an important means for B cell survival when deletion is threatened.

Secondly, it is possible that autophagy may act as a support mechanism for withstanding cellular stress incurred by DNA damage during the action of DNA endonucleases. *Rag1/2* expression begins at the Pro-B stage, with rearrangement of the *IgH* locus. *Rag1/2* is then down-regulated by signals from the pre-BCR and by IL-7, forcing allelic exclusion, then re-expressed to allow *IgL* rearrangement[294]. The formation of double-stranded breaks (DSBs) by Rag leads to phosphorylation of ataxia telangiectasia mutated (ATM) kinase, which both phosphorylates many components of the DNA damage response, and also directly stabilizes the DSBs[295;296]. ATM activates autophagy via LKB1 mediated phosphorylation of AMPK, which in turn also inhibits mTORC1 signaling through TSC2[297]. Foxo3a is also up-regulated during DSB formation, and interacts with ATM[298]. Interestingly, during pre-B development, IL-7 signaling must be attenuated for *Rag* re-expression and *IgL* rearrangement to occur, and this event is associated with up-regulation of Foxo3a due to suppression of Akt signaling[299;300]. It could be inferred therefore, that autophagy is activated in this circumstance.

One significant omission from the data collected on autophagy in the bone marrow is that the phenotyping panel did not include markers for pro-B cells. This unfortunately to an extent limits the ability of my results to support the hypotheses outlined above. The study of autophagy with more detailed bone marrow B cell immunophenotyping is therefore clearly warranted.

Following egress from the bone marrow, there is a global reduction in B cell Cy-

toID uptake, commensurate with a decrease in autophagy. This may be explained by the conclusion of the process of receptor formation and testing, and the emergence into maturity. Within the peripheral B cell pool, there are subset specific differences in autophagy. Notably, there was significantly more CytoID uptake in marginal zone (MZ) than follicular (FO) B cells. MZ B cells are a population of innate-like lymphocytes located at the splenic MZ, and in contrast to FO B cells, typically have a polyreactive BCR, analogous to a TLR[301]. MZ B cells are responsible for the T-independent adaptive immune response, and because they express high levels of TLRs, are able to respond rapidly to infection through dual receptor ligation, which leads to the production of high levels of low specificity immunoglobulin[302]. MZ B cells are also a major source of natural immunoglobulin, important in clearance of damaged and dead cells. Many of these functions may be associated with activation of autophagy. However, it appears that autophagy is redundant in the formation of MZ B cells, as *Atg5*$^{-/-}$ mice do not have a significant difference in this population compared with the wild-type[232].

There is a degree of discordance in the data however, in the case of plasma cells. Using CytoID, I found higher uptake in these cells than the remainder of the peripheral B cell compartment in the control mice, but interestingly in the NZB/W mice, this differential was not present. However, in contrast, the expression of p62 in plasma cells was in fact higher in both control and diseased mice. One potential explanation for this finding may indicate the limitation of p62 as a universal marker of flux. Plasma cells are subject to profound cellular stress caused by their extremely high output of immunoglobulin. This leads to activation of the UPR, which is associated with increased expression of p62, performing its role as a ubiquitin binding protein[303]. In this situation therefore, p62 levels may be elevated due to transcriptional regulation, limiting its utility as a marker of autophagy.

5.4.2 Pre-disease activation of autophagy in the NZB/W mouse model of SLE

A novel finding from the data presented in this chapter is that autophagy is enhanced in the B cells of the NZB/W mice, notably even before expression of disease. Much of the discussion applicable to this observation has been outlined in chapter 4. However, the apparently intrinsic activation of autophagy in the pre-disease mice will be considered further, as will the stage-specific findings. As has been described above, the genetic abnormalities leading to the disease phenotype of the NZB/W mouse are associated with B cell hyperactivation. How autophagy may be enhanced is not clear. A study of the expression and phosphorylation state of pathways associated both with activation and inhibition of autophagy has been conducted in congenic mice carrying the *Sle1-3* alleles[304]. There is phosphorylation of Bcl-2, which leads to its dissociation from beclin-1 and therefore initiation of autophagy[273]. However, mTOR is also activated, which would tend to suppress autophagy. The relative importance and net effect of these pathways is unclear.

The maximal differences in autophagy are seen in the bone marrow, in the pre-, immature, and mature B cell stages. It is possible, as has been described, that intrinsic activation of autophagy allows autoreactive B cells to survive receptor testing and to enter the periphery (figure 7.1. It is also possible that differential activation of autophagy reflects the stress response to receptor editing in cells that have generated an autoreactive BCR. However, the currently available data cannot confirm or refute these hypotheses.

5.4.3 Limitations

As was outlined in the introduction to this chapter, the use of a model system eliminates many of the potentially confounding factors inherent to the study of human

disease. The similarity of the results obtained in patients to the NZB/W mice suggests that the human data is not skewed by the possible biases listed above. However, there is discrepancy between the results obtained in $CD4^+$ T cells; using MIFC in SLE patients, there was found to be higher autophagosome density in these cells, whereas in the NZB/W mice, using CytoID, there was no difference between the diseased and control mice. The latter finding is discordant with the results published by Gros *et al.*[247]. Autophagy was determined by different experimental techniques in all cases, and therefore direct comparison, given only one assay, must be undertaken with a degree of caution.

One final limitation that must be raised is that, owing to limited sample availability and the requirement for relatively complex immunophenotyping, the bone marrow data that I have presented uses only one methodology for the determination of autophagy. It is therefore also not possible to exclude a defect in autophagic flux. Further work should thus include multimodal analysis of autophagy in developing B cells.

6 Autophagy is required for plasmablast development

6.1 Introduction

In the foregoing experiments, I have demonstrated activation of autophagy in the B cells of humans and mice with SLE, with notable findings in the early, bone marrow stages of development. I next examined the requirement for autophagy in the formation of antigen-secreting plasma cells.

Plasma cells are required to produce very high quantities of immunoglobulin, and in order to do so acquire a number of specialized adaptations during differentiation. The differentiation programme of plasma cells involves extinguishing expression of genes associated with cell division and growth, and activation of the UPR, whilst increasing the capacity of the protein synthesis machinery[305;306].

The UPR is a conserved mechanism for the transduction of ER stress, activated when the protein folding capacity of the ER is exceeded. The status of the ER is detected by three principal sensors: activating transcription factor 6 (ATF6), protein kinase RNA-like endoplasmic reticulum kinase (PERK), and inositol-requiring protein 1α (IRE1α). Activation of these sensors by misfolded proteins triggers two major waves of response. The first series of effects are the suppression of protein translation through phosphorylation of eukaryotic translation initiator factor 2α (eIF2α) by PERK[307]}, an increase in mRNA decay mediated by IRE1α[308], and activation of

autophagy by JNK, again by IRE1α, and also by activating transcription factor 4 (ATF4) and C/EBP homologous protein (CHOP), downstream of PERK[309;310]. The second wave of the UPR is characterized by initiation of a broad gene expression program by the transcription factors X-box binding protein-1 (XBP1s), ATF4, and ATF6f, leading to up-regulation of endoplasmic reticulum-associated decay (ERAD) components, thereby enhancing the capacity of the ER to handle defective proteins[311]. The role of autophagy in the persistent UPR is less clear, with some data suggesting that XBP-1s (the active form of XBP-1) in fact down-regulates autophagy, in least in neurons[312].

6.1.1 The *Atg7$^{Flox/Flox}$*-*Vav*-Cre mouse

To address the importance of autophagy in plasma cell formation, I utilized the *Atg7$^{Flox/Flox}$*-*Vav*-Cre mouse[313]. This mouse, denoted as Vav-Atg7$^{-/-}$, was created by crossing *Atg7$^{Flox/Flox}$* with *Vav*-iCre mice, resulting in conditional deletion of *Atg7*[313]. The Atg7$^{Flox/Flox}$ mouse is produced on a C57BL/6/CBA background, and the *Vav-iCre* mouse is produced on a C57BL/6 background.

Atg7 has an E1-like function, activating Atg12 for conjugation with Atg5[12], and is essential for autophagosome elongation. However, because knockout of critical autophagy genes is lethal, it is necessary to use a tissue specific deletion model for the study of autophagy deficiency *in vivo*[314;315]. The conditional knockout system employed in the Vav-Atg7$^{-/-}$ mouse uses Cre-Lox recombination, excising the loxP flanked *Atg7* gene with Cre recombinase under the control of the promoter for the proto-oncogene *Vav*[316]. Vav transduces signals from a number of surface receptors for Rho GTP binding proteins, and is expressed by all haematopoietic cells[317;318]. Atg7 is therefore deleted in all cells of the immune system in the Vav-Atg7$^{-/-}$ mouse. The Vav-Atg7$^{-/-}$ mouse has already been characterized in detail, and both efficient deletion of *Atg7* and severe functional impairment of autophagy has been demon-

strated[313]. The phenotype of the Vav-Atg7$^{-/-}$ mouse is of progressive bone marrow failure, with mortality typically occurring by 12-weeks. There is lymphopenia for CD4^{+} and CD8^{+} T cells, and B cells. Vav-Atg7$^{-/-}$ T cells have increased active caspase-3 staining, indicating apoptosis, and increased mitochondrial density with higher levels of mitochondrial superoxide[313]. A major cause of the cytopenia observed in this model is the dependency of haematopoietic stem cells on autophagy for maintenance and self-renewal[86;233].

6.2 Results

6.2.1 There is abnormal B cell development in the Vav-Atg7$^{-/-}$ mouse

I first examined the B cell pool of female 8-week-old Vav-Atg7$^{-/-}$ mouse, to establish the degree of conformation of this model to other published work. Bone marrow and splenic B cells were extracted and immunophenotyping performed using flow cytometry (figure 6.1).

The results I obtained were in close agreement with the reported phenotype of autophagy deficiency[232]. In the bone marrow which was as described, hypocellular[233], there was an excess of pro- or pre-B cells, with a substantially smaller proportion of immature and mature B cells. The phenotyping panel unfortunately did not include markers to differentiate between pro- and pre-B cells. However, in the periphery, although B cell numbers were reduced[233], there were normal proportions of mature B cells in the spleen. This supports the data presented in chapter 5; that autophagy is primarily activated in the bone marrow during development, but is down-regulated in the periphery once maturity is reached. T cells from the Vav-Atg7$^{-/-}$ mouse have increased mitochondrial density. To determine if there are similar findings in Vav-Atg7$^{-/-}$ B cells, I used the mitochondrial dyes Mitotracker Deep Red and Mitotracker Green, measuring their fluorescence by flow cytome-

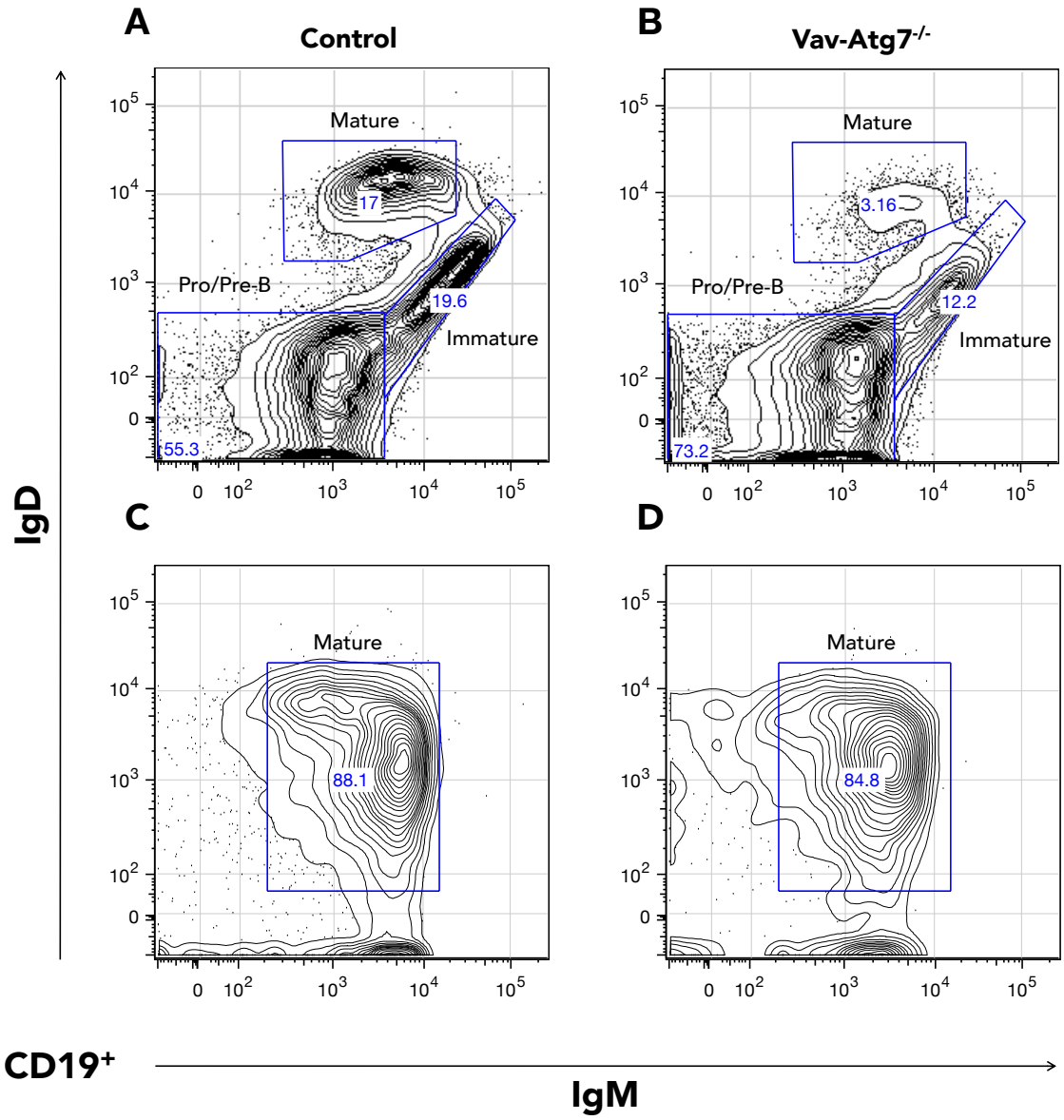

Figure 6.1: **CD19$^+$ B cell populations in Vav-Atg7$^{-/-}$ mice. A&B**. Percentage mature IgM$^+$IgG$^+$ B cells in bone marrow are markedly decreased in Vav-Atg7$^{-/-}$ mice, with an increased proportion of Pre-B cells. However, in the spleen, the percentages of mature B cells are similar (**C&D**). Representative data from n=4 mice of each phenotype.

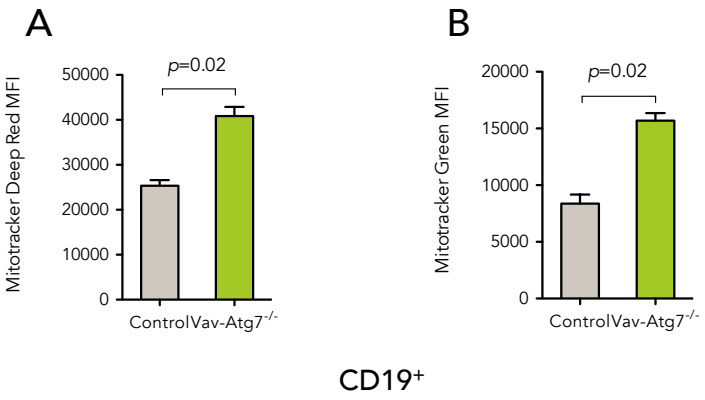

Figure 6.2: **Mitochondrial density in Vav-Atg7$^{-/-}$ B cells**. There is higher mitochondrial mass in Vav-Atg7$^{-/-}$ B cells, measured by MitoTracker Deep Red and Green (**A**) and (**B**), compared with control mice. n=5 per group. Mann-Whitney U test used for comparisons.

try. These are carbocyanine-based probes that selectively stain mitochondria, differing in emission frequencies, and can therefore be used as markers of mitochondrial mass. I found increased mitochondrial density with both dyes in Vav-Atg7$^{-/-}$ B cells compared with controls (figure 6.2).

6.2.2 Autophagy is required for normal plasmablast differentiation

6.2.2.1 Vav-Atg7$^{-/-}$ B cells do not efficiently form plasmablasts

Next, I determined the requirement for autophagy in the differentiation of B cells to immunoglobulin secreting plasmablasts. B cells were isolated from the spleens of female 8-week-old Vav-Atg7$^{-/-}$ and control litter mates using negative magnetic bead selection. B cells were then stimulated with LPS and IL-4 for 72 hours to induce differentiation into plasmablasts. Following the culture period, the proportion of viable, CD138^{+} cells was determined. There was decreased viability in the Vav-Atg7$^{-/-}$ cells, and substantially fewer plasmablasts were formed (figure 6.3). To

further confirm the deficit in plasmablast differentiation, an ELISA was performed to examine immunoglobulin production (figure 6.3B). There was significantly less IgM secreted into the supernatant of the Vav-Atg7$^{-/-}$ plasmablast culture. Little class switching had occurred in either the Atg7$^{-/-}$ or the control experiment, and there was no significant difference in IgG production, which was modest in both.

6.2.3 Pharmacologic inhibition of autophagy in human B cells prevents their differentiation into plasmablasts

Following on from the results obtained in the Vav-Atg7$^{-/-}$ mice, I next wished to establish if human B cells were also dependent on autophagy for efficient differentiation. I used the selective class III PI3K inhibitor 3-MA to pharmacologically inhibit autophagy. B cells were isolated by negative magnetic selection from healthy donors. In order to induce plasmablast differentiation, cells were stimulated according to a protocol adapted from Jourdan et al[319]. B cells were stimulated with the type B CpG ODN2006 in the presence of CD40 ligation with an anti-CD40 antibody, and IL-10 and IL-15. Plasmablasts were defined as CD19^{+}CD38^{++}. I found that 3-MA at a 5μM concentration largely abrogated plasmablast formation in this experimental system (figure 6.4). Whilst 3-MA is widely used as an inhibitor of autophagy, it has been suggested that in some contexts it may actually act to stimulate autophagy, via a dual inhibitory effect on class I PI3K[320]. To confirm that 3-MA was inhibiting autophagy in cultured human primary B cells, I stimulated isolated cells from healthy human donors for 72 hours using the protocol described above in the presence or absence of 3-MA (5μM). During the last hour of culture, bafilomycin A_1 was added to a concentration of 100nM. The addition of an autophagosome-lysosome inhibitor served to enhance LC3 levels by inhibition of autophagic flux, thereby allowing easier immunodetection of this protein. The cultured cells were lysed, and the ratio of LC3-II to β-actin determined using western blotting. I found

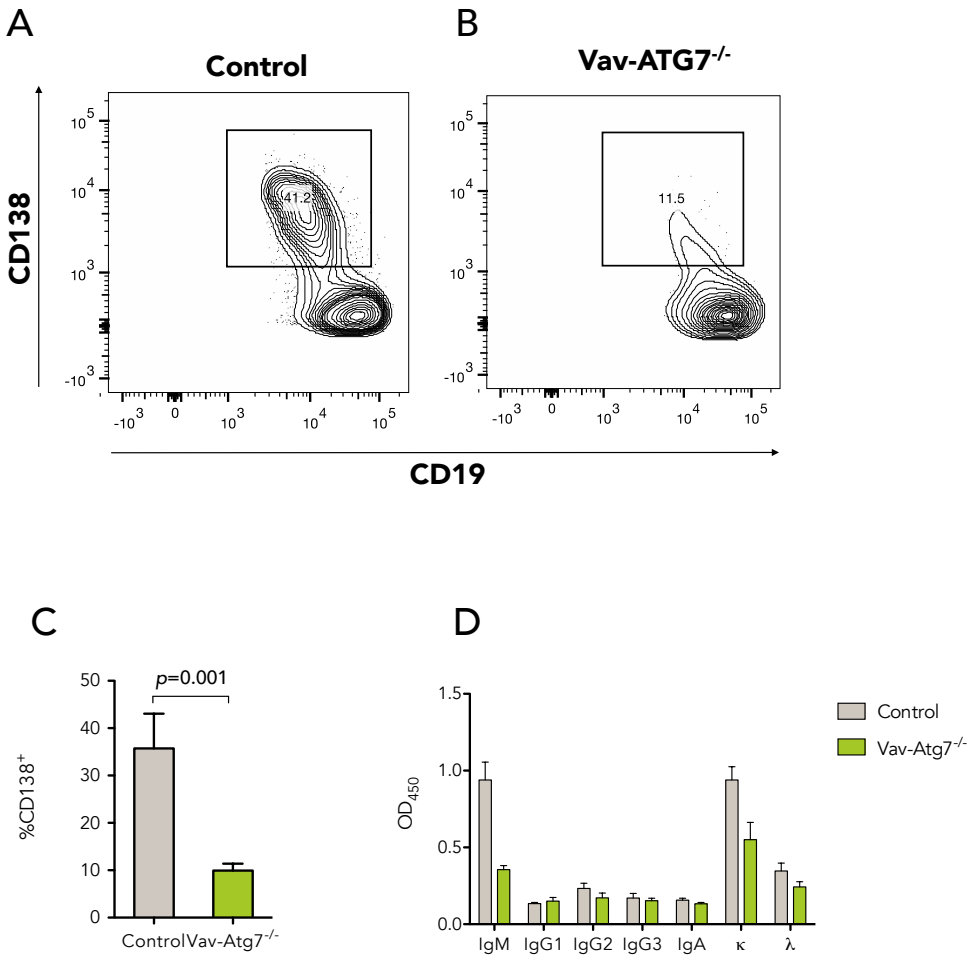

Figure 6.3: **Plasma cell differentiation is impaired *in vitro* in Vav-Atg7$^{-/-}$ B cells**. B cells from Vav-Atg7$^{-/-}$ or control mice were stimulated with LPS (10µg/ml) and IL-4 (10ng/ml) for 72 hours. Following the culture period, there was significant impairment of differentiation into plasma cells in Vav-Atg7$^{-/-}$B cells (A) compared with controls (B), and (C). Accordingly, there was less immunoglobulin secretion in the Vav-Atg7$^{-/-}$ culture. Representative of 2 independent experiments, n=5 per group. C. Mann-Whitney U test used for comparison.

that 3-MA treatment reduced the level of lipidated LC3, indicative of inhibition of autophagy (figure 6.5).

To determine to what extent 3-MA inhibited cell division, I examined dilution of the dye CFSE by flow cytometry. CFSE covalently binds to lysine residues within the stained cell, and due to this attachment is stably retained. CFSE is therefore distributed into daughter cells during division. There were fewer cell divisions in the 3-MA treated cells than in the control, untreated culture (figure 6.4).

6.3 Discussion

6.3.1 Autophagy is required for the efficient differentiation of plasmablasts

The data I have obtained reveal that autophagy is required for plasmablast formation. The potential roles that autophagy might play in this process will now be considered.

6.3.1.1 Autophagy and cell proliferation

Autophagy has a well-described modulatory effect on cell proliferation through its effects on cellular energy metabolism. Interestingly, the extent to which cell types are affected by loss of autophagy is variable, and in some circumstances it may in fact promote tumorigenesis[321]. Reports of the effects of autophagy deficiency on lymphocyte proliferation vary. *Atg5*$^{-/-}$ T cells have impaired division following TCR stimulation or treatment with PMA and ionomycin[223]. However, *Atg5*$^{-/-}$ B cells have been previously described as having essentially normal early *in vitro* proliferation in response to LPS[232;238]. Whilst I did not examine Vav-Atg7$^{-/-}$ B cells, human B cells treated with 3-MA exhibited a significant reduction in division, as assessed by CFSE dilution. Why differences between T and B cells should exist is not clear, but their

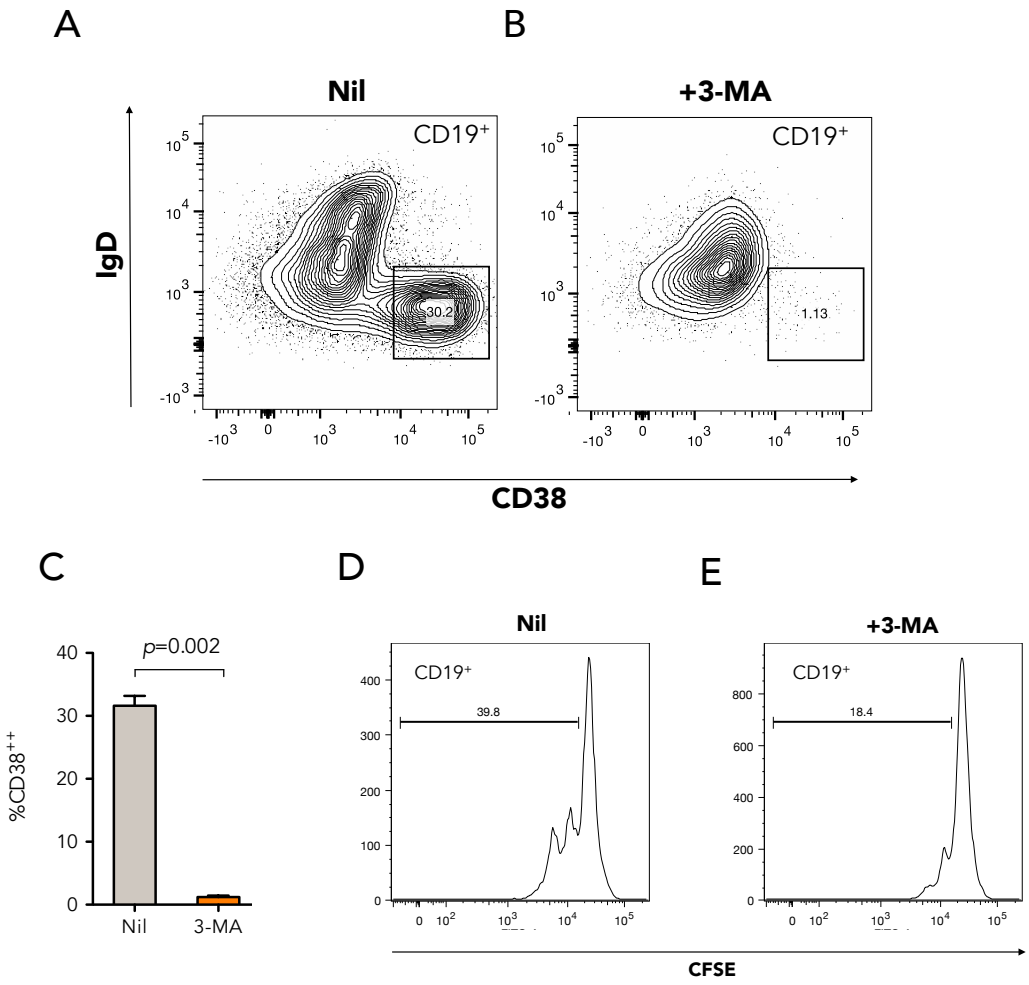

in

Figure 6.4: **Pharmacological inhibition of autophagy in human plasmablast differentiation *in vitro***. B cells from healthy human donors were stimulated with ODN2006 (5µM), IL-10 (50ng/ml), IL-15 (10ng/ml), and monoclonal mouse anti-CD40L (1µg/ml) for 72 hours in the presence or absence of the autophagy inhibitor 3-MA (5µM). There was almost complete inhibition of differentiation into $CD19^{+}IgD^{-}CD38^{++}$ plasmablasts (**A**-**C**), associated with impairment of cell division as assessed by CFSE dilution (**D**&**E**). C. Mann-Whitney U test used for comparison.

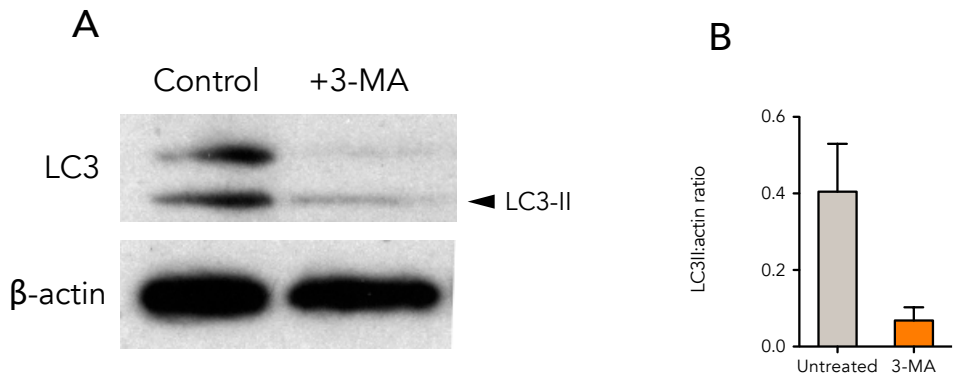

Figure 6.5: **3-MA inhibits autophagy in human B cells**. B cells were stimulated with the type B CpG ODN2006 in the presence of CD40 ligation with an anti-CD40 antibody, and IL-10 and IL-15, with or without 5mM 3-MA, for 72 hours. Bafilomycin A_1 was added to a concentration of 100nM for the final hour of culture. **A**. Immunoblotting for LC3, representative of 2 independent experiments. **B**. LC3-II:actin ratio, n=2 per group.

metabolic demands may perhaps differ, *e.g.* cytokine production *vs.* endoplasmic reticulum expansion.

6.3.1.2 Autophagy and plasmablast differentiation

Results generated in Vav-Atg7$^{-/-}$ and human B cells demonstrate that autophagy is required for plasmablast formation. As described above, the importance of the UPR in plasmablast function is well established. The UPR is associated with activation of autophagy through JNK signaling, and the two pathways have significant overlap in function. It is likely therefore that autophagy acts in concert with the UPR to contain the cellular stress associated with immunoglobulin production. My data demonstrates that following culture, there is significantly less viability in the Vav-Atg7$^{-/-}$ plasmablasts than in the control population. Many cell survival functions performed by autophagy may explain this finding, and one of which I examined

was mitophagy. There was higher mitochondrial density in the B cells of the Vav-Atg7$^{-/-}$ mice, suggestive of disrupted mitophagy. Mitophagy is required for the clearance of damaged and defective mitochondria, which would otherwise predispose the cell to apoptosis[40]. It is therefore possible that this at least in part accounts for the impaired viability observed in the autophagy deficient cells.

During the production of the results presented in this chapter, two groups reported largely similar findings, but with significant differences in detail, both using the same *CD19*-Cre-*Atg5*$^{Flox/Flox}$ conditional knockout mouse model[238;239]. The *CD19*-Cre-*Atg5*$^{Flox/Flox}$ mouse selectively deletes *Atg5* in B cells, and therefore relevant *in vivo* experimentation is possible, which is not the case in the Vav-Atg7$^{-/-}$ mouse, which has autophagy deficiency throughout its immune system. Despite this, however, the immunophenotype of the Vav-Atg7$^{-/-}$ mouse does appear to be largely similar to the *CD19*-Cre-*Atg5*$^{Flox/Flox}$, in that the mature B cell pool appears to be proportionally normal. The numerical and likely functional deficit in T cells would be expected to limit the immune response to T-dependent antigens, rendering comparisons of terminal B cell differentiation difficult.

Whilst Conway *et al*., Pengo *et al*. and I draw the same conclusion, that autophagy is required for plasmablast differentiation; there are important variations in our results[238;239]. Conway *et al*. and I found that *in vitro* plasma cell development was substantially impaired, with reduced antibody secretion following LPS stimulation. However, Pengo *et al*. detected no difference in CD138^{+} cell proportion after a similar culture period, and no defect in proliferation. Despite this discrepancy, they found approximately twice the proportion of apoptotic cells in the *Atg5*$^{-/-}$ culture versus the control, whereas Conway *et al.* detected no increase in apoptosis. Why these differences should occur is not clear. All three experiments used different concentrations of LPS (10 or 20μg/ml), and my culture was supplemented with IL-4. It is possible that autophagy has varying importance dependent on the de-

gree and nature of stimulation. It may also be the case that B cells isolated from the Vav-Atg7$^{-/-}$ mouse, which has generalized dysfunction of the immune system, may be inherently more susceptible to apoptosis and less amenable to plasmablast formation, due to diminished cytokine support. Alternatively, *Atg7* deletion may lead to a phenotype distinct from *Atg5* knockout, rather than generic autophagy deficiency[322].

Whilst I noted increased mitochondrial density in autophagy-deficient B cells, Pengo *et al*. found that mitochondria-associated proteins were not over-represented, using stable isotope labeling in cell culture (SILAC) followed by mass spectrometry. They did however, detect an increase in ER-resident proteins, and components of the immunoglobulin molecule. Dye labeling of mitochondria, and mass spectrometric identification of mitochondria-associated proteins are very different techniques, but apparently intact mitophagy in B cells would be a finding against expectation.

There are further significant differences in the findings of Conway *et al*. and Pengo *et al*. Notably, Conway *et al*. detect substantially fewer plasma cells in the bone marrow of *CD19*-Cre-*Atg5*$^{Flox/Flox}$ mice, whereas Pengo *et al*. find no difference compared with controls. The immunophenotyping strategies adopted by the two groups are different, with Pengo *et al*. gating on IRF4^{+}B220^{-}CD138^{+}, whilst Conway *et al*. define plasma cells as CD19^{+}CD138^{+}. CD138 is also expressed during the pre-B stage of B cell development, and so the former gating definition is to be favored[323]. Interestingly, Conway *et al*. find that serum immunoglobulin levels are not reduced in the *CD19*-Cre-*Atg5*$^{Flox/Flox}$ mouse. Examining differences at the mRNA transcript level, Conway *et al*. detected impaired expression of the transcription factors XBP-1 and PRDM1 in *CD19*-Cre-*Atg5*$^{Flox/Flox}$ B cells stimulated with LPS, whereas Pengo *et al*. found that levels of these transcripts were in fact increased.

However, both authors agree that the antibody response to both TD and TI im-

munization is impaired in the conditional knockout. In the TD response, processing of the antigen by the B cell with subsequent presentation to its cognate $CD4^+$ T cell provides co-stimulation and leads to B cell proliferation. The TI response is independent of T cell help, and is elicited by engagement of TLRs, or multivalent binding of antigen to the BCR. The TI response does not lead to SHM or CSR. Interestingly, Pengo *et al*. found that the antibody response to NP-Ficoll, a TI hapten that resists clearance and leads to long-term production of immunoglobulin by B1a cells[324], was in fact enhanced in the *CD19*-Cre-$Atg5^{Flox/Flox}$ mouse. Why this should be the case is not clear. Equally intriguingly, they also find that immunoglobulin secretion appears to be increased in autophagy deficient B cells. Conway *et al*. detected increased intracellular and surface immunoglobulin levels, but impaired secretion.

Overall, there is substantial variation in the details of the phenotype of murine B cells deficient in autophagy, with reconciliation of some of the experimental results proving difficult. Further work needs to be done to confidently establish the role of autophagy in B cell development and homeostasis.

7 Conclusions

In the work presented in this thesis, I have demonstrated activation of autophagy in immune cells in SLE, notably in B lymphocytes, which represents a novel finding. Similarly, the roles autophagy might play in B cell function have been relatively less explored compared with T cells. For this reason, autophagy in B cells was specifically chosen for more detailed study investigation. In order to overcome the limitations imposed by small sample quantities available from diseased patients, novel flow-based assays were developed and utilized.

Examination of the peripheral B cell compartment in SLE indicates that autophagy is principally enhanced in the naïve subpopulation. A potential explanation for this observation is that autophagy is acting to sustain self-reactive B cells newly egressed from the bone marrow, which would appropriately undergo apoptosis to avoid the development of autoimmunity. To explore these findings more completely, I assayed the central and peripheral B cell populations of the NZB/W murine model of SLE, which allows exclusion of the potentially confounding variable of pharmacologic intervention, and also allows access to developing B cells in the bone marrow. The observations made in the peripheral B cell pool of the NZB/W mouse recapitulated those in SLE patients, with autophagy activation prominent in less mature cells. In the bone marrow, there were strikingly higher levels of autophagy in developing B cells, with a greater differential between control and NZB/W mice. Examining NZB/W mice of differing ages, I observed increased autophagy in the

disease model even before the clinical onset of lupus. Finally, gaining insight into the functional properties of autophagy, I noted a requirement for this process in the efficient differentiation of murine and human plasmablasts.

These results require explanation, and to determine the role of autophagy in the pathogenesis of SLE, and in normal and autoreactive B cell development, much more work needs to be done. Firstly, cause and effect need to be established in the observation that autophagy is increased in SLE. The data I have collected so far do not permit it to be concluded whether enhancement of autophagy is potentially requisite to the development of disease, or if it is a reactive phenomenon driven by threatened cell death. It is even possible that autophagy may be acting in some capacity as a pro-cell death mechanism, thereby limiting autoimmunity. This question may be resolved experimentally by the use of a model of SLE established in an autophagy-deficient background. Should modulation of autophagy prove to prevent or reduce the severity of experimental SLE, then a strong argument would be created for the trial of autophagy-modifying agents in human autoimmune disease. The detection of differential autophagy during B cell developmental stages in both normal and diseased mice suggests as yet undefined roles for this process in B cell ontogeny. In murine models deficient in autophagy in haematopoietic cells, there is a developmental block at the pro- to pre-B cell transition, which is however surmountable, as there is a relatively normal peripheral mature B2 cell pool. Conditional deletion of autophagy genes under the control of the CD19 promotor is not however associated with early developmental defects, which is in keeping with maximal activation of autophagy at the pro-B cell stage. This observation corresponds to equivalent findings in T cell development at the 'double negative' thymocyte stage. The seemingly specific nature of this block is interesting and does not have an obvious explanation. The pro-B cell stage is associated with the recombination of the immunoglobulin heavy chain locus, which might, through the generation

of DNA damage, recruit autophagy as a mechanism to counter stress. However, since autophagy seems to be redundant at the pre-B cell stage, when light chain recombination occurs, it may be that signaling from the pre-BCR, aided by surrogate light chains, provides the necessary survival stimulus and autophagy is no longer required. This hypothesis, outlined in figure 7.1, again requires further investigation, as does the explanation for the difference in autophagy seen in the NZB/W mouse model of lupus.

Autophagy may be modulated by a number of FDA approved pharmaceutical agents, and therefore represents an interesting target for the treatment of autoimmune disease. Inhibition of autophagy may be one mode of action of hydroxychloroquine in SLE, and this potential for rapid therapeutic translation is further supportive of the need for further investigation.

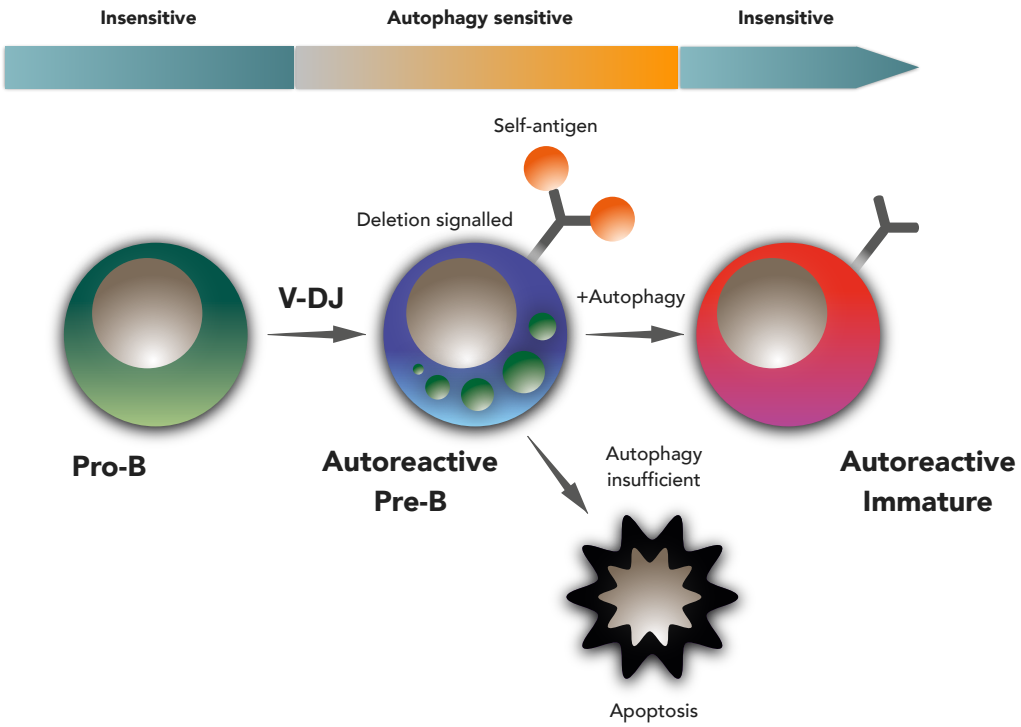

Figure 7.1: **Autophagy in B cell autoimmunity**. Following generation of an autoreactive surface Ig molecule, apoptosis is induced should editing fail. I hypothesize that autophagy is activated and aids autoreactive cell survival.

Bibliography

[1] Nakatogawa, H, Suzuki, K, Kamada, Y, & Ohsumi, Y. (2009) Dynamics and diversity in autophagy mechanisms: lessons from yeast. *Nature Reviews Molecular Cell Biology* **10**, 458–467.

[2] Tooze, S. A & Yoshimori, T. (2010) The origin of the autophagosomal membrane. *Nature Cell Biology* **12**, 831–835.

[3] Hamasaki, M, Furuta, N, Matsuda, A, Nezu, A, Yamamoto, A, Fujita, N, Oomori, H, Noda, T, Haraguchi, T, Hiraoka, Y, Amano, A, & Yoshimori, T. (2013) Autophagosomes form at ER-mitochondria contact sites. *Nature* **495**, 389–393.

[4] Mizushima, N. (2010) The role of the Atg1/ULK1 complex in autophagy regulation. *Current Opinion in Cell Biology* **22**, 132–139.

[5] Kim, J, Kundu, M, Viollet, B, & Guan, K.-L. (2011) AMPK and mTOR regulate autophagy through direct phosphorylation of Ulk1. *Nature Cell Biology* **13**, 132–141.

[6] Gammoh, N, Florey, O, Overholtzer, M, & Jiang, X. (2012) Interaction between FIP200 and ATG16L1 distinguishes ULK1 complex–dependent and –independent autophagy. *Nature Structural & Molecular Biology* **20**, 144–149.

[7] McAlpine, F, Williamson, L. E, Tooze, S. A, & Chan, E. Y. W. (2013) Regulation of nutrient-sensitive autophagy by uncoordinated 51-like kinases 1 and 2. *Autophagy* **9**, 361–373.

[8] Simonsen, A & Tooze, S. A. (2009) Coordination of membrane events during autophagy by multiple class III PI3-kinase complexes. *The Journal of Cell Biology* **186**, 773–782.

[9] Axe, E. L, Walker, S. A, Manifava, M, Chandra, P, Roderick, H. L, Habermann, A, Griffiths, G, & Ktistakis, N. T. (2008) Autophagosome formation from membrane compartments enriched in phosphatidylinositol 3-phosphate and dynamically connected to the endoplasmic reticulum. *The Journal of Cell Biology* **182**, 685–701.

[10] Okkenhaug, K. (2013) Signaling by the Phosphoinositide 3-Kinase Family in Immune Cells. *Annual Review of Immunology* **31**, 675–704.

[11] Polson, H. E. J, de Lartigue, J, Rigden, D. J, Reedijk, M, Urbé, S, Clague, M. J, & Tooze, S. A. (2010) Mammalian Atg18 (WIPI2) localizes to omegasome-anchored phagophores and positively regulates LC3 lipidation. *Autophagy* **6**, 506–522.

[12] Mizushima, N, Noda, T, Yoshimori, T, Tanaka, Y, Ishii, T, George, M. D, Klionsky, D. J, Ohsumi, M, & Ohsumi, Y. (1998) A protein conjugation system essential for autophagy. *Nature* **395**, 395–398.

[13] Mizushima, N, Sugita, H, Yoshimori, T, & Ohsumi, Y. (1998) A new protein conjugation system in human. The counterpart of the yeast Apg12p conjugation system essential for autophagy. *The Journal of Biological Chemistry* **273**, 33889–33892.

[14] Mizushima, N. (2003) Mouse Apg16L, a novel WD-repeat protein, targets to the autophagic isolation membrane with the Apg12-Apg5 conjugate. *Journal of Cell Science* **116**, 1679–1688.

[15] Fujita, N, Itoh, T, Omori, H, Fukuda, M, Noda, T, & Yoshimori, T. (2008) The Atg16L complex specifies the site of LC3 lipidation for membrane biogenesis in autophagy. *Molecular Biology of the Cell* **19**, 2092–2100.

[16] Ichimura, Y, Kirisako, T, Takao, T, Satomi, Y, Shimonishi, Y, Ishihara, N, Mizushima, N, Tanida, I, Kominami, E, Ohsumi, M, Noda, T, & Ohsumi, Y. (2000) A ubiquitin-like system mediates protein lipidation. *Nature* **408**, 488–492.

[17] Hanada, T, Noda, N. N, Satomi, Y, Ichimura, Y, Fujioka, Y, Takao, T, Inagaki, F, & Ohsumi, Y. (2007) The Atg12-Atg5 Conjugate Has a Novel E3-like Activity for Protein Lipidation in Autophagy. *The Journal of Biological Chemistry* **282**, 37298–37302.

[18] Nair, U, Yen, W.-L, Mari, M, Cao, Y, Xie, Z, Baba, M, Reggiori, F, & Klionsky, D. J. (2012) A role for Atg8-PE deconjugation in autophagosome biogenesis. *Autophagy* **8**, 780–793.

[19] Kirisako, T, Ichimura, Y, Okada, H, Kabeya, Y, Mizushima, N, Yoshimori, T, Ohsumi, M, Takao, T, Noda, T, & Ohsumi, Y. (2000) The reversible modification regulates the membrane-binding state of Apg8/Aut7 essential for autophagy and the cytoplasm to vacuole targeting pathway. *The Journal of Cell Biology* **151**, 263–276.

[20] Nakatogawa, H, Ichimura, Y, & Ohsumi, Y. (2007) Atg8, a Ubiquitin-like Protein Required for Autophagosome Formation, Mediates Membrane Tethering and Hemifusion. *Cell* **130**, 165–178.

[21] Mizushima, N, Yoshimori, T, & Levine, B. (2010) Methods in mammalian autophagy research. *Cell* **140**, 313–326.

[22] Fass, E, Shvets, E, Degani, I, Hirschberg, K, & Elazar, Z. (2006) Microtubules support production of starvation-induced autophagosomes but not their targeting and fusion with lysosomes. *The Journal of Biological Chemistry* **281**, 36303–36316.

[23] Lee, J.-A, Beigneux, A, Ahmad, S. T, Young, S. G, & Gao, F.-B. (2007) ESCRT-III Dysfunction Causes Autophagosome Accumulation and Neurodegeneration. *Current Biology* **17**, 1561–1567.

[24] Liang, C, Lee, J.-s, Inn, K.-S, Gack, M. U, Li, Q, Roberts, E. A, Vergne, I, Deretic, V, Feng, P, Akazawa, C, & Jung, J. U. (2008) Beclin1-binding UVRAG targets the class C Vps complex to coordinate autophagosome maturation and endocytic trafficking. *Nature Cell Biology* **10**, 776–787.

[25] Gutierrez, M. G. (2004) Rab7 is required for the normal progression of the autophagic pathway in mammalian cells. *Journal of Cell Science* **117**, 2687–2697.

[26] Berg, T. O, Fengsrud, M, Strømhaug, P. E, Berg, T, & Seglen, P. O. (1998) Isolation and characterization of rat liver amphisomes. Evidence for fusion of autophagosomes with both early and late endosomes. *The Journal of Biological Chemistry* **273**, 21883–21892.

[27] Korolchuk, V. I, Saiki, S, Lichtenberg, M, Siddiqi, F. H, Roberts, E. A, Imarisio, S, Jahreiss, L, Sarkar, S, Futter, M, Menzies, F. M, O'Kane, C. J, Deretic, V, & Rubinsztein, D. C. (2011) Lysosomal positioning coordinates cellular nutrient responses. *Nature Cell Biology* **13**, 453–460.

[28] Settembre, C, Di Malta, C, Polito, V. A, Arencibia, M. G, Vetrini, F, Erdin, S, Erdin, S. U, Huynh, T, Medina, D, Colella, P, Sardiello, M, Rubinsztein, D. C, & Ballabio, A. (2011) TFEB Links Autophagy to Lysosomal Biogenesis. *Science* **332**, 1429–1433.

[29] Nair, U, Jotwani, A, Geng, J, Gammoh, N, Richerson, D, Yen, W.-L, Griffith, J, Nag, S, Wang, K, Moss, T, Baba, M, McNew, J. A, Jiang, X, Reggiori, F, Melia, T. J, & Klionsky, D. J. (2011) SNARE Proteins Are Required for Macroautophagy. *Cell* **146**, 290–302.

[30] Yamamoto, A, Tagawa, Y, Yoshimori, T, Moriyama, Y, Masaki, R, & Tashiro, Y. (1998) Bafilomycin A1 prevents maturation of autophagic vacuoles by inhibiting fusion between autophagosomes and lysosomes in rat hepatoma cell line, H-4-II-E cells. *Cell Structure and Function* **23**, 33–42.

[31] Pankiv, S, Clausen, T. H, Lamark, T, Brech, A, Bruun, J. A, Outzen, H, Overvatn, A, Bjorkoy, G, & Johansen, T. (2007) p62/SQSTM1 Binds Directly to Atg8/LC3 to Facilitate Degradation of Ubiquitinated Protein Aggregates by Autophagy. *Journal of Biological Chemistry* **282**, 24131–24145.

[32] Bjorkoy, G. (2005) p62/SQSTM1 forms protein aggregates degraded by autophagy and has a protective effect on huntingtin-induced cell death. *The Journal of Cell Biology* **171**, 603–614.

[33] Mathew, R, Karp, C. M, Beaudoin, B, Vuong, N, Chen, G, Chen, H.-Y, Bray, K, Reddy, A, Bhanot, G, Gelinas, C, DiPaola, R. S, Karantza-Wadsworth, V, & White, E. (2009) Autophagy Suppresses Tumorigenesis through Elimination of p62. *Cell* **137**, 1062–1075.

[34] Komatsu, M, Waguri, S, Koike, M, Sou, Y.-S, Ueno, T, Hara, T, Mizushima, N, Iwata, J.-i, Ezaki, J, Murata, S, Hamazaki, J, Nishito, Y, Iemura, S.-I, Natsume,

T, Yanagawa, T, Uwayama, J, Warabi, E, Yoshida, H, Ishii, T, Kobayashi, A, Yamamoto, M, Yue, Z, Uchiyama, Y, Kominami, E, & Tanaka, K. (2007) Homeostatic levels of p62 control cytoplasmic inclusion body formation in autophagy-deficient mice. *Cell* **131**, 1149–1163.

[35] Johansen, T & Lamark, T. (2011) Selective autophagy mediated by autophagic adapter proteins. *Autophagy* **7**, 279–296.

[36] Kirkin, V, Lamark, T, Sou, Y.-S, Bjoslashrkoslashy, G, Nunn, J. L, Bruun, J.-A, Shvets, E, McEwan, D. G, Clausen, T. H, Wild, P, Bilusic, I, Theurillat, J.-P, Oslashvervatn, A, Ishii, T, Elazar, Z, Komatsu, M, Dikic, I, & Johansen, T. (2009) A Role for NBR1 in Autophagosomal Degradation of Ubiquitinated Substrates. *Molecular Cell* **33**, 505–516.

[37] Yang, J.-Q, Liu, H, Diaz-Meco, M. T, & Moscat, J. (2010) NBR1 is a new PB1 signalling adapter in Th2 differentiation and allergic airway inflammation in vivo. *The EMBO Journal* **29**, 3421–3433.

[38] Thurston, T. L. M, Wandel, M. P, von Muhlinen, N, Foeglein, Á, & Randow, F. (2013) Galectin 8 targets damaged vesicles for autophagy to defend cells against bacterial invasion. *Nature* **482**, 414–418.

[39] Thurston, T. L. M, Ryzhakov, G, Bloor, S, von Muhlinen, N, & Randow, F. (2009) The TBK1 adaptor and autophagy receptor NDP52 restricts the proliferation of ubiquitin-coated bacteria. *Nature Immunology* **10**, 1215–1221.

[40] Youle, R. J & Narendra, D. P. (2011) Mechanisms of mitophagy. *Nature Reviews Molecular Cell Biology* **12**, 9–14.

[41] Andersen, J. L & Kornbluth, S. (2013) The Tangled Circuitry of Metabolism and Apoptosis. *Molecular Cell* **49**, 399–410.

[42] Schweers, R. L, Zhang, J, Randall, M. S, Loyd, M. R, Li, W, Dorsey, F. C, Kundu, M, Opferman, J. T, Cleveland, J. L, Miller, J. L, & Ney, P. A. (2007) NIX is required for programmed mitochondrial clearance during reticulocyte maturation. *Proceedings of the National Academy of Sciences* **104**, 19500–19505.

[43] Al Rawi, S, Louvet-Vallee, S, Djeddi, A, Sachse, M, Culetto, E, Hajjar, C, Boyd, L, Legouis, R, & Galy, V. (2011) Postfertilization Autophagy of Sperm Organelles Prevents Paternal Mitochondrial DNA Transmission. *Science* **334**, 1144–1147.

[44] Sandoval, H, Thiagarajan, P, Dasgupta, S. K, Schumacher, A, Prchal, J. T, Chen, M, & Wang, J. (2008) Essential role for Nix in autophagic maturation of erythroid cells. *Nature* **454**, 232–235.

[45] Aerbajinai, W. (2003) The proapoptotic factor Nix is coexpressed with Bcl-xL during terminal erythroid differentiation. *Blood* **102**, 712–717.

[46] Novak, I, Kirkin, V, McEwan, D. G, Zhang, J, Wild, P, Rozenknop, A, Rogov, V, hr, F. L. o, Popovic, D, Occhipinti, A, Reichert, A. S, Terzic, J, tsch, V. D. o, Ney, P. A, & Dikic, I. (2009) scientific report. *EMBO reports* **11**, 45–51.

[47] Valente, E. M. (2004) Hereditary Early-Onset Parkinson's Disease Caused by Mutations in PINK1. *Science* **304**, 1158–1160.

[48] Kitada, T, Asakawa, S, Hattori, N, Matsumine, H, Yamamura, Y, Minoshima, S, Yokochi, M, Mizuno, Y, & Shimizu, N. (1998) Mutations in the parkin gene cause autosomal recessive juvenile parkinsonism. *Nature* **392**, 605–608.

[49] Laplante, M & Sabatini, D. M. (2012) mTOR Signaling in Growth Control and Disease. *Cell* **149**, 274–293.

[50] Nicklin, P, Bergman, P, Zhang, B, Triantafellow, E, Wang, H, Nyfeler, B, Yang, H, Hild, M, Kung, C, Wilson, C, Myer, V. E, MacKeigan, J. P, Porter, J. A, Wang, Y. K, Cantley, L. C, Finan, P. M, & Murphy, L. O. (2009) Bidirectional Transport of Amino Acids Regulates mTOR and Autophagy. *Cell* **136**, 521–534.

[51] Sancak, Y, Bar-Peled, L, Zoncu, R, Markhard, A. L, Nada, S, & Sabatini, D. M. (2010) Ragulator-Rag Complex Targets mTORC1 to the Lysosomal Surface and Is Necessary for Its Activation by Amino Acids. *Cell* **141**, 290–303.

[52] Jung, C. H, Jun, C. B, Ro, S.-H, Kim, Y.-M, Otto, N. M, Cao, J, Kundu, M, & Kim, D.-H. (2009) ULK-Atg13-FIP200 complexes mediate mTOR signaling to the autophagy machinery. *Molecular Biology of the Cell* **20**, 1992–2003.

[53] Hosokawa, N, Hara, T, Kaizuka, T, Kishi, C, Takamura, A, Miura, Y, Iemura, S.-I, Natsume, T, Takehana, K, Yamada, N, Guan, J.-L, Oshiro, N, & Mizushima, N. (2009) Nutrient-dependent mTORC1 association with the ULK1-Atg13-FIP200 complex required for autophagy. *Molecular Biology of the Cell* **20**, 1981–1991.

[54] Ganley, I. G, Lam, D. H, Wang, J, Ding, X, Chen, S, & Jiang, X. (2009) ULK1.ATG13.FIP200 complex mediates mTOR signaling and is essential for autophagy. *The Journal of Biological Chemistry* **284**, 12297–12305.

[55] Nazio, F, Strappazzon, F, Antonioli, M, Bielli, P, Cianfanelli, V, Bordi, M, Gretzmeier, C, Dengjel, J, Piacentini, M, Fimia, G. M, & Cecconi, F. (2013) mTOR inhibits autophagy by controlling ULK1 ubiquitylation, self-association and function through AMBRA1 and TRAF6. *Nature Cell Biology* **15**, 1–13.

[56] Powell, J. D & Delgoffe, G. M. (2010) The mammalian target of rapamycin: linking T cell differentiation, function, and metabolism. *Immunity* **33**, 301–311.

[57] Delgoffe, G. M, Kole, T. P, Zheng, Y, Zarek, P. E, Matthews, K. L, Xiao, B, Worley, P. F, Kozma, S. C, & Powell, J. D. (2009) The mTOR Kinase Differentially Regulates Effector and Regulatory T Cell Lineage Commitment. *Immunity* **30**, 832–844.

[58] Battaglia, M. (2005) Rapamycin selectively expands CD4+CD25+FoxP3+ regulatory T cells. *Blood* **105**, 4743–4748.

[59] Donahue, A. C & Fruman, D. A. (2007) Distinct signaling mechanisms activate the target of rapamycin in response to different B-cell stimuli. *European Journal of Immunology* **37**, 2923–2936.

[60] Wicker, L. S, Boltz, R. C, Matt, V, Nichols, E. A, Peterson, L. B, & Sigal, N. H. (1990) Suppression of B cell activation by cyclosporin A, FK506 and rapamycin. *European journal of immunology* **20**, 2277–2283.

[61] Hardie, D. G, Ross, F. A, & Hawley, S. A. (2012) AMPK: a nutrient and energy sensor that maintains energy homeostasis. *Nature Reviews Molecular Cell Biology* **13**, 251–262.

[62] Gwinn, D. M, Shackelford, D. B, Egan, D. F, Mihaylova, M. M, Mery, A, Vasquez, D. S, Turk, B. E, & Shaw, R. J. (2008) AMPK Phosphorylation of Raptor Mediates a Metabolic Checkpoint. *Molecular Cell* **30**, 214–226.

[63] Inoki, K, Zhu, T, & Guan, K.-L. (2003) TSC2 mediates cellular energy response to control cell growth and survival. *Cell* **115**, 577–590.

[64] Pearce, E. L & Pearce, E. J. (2013) Metabolic Pathways in Immune Cell Activation and Quiescence. *Immunity* **38**, 633–643.

[65] Shi, L. Z, Wang, R, Huang, G, Vogel, P, Neale, G, Green, D. R, & Chi, H. (2011) HIF1 -dependent glycolytic pathway orchestrates a metabolic checkpoint for

the differentiation of TH17 and Treg cells. *Journal of Experimental Medicine* **208**, 1367–1376.

[66] Michalek, R. D, Gerriets, V. A, Jacobs, S. R, Macintyre, A. N, MacIver, N. J, Mason, E. F, Sullivan, S. A, Nichols, A. G, & Rathmell, J. C. (2011) Cutting Edge: Distinct Glycolytic and Lipid Oxidative Metabolic Programs Are Essential for Effector and Regulatory CD4+ T Cell Subsets. *The Journal of Immunology* **186**, 3299–3303.

[67] Scherz-Shouval, R, Shvets, E, Fass, E, Shorer, H, Gil, L, & Elazar, Z. (2007) Reactive oxygen species are essential for autophagy and specifically regulate the activity of Atg4. *The EMBO Journal* **26**, 1749–1760.

[68] Nunnari, J & Suomalainen, A. (2012) Mitochondria: In Sickness and in Health. *Cell* **148**, 1145–1159.

[69] Copetti, T, Bertoli, C, Dalla, E, Demarchi, F, & Schneider, C. (2009) p65/RelA Modulates BECN1 Transcription and Autophagy. *Molecular and Cellular Biology* **29**, 2594–2608.

[70] Criollo, A, Senovilla, L, Authier, H. e. l. e. n, Maiuri, M. C, Morselli, E, Vitale, I, Kepp, O, Tasdemir, E, Galluzzi, L, Shen, S, Tailler, M, Delahaye, N, Tesniere, A, De Stefano, D, Ben Younes, A. e. n, Harper, F, Pierron, G. e. r, Lavandero, S, Zitvogel, L, Israel, A, Baud, V. e. r, & Kroemer, G. (2009) The IKK complex contributes to the induction of autophagy. *The EMBO Journal* **29**, 619–631.

[71] Comb, W. C, Cogswell, P, Sitcheran, R, & Baldwin, A. S. (2011) IKK-dependent, NF-κB-independent control of autophagic gene expression. *Oncogene* **30**, 1727–1732.

[72] Comb, W. C, Hutti, J. E, Cogswell, P, Cantley, L. C, & Baldwin, A. S. (2012)

p85α SH2 domain phosphorylation by IKK promotes feedback inhibition of PI3K and Akt in response to cellular starvation. *Molecular Cell* **45**, 719–730.

[73] Djavaheri-Mergny, M, Amelotti, M, Mathieu, J, Besancon, F, Bauvy, C, Souquere, S, Pierron, G, & Codogno, P. (2006) NF- B Activation Represses Tumor Necrosis Factor- -induced Autophagy. *The Journal of Biological Chemistry* **281**, 30373–30382.

[74] Nivon, M, Richet, E, Codogno, P, Arrigo, A.-P, & Kretz-Remy, C. (2009) Autophagy activation by NFkappaB is essential for cell survival after heat shock. *Autophagy* **5**, 766–783.

[75] Hoeflich, K. P, Luo, J, Rubie, E. A, Tsao, M.-S, Jin, O. U, & Woodgett, J. R. (2000) Requirement for glycogen synthase kinase-3β in cell survival and NF-κB activation. *Nature* **406**, 86–90.

[76] Cross, D. A, Alessi, D. R, Cohen, P, Andjelkovich, M, & Hemmings, B. A. (1995) Inhibition of glycogen synthase kinase-3 by insulin mediated by protein kinase B. *Nature* **378**, 785–789.

[77] Doble, B. W. (2003) GSK-3: tricks of the trade for a multi-tasking kinase. *Journal of Cell Science* **116**, 1175–1186.

[78] Lin, S. Y, Li, T. Y, Liu, Q, Zhang, C, Li, X, Chen, Y, Zhang, S. M, Lian, G, Liu, Q, Ruan, K, Wang, Z, Zhang, C. S, Chien, K. Y, Wu, J, Li, Q, Han, J, & Lin, S. C. (2012) GSK3-TIP60-ULK1 Signaling Pathway Links Growth Factor Deprivation to Autophagy. *Science* **336**, 477–481.

[79] Parr, C, Carzaniga, R, Gentleman, S. M, Van Leuven, F, Walter, J, & Sastre, M. (2012) Glycogen Synthase Kinase 3 Inhibition Promotes Lysosomal Biogenesis and Autophagic Degradation of the Amyloid- Precursor Protein. *Molecular and Cellular Biology* **32**, 4410–4418.

[80] Calnan, D. R & Brunet, A. (2008) The FoxO code. *Oncogene* **27**, 2276–2288.

[81] Mammucari, C, Milan, G, Romanello, V, Masiero, E, Rudolf, R, Del Piccolo, P, Burden, S. J, Di Lisi, R, Sandri, C, Zhao, J, Goldberg, A. L, Schiaffino, S, & Sandri, M. (2007) FoxO3 Controls Autophagy in Skeletal Muscle In Vivo. *Cell Metabolism* **6**, 458–471.

[82] Sengupta, A, Molkentin, J. D, & Yutzey, K. E. (2009) FoxO Transcription Factors Promote Autophagy in Cardiomyocytes. *Journal of Biological Chemistry* **284**, 28319–28331.

[83] Zhao, J, Brault, J. J, Schild, A, Cao, P, Sandri, M, Schiaffino, S, Lecker, S. H, & Goldberg, A. L. (2007) FoxO3 Coordinately Activates Protein Degradation by the Autophagic/Lysosomal and Proteasomal Pathways in Atrophying Muscle Cells. *Cell Metabolism* **6**, 472–483.

[84] Brunet, A, Bonni, A, Zigmond, M. J, Lin, M. Z, Juo, P, Hu, L. S, Anderson, M. J, Arden, K. C, Blenis, J, & Greenberg, M. E. (1999) Akt promotes cell survival by phosphorylating and inhibiting a Forkhead transcription factor. *Cell* **96**, 857–868.

[85] Greer, E. L, Oskoui, P. R, Banko, M. R, Maniar, J. M, Gygi, M. P, Gygi, S. P, & Brunet, A. (2007) The Energy Sensor AMP-activated Protein Kinase Directly Regulates the Mammalian FOXO3 Transcription Factor. *Journal of Biological Chemistry* **282**, 30107–30119.

[86] Warr, M. R, Binnewies, M, Flach, J, Reynaud, D, Garg, T, Malhotra, R, Debnath, J, & Passegué, E. (2013) FOXO3A directs a protective autophagy program in haematopoietic stem cells. *Nature* pp. 1–7.

[87] Lee, J. C, Espéli, M, Anderson, C. A, Linterman, M. A, Pocock, J. M, Williams, N. J, Roberts, R, Viatte, S, Fu, B, Peshu, N, Hien, T. T, Phu, N. H, Wesley,

E, Edwards, C, Ahmad, T, Mansfield, J. C, Gearry, R, Dunstan, S, Williams, T. N, Barton, A, Vinuesa, C. G, Consortium, U. I. G, Phillips, A, Mowat, C, Drummond, H, Kennedy, N, Lees, C. W, Satsangi, J, Taylor, K, Prescott, N. J, Mathew, C. G, Simpson, P, Simmons, A, Khan, M, Newman, W. G, Hawkey, C, Hart, A, Wilson, D. C, Henderson, P, Barrett, J. C, Parkes, M, Lyons, P. A, & Smith, K. G. C. (2013) Human SNP Links Differential Outcomes in Inflammatory and Infectious Disease to a FOXO3-Regulated Pathway. *Cell* pp. 1–13.

[88] Liang, X. H, Jackson, S, Seaman, M, Brown, K, Kempkes, B, Hibshoosh, H, & Levine, B. (1999) Induction of autophagy and inhibition of tumorigenesis by beclin 1. *Nature* **402**, 672–676.

[89] Yue, Z, Jin, S, Yang, C, Levine, A. J, & Heintz, N. (2003) Beclin 1, an autophagy gene essential for early embryonic development, is a haploinsufficient tumor suppressor. *Proceedings of the National Academy of Sciences* **100**, 15077–15082.

[90] Oberstein, A, Jeffrey, P. D, & Shi, Y. (2007) Crystal Structure of the Bcl-XL-Beclin 1 Peptide Complex: Beclin-1 is a BH3-only protein. *Journal of Biological Chemistry* **282**, 13123–13132.

[91] Pattingre, S, Tassa, A, Qu, X, Garuti, R, Liang, X. H, Mizushima, N, Packer, M, Schneider, M. D, & Levine, B. (2005) Bcl-2 Antiapoptotic Proteins Inhibit Beclin 1-Dependent Autophagy. *Cell* **122**, 927–939.

[92] Maiuri, M. C, Le Toumelin, G, Criollo, A, Rain, J.-C, Gautier, F, Juin, P, Tasdemir, E, Pierron, G, Troulinaki, K, & Tavernarakis, N. (2007) Functional and physical interaction between Bcl-XL and a BH3-like domain in Beclin-1. *The EMBO Journal* **26**, 2527–2539.

[93] Daido, S, Kanzawa, T, Yamamoto, A, Takeuchi, H, Kondo, Y, & Kondo, S.

(2004) Pivotal role of the cell death factor BNIP3 in ceramide-induced autophagic cell death in malignant glioma cells. *Cancer Research* **64**, 4286–4293.

[94] Abedin, M. J, Wang, D, McDonnell, M. A, Lehmann, U, & Kelekar, A. (2006) Autophagy delays apoptotic death in breast cancer cells following DNA damage. *Cell Death and Differentiation* **14**, 500–510.

[95] Noble, C. G, Dong, J. M, Manser, E, & Song, H. (2008) Bcl-xL and UVRAG Cause a Monomer-Dimer Switch in Beclin1. *Journal of Biological Chemistry* **283**, 26274–26282.

[96] Adi-Harel, S, Erlich, S, Schmukler, E, Cohen-Kedar, S, Segev, O, Mizrachy, L, Hirsch, J. A, & Pinkas-Kramarski, R. (2010) Beclin 1 self-association is independent of autophagy induction by amino acid deprivation and rapamycin treatment. *Journal of Cellular Biochemistry* **110**, 1262–1271.

[97] Zalckvar, E, Berissi, H, Mizrachy, L, Idelchuk, Y, Koren, I, Eisenstein, M, Sabanay, H, Pinkas-Kramarski, R, & Kimchi, A. (2009) DAP-kinase-mediated phosphorylation on the BH3 domain of beclin 1 promotes dissociation of beclin 1 from Bcl-XL and induction of autophagy. *EMBO reports* **10**, 285–292.

[98] Shi, C. S & Kehrl, J. H. (2010) TRAF6 and A20 Regulate Lysine 63-Linked Ubiquitination of Beclin-1 to Control TLR4-Induced Autophagy. *Science Signaling* **3**, ra42–ra42.

[99] Goldblatt, F & O'Neill, S. G. (2013) Clinical aspects of autoimmune rheumatic diseases. *The Lancet* **382**, 797–808.

[100] McCarty, D. J, Manzi, S, Medsger, T. A, Ramsey-Goldman, R, LaPorte, R. E, & Kwoh, C. K. (1995) Incidence of systemic lupus erythematosus. Race and gender differences. *Arthritis and Rheumatism* **38**, 1260–1270.

[101] Johnson, A. E, Gordon, C, Palmer, R. G, & Bacon, P. A. (1995) The prevalence and incidence of systemic lupus erythematosus in Birmingham, England. *Arthritis and Rheumatism* **38**, 551–558.

[102] Alarcon-Segovia, D, Alarcon-Riquelme, M. E, Cardiel, M. H, Caeiro, F, Massardo, L, Villa, A. R, Pons-Estel, B. A, & on behalf of the Grupo Latinoamericano de Estudio del Lupus Eritematoso (GLADEL). (2005) Familial aggregation of systemic lupus erythematosus, rheumatoid arthritis, and other autoimmune diseases in 1,177 lupus patients from the GLADEL cohort. *Arthritis and Rheumatism* **52**, 1138–1147.

[103] Manderson, A. P, Botto, M, & Walport, M. J. (2004) The Role of Complement in the Development of Systemic Lupus Erythematosus. *Annual Review of Immunology* **22**, 431–456.

[104] Rhodes, B & Vyse, T. J. (2008) The genetics of SLE: an update in the light of genome-wide association studies. *Rheumatology (Oxford, England)* **47**, 1603–1611.

[105] Project, T. E & Consortium. (2013) An integrated encyclopedia of DNA elements in the human genome. *Nature* **488**, 57–74.

[106] Gateva, V, Sandling, J. K, Hom, G, Taylor, K. E, Chung, S. A, Sun, X, Ortmann, W, Kosoy, R, Ferreira, R. C, Nordmark, G, Gunnarsson, I, Svenungsson, E, Padyukov, L, Sturfelt, G, Jönsen, A, Bengtsson, A. A, Rantapää-Dahlqvist, S, Baechler, E. C, Brown, E. E, Alarcón, G. S, Edberg, J. C, Ramsey-Goldman, R, McGwin, G, Reveille, J. D, Vila, L. M, Kimberly, R. P, Manzi, S, Petri, M. A, Lee, A, Gregersen, P. K, Seldin, M. F, Rönnblom, L, Criswell, L. A, Syvänen, A.-C, Behrens, T. W, & Graham, R. R. (2009) A large-scale replication study

identifies TNIP1, PRDM1, JAZF1, UHRF1BP1 and IL10 as risk loci for systemic lupus erythematosus. *Nature Genetics* **41**, 1228–1233.

[107] Han, J.-W, Zheng, H.-F, Cui, Y, Sun, L.-D, Ye, D.-Q, Hu, Z, Xu, J.-H, Cai, Z.-M, Huang, W, Zhao, G.-P, Xie, H.-F, Fang, H, Lu, Q.-J, Xu, J.-H, Li, X.-P, Pan, Y.-F, Deng, D.-Q, Zeng, F.-Q, Ye, Z.-Z, Zhang, X.-Y, Wang, Q.-W, Hao, F, Ma, L, Zuo, X.-B, Zhou, F.-S, Du, W.-H, Cheng, Y.-L, Yang, J.-Q, Shen, S.-K, Li, J, Sheng, Y.-J, Zuo, X.-X, Zhu, W.-F, Gao, F, Zhang, P.-L, Guo, Q, Li, B, Gao, M, Xiao, F.-L, Quan, C, Zhang, C, Zhang, Z, Zhu, K.-J, Li, Y, Hu, D.-Y, Lu, W.-S, Huang, J.-L, Liu, S.-X, Li, H, Ren, Y.-Q, Wang, Z.-X, Yang, C.-J, Wang, P.-G, Zhou, W.-M, Lv, Y.-M, Zhang, A.-P, Zhang, S.-Q, Lin, D, Li, Y, Low, H. Q, Shen, M, Zhai, Z.-F, Wang, Y, Zhang, F.-Y, Yang, S, Liu, J.-J, & Zhang, X.-J. (2009) Genome-wide association study in a Chinese Han population identifies nine new susceptibility loci for systemic lupus erythematosus. *Nature Genetics* **41**, 1234–1237.

[108] for Systemic Lupus Erythematosus Genetics SLEGEN, I. C, Harley, J. B, Alarcon-Riquelme, M. E, Criswell, L. A, Jacob, C. O, Kimberly, R. P, Moser, K. L, Tsao, B. P, Vyse, T. J, Langefeld, C. D, Nath, S. K, Guthridge, J. M, Cobb, B. L, Mirel, D. B, Marion, M. C, Williams, A. H, Divers, J, Wang, W, Frank, S. G, Namjou, B, Gabriel, S. B, Lee, A. T, Gregersen, P. K, Behrens, T. W, Taylor, K. E, Fernando, M, Zidovetzki, R, Gaffney, P. M, Edberg, J. C, Rioux, J. D, Ojwang, J. O, James, J. A, Merrill, J. T, Gilkeson, G. S, Seldin, M. F, Yin, H, Baechler, E. C, Li, Q.-Z, Wakeland, E. K, Bruner, G. R, Kaufman, K. M, & Kelly, J. A. (2008) Genome-wide association scan in women with systemic lupus erythematosus identifies susceptibility variants in ITGAM, PXK, KIAA1542 and other loci. *Nature Genetics* **40**, 204–210.

[109] Nalbandian, G, Paharkova-Vatchkova, V, Mao, A, Nale, S, & Kovats, S. (2005)

The selective estrogen receptor modulators, tamoxifen and raloxifene, impair dendritic cell differentiation and activation. *Journal of Immunology* **175**, 2666–2675.

[110] Carreras, E, Turner, S, Paharkova-Vatchkova, V, Mao, A, Dascher, C, & Kovats, S. (2008) Estradiol acts directly on bone marrow myeloid progenitors to differentially regulate GM-CSF or Flt3 ligand-mediated dendritic cell differentiation. *Journal of immunology (Baltimore, Md : 1950)* **180**, 727–738.

[111] Zoller, A. L & Kersh, G. J. (2006) Estrogen induces thymic atrophy by eliminating early thymic progenitors and inhibiting proliferation of beta-selected thymocytes. *Journal of Immunology* **176**, 7371–7378.

[112] Medina, K. L, Strasser, A, & Kincade, P. W. (2000) Estrogen influences the differentiation, proliferation, and survival of early B-lineage precursors. *Blood* **95**, 2059–2067.

[113] Sakiani, S, Olsen, N. J, & Kovacs, W. J. (2012) Gonadal steroids and humoral immunity. *Nature Reviews Endocrinology* **9**, 56–62.

[114] Oertelt-Prigione, S. (2012) The influence of sex and gender on the immune response. *Autoimmunity Reviews* **11**, A479–A485.

[115] Sánchez-Guerrero, J, González-Pérez, M, Durand-Carbajal, M, Lara-Reyes, P, Jiménez-Santana, L, Romero-Díaz, J, & Cravioto, M.-d.-C. (2007) Menopause hormonal therapy in women with systemic lupus erythematosus. *Arthritis and Rheumatism* **56**, 3070–3079.

[116] Kaufman, K. M, Zhao, J, Kelly, J. A, Hughes, T, Adler, A, Sanchez, E, Ojwang, J. O, Langefeld, C. D, Ziegler, J. T, Williams, A. H, Comeau, M. E, Marion, M. C, Glenn, S. B, Cantor, R. M, Grossman, J. M, Hahn, B. H, Song, Y. W,

Yu, C. Y, James, J. A, Guthridge, J. M, Brown, E. E, Alarcon, G. S, Kimberly, R. P, Edberg, J. C, Ramsey-Goldman, R, Petri, M. A, Reveille, J. D, Vila, L. M, Anaya, J. M, Boackle, S. A, Stevens, A. M, Freedman, B. I, Criswell, L. A, Bernardo A Pons-Estel on behalf of the Argentine Collaborative Group, Lee, J. H, Lee, J. S, Chang, D. M, Scofield, R. H. A, Gilkeson, G. S, Merrill, J. T, Niewold, T. B, Vyse, T. J, Bae, S.-C, Marta E Alarcon-Riquelme on behalf of the BIOLUPUS network, Jacob, C. O, Moser Sivils, K, Gaffney, P. M, Harley, J. B, Sawalha, A. H, & Tsao, B. P. (2013) Fine mapping of Xq28: both MECP2 and IRAK1 contribute to risk for systemic lupus erythematosus in multiple ancestral groups. *Annals of the Rheumatic Diseases* **72**, 437–444.

[117] Sasidhar, M. V, Itoh, N, Gold, S. M, Lawson, G. W, & Voskuhl, R. R. (2012) The XX sex chromosome complement in mice is associated with increased spontaneous lupus compared with XY. *Annals of the Rheumatic Diseases* **71**, 1418–1422.

[118] Scofield, R. H, Bruner, G. R, Namjou, B, Kimberly, R. P, Ramsey-Goldman, R, Petri, M, Reveille, J. D, Alarcón, G. S, Vila, L. M, Reid, J, Harris, B, Li, S, Kelly, J. A, & Harley, J. B. (2008) Klinefelter's syndrome (47,XXY) in male systemic lupus erythematosus patients: Support for the notion of a gene-dose effect from the X chromosome. *Arthritis and Rheumatism* **58**, 2511–2517.

[119] James, J. A, Kaufman, K. M, Farris, A. D, Taylor-Albert, E, Lehman, T. J, & Harley, J. B. (1997) An increased prevalence of Epstein-Barr virus infection in young patients suggests a possible etiology for systemic lupus erythematosus. *Journal of Clinical Investigation* **100**, 3019–3026.

[120] James, J. A, Neas, B. R, Moser, K. L, Hall, T, Bruner, G. R, Sestak, A. L, & Harley, J. B. (2001) Systemic lupus erythematosus in adults is associated with previous Epstein-Barr virus exposure. *Arthritis and Rheumatism* **44**, 1122–1126.

[121] McClain, M. T, Heinlen, L. D, Dennis, G. J, Roebuck, J, Harley, J. B, & James, J. A. (2004) Early events in lupus humoral autoimmunity suggest initiation through molecular mimicry. *Nature Medicine* **11**, 85–89.

[122] Larsen, M, Sauce, D, Deback, C, Arnaud, L, Mathian, A, Miyara, M, Boutolleau, D, Parizot, C, Dorgham, K, Papagno, L, Appay, V, Amoura, Z, & Gorochov, G. (2011) Exhausted Cytotoxic Control of Epstein-Barr Virus in Human Lupus. *PLoS Pathogens* **7**, e1002328.

[123] Katz, U & Zandman-Goddard, G. (2010) Drug-induced lupus: an update. *Autoimmunity Reviews* **10**, 46–50.

[124] Costenbader, K. H, Kim, D. J, Peerzada, J, Lockman, S, Nobles-Knight, D, Petri, M, & Karlson, E. W. (2004) Cigarette smoking and the risk of systemic lupus erythematosus: A meta-analysis. *Arthritis and Rheumatism* **50**, 849–857.

[125] Parks, C. G, Cooper, G. S, Nylander-French, L. A, Sanderson, W. T, Dement, J. M, Cohen, P. L, Dooley, M. A, Treadwell, E. L, St Clair, E. W, Gilkeson, G. S, Hoppin, J. A, & Savitz, D. A. (2002) Occupational exposure to crystalline silica and risk of systemic lupus erythematosus: A population-based, case-control study in the Southeastern United States. *Arthritis and Rheumatism* **46**, 1840–1850.

[126] Sarzi-Puttini, P, Atzeni, F, Iaccarino, L, & Doria, A. (2005) Environment and systemic lupus erythematosus: An overview. *Autoimmunity* **38**, 465–472.

[127] Nagata, S, Hanayama, R, & Kawane, K. (2010) Autoimmunity and the clearance of dead cells. *Cell* **140**, 619–630.

[128] Rhodes, B, Furnrohr, B. G, Roberts, A. L, Tzircotis, G, Schett, G, Spector, T. D, & Vyse, T. J. (2012) The rs1143679 (R77H) lupus associated variant of ITGAM

(CD11b) impairs complement receptor 3 mediated functions in human monocytes. *Annals of the Rheumatic Diseases* **71**, 2028–2034.

[129] Baumann, I, Kolowos, W, Voll, R. E, Manger, B, Gaipl, U, Neuhuber, W. L, Kirchner, T, Kalden, J. R, & Herrmann, M. (2002) Impaired uptake of apoptotic cells into tingible body macrophages in germinal centers of patients with systemic lupus erythematosus. *Arthritis and Rheumatism* **46**, 191–201.

[130] Scott, R. S, McMahon, E. J, Pop, S. M, Reap, E. A, Caricchio, R, Cohen, P. L, Earp, H. S, & Matsushima, G. K. (2001) Phagocytosis and clearance of apoptotic cells is mediated by MER. *Nature* **411**, 207–211.

[131] Lu, Q & Lemke, G. (2001) Homeostatic regulation of the immune system by receptor tyrosine kinases of the Tyro 3 family. *Science* **293**, 306–311.

[132] Gilliet, M, Cao, W, & Liu, Y.-J. (2008) Plasmacytoid dendritic cells: sensing nucleic acids in viral infection and autoimmune diseases. *Nature reviews Immunology* **8**, 594–606.

[133] Banchereau, J & Pascual, V. (2006) Type I Interferon in Systemic Lupus Erythematosus and Other Autoimmune Diseases. *Immunity* **25**, 383–392.

[134] Dall'Era, M. C. (2005) Type I interferon correlates with serological and clinical manifestations of SLE. *Annals of the Rheumatic Diseases* **64**, 1692–1697.

[135] Baechler, E. C, Batliwalla, F. M, Karypis, G, Gaffney, P. M, Ortmann, W. A, Espe, K. J, Shark, K. B, Grande, W. J, Hughes, K. M, Kapur, V, Gregersen, P. K, & Behrens, T. W. (2003) Interferon-inducible gene expression signature in peripheral blood cells of patients with severe lupus. *Proceedings of the National Academy of Sciences of the United States of America* **100**, 2610–2615.

[136] Merrill, J. T, Wallace, D. J, Petri, M, Kirou, K. A, Yao, Y, White, W. I, Robbie, G, Levin, R, Berney, S. M, Chindalore, V, Olsen, N, Richman, L, Le, C, Jallal, B, White, B, & for the Lupus Interferon Skin Activity (LISA) Study Investigators. (2011) Safety profile and clinical activity of sifalimumab, a fully human anti-interferon monoclonal antibody, in systemic lupus erythematosus: a phase I, multicentre, double-blind randomised study. *Annals of the Rheumatic Diseases* **70**, 1905–1913.

[137] Barrat, F. J. (2005) Nucleic acids of mammalian origin can act as endogenous ligands for Toll-like receptors and may promote systemic lupus erythematosus. *Journal of Experimental Medicine* **202**, 1131–1139.

[138] Lande, R, Gregorio, J, Facchinetti, V, Chatterjee, B, Wang, Y.-H, Homey, B, Cao, W, Wang, Y.-H, Su, B, Nestle, F. O, Zal, T, Mellman, I, Schröder, J.-M, Liu, Y.-J, & Gilliet, M. (2007) Plasmacytoid dendritic cells sense self-DNA coupled with antimicrobial peptide. *Nature* **449**, 564–569.

[139] Guiducci, C, Gong, M, Xu, Z, Gill, M, Chaussabel, D, Meeker, T, Chan, J. H, Wright, T, Punaro, M, Bolland, S, Soumelis, V, Banchereau, J, Coffman, R. L, Pascual, V, & Barrat, F. J. (2010) TLR recognition of self nucleic acids hampers glucocorticoid activity in lupus. *Nature* **465**, 937–941.

[140] Kondo, M, Weissman, I. L, & Akashi, K. (1997) Identification of clonogenic common lymphoid progenitors in mouse bone marrow. *Cell* **91**, 661–672.

[141] Busslinger, M. (2004) Transcriptional Control of Early B Cell Development 1. *Annual Review of Immunology* **22**, 55–79.

[142] Wardemann, H, Yurasov, S, Schaefer, A, Young, J. W, Meffre, E, & Nussenzweig, M. C. (2003) Predominant autoantibody production by early human B cell precursors. *Science* **301**, 1374–1377.

[143] Keenan, R. A, De Riva, A, Corleis, B, Hepburn, L, Licence, S, Winkler, T. H, & Martensson, I. L. (2008) Censoring of Autoreactive B Cell Development by the Pre-B Cell Receptor. *Science* **321**, 696–699.

[144] Radic, M. Z & Zouali, M. (1996) Receptor editing, immune diversification, and self-tolerance. *Immunity* **5**, 505–511.

[145] Sekiguchi, D. R, Eisenberg, R. A, & Weigert, M. (2002) Secondary Heavy Chain Rearrangement: A Mechanism for Generating Anti-double-stranded DNA B Cells. *Journal of Experimental Medicine* **197**, 27–39.

[146] Witsch, E. J. (2006) Light chain editing generates polyreactive antibodies in chronic graft-versus-host reaction. *Journal of Experimental Medicine* **203**, 1761–1772.

[147] Yurasov, S, Tiller, T, Tsuiji, M, Velinzon, K, Pascual, V, Wardemann, H, & Nussenzweig, M. C. (2006) Persistent expression of autoantibodies in SLE patients in remission. *Journal of Experimental Medicine* **203**, 2255–2261.

[148] Yurasov, S. (2005) Defective B cell tolerance checkpoints in systemic lupus erythematosus. *Journal of Experimental Medicine* **201**, 703–711.

[149] Cappione, III, A, Anolik, J. H, Pugh-Bernard, A, Barnard, J, Dutcher, P, Silverman, G, & Sanz, I. (2005) Germinal center exclusion of autoreactive B cells is defective in human systemic lupus erythematosus. *Journal of Clinical Investigation* **115**, 3205–3216.

[150] Mackay, F, Schneider, P, Rennert, P, & Browning, J. (2003) BAFF ANDAPRIL: A Tutorial on B Cell Survival. *Annual Review of Immunology* **21**, 231–264.

[151] Enders, A, Bouillet, P, Puthalakath, H, Xu, Y, Tarlinton, D. M, & Strasser, A. (2003) Loss of the Pro-Apoptotic BH3-only Bcl-2 Family Member Bim Inhibits

BCR Stimulation-induced Apoptosis and Deletion of Autoreactive B Cells. *Journal of Experimental Medicine* **198**, 1119–1126.

[152] Todd, D. J, Lee, A.-H, & Glimcher, L. H. (2008) The endoplasmic reticulum stress response in immunity and autoimmunity. *Nature Reviews Immunology* **8**, 663–674.

[153] Reimold, A. M, Iwakoshi, N. N, Manis, J, Vallabhajosyula, P, Szomolanyi-Tsuda, E, Gravallese, E. M, Friend, D, Grusby, M. J, Alt, F, & Glimcher, L. H. (2001) Plasma cell differentiation requires the transcription factor XBP-1. *Nature* **412**, 300–307.

[154] Nutt, S. L, Taubenheim, N, Hasbold, J, Corcoran, L. M, & Hodgkin, P. D. (2011) The genetic network controlling plasma cell differentiation. *Seminars in Immunology* pp. 1–9.

[155] Zhang, K, Wong, H. N, Song, B, Miller, C. N, Scheuner, D, & Kaufman, R. J. (2005) The unfolded protein response sensor IRE1α is required at 2 distinct steps in B cell lymphopoiesis. *Journal of Clinical Investigation* **115**, 268–281.

[156] Odendahl, M, Jacobi, A, Hansen, A, Feist, E, Hiepe, F, Burmester, G.-R, Lipsky, P. E, Radbruch, A, & Dorner, T. (2000) Disturbed peripheral B lymphocyte homeostasis in systemic lupus erythematosus. *Journal of Immunology* **165**, 5970–5979.

[157] Jacobi, A. M, Odendahl, M, Reiter, K, Bruns, A, Burmester, G. R, Radbruch, A, Valet, G. n, Lipsky, P. E, & D rner, T. (2003) Correlation between circulating CD27high plasma cells and disease activity in patients with systemic lupus erythematosus. *Arthritis and Rheumatism* **48**, 1332–1342.

[158] Cassese, G, Lindenau, S, de Boer, B, Arce, S, Hauser, A, Riemekasten, G, Berek, C, Hiepe, F, Krenn, V, Radbruch, A, & Manz, R. A. (2001) Inflamed kidneys of

NZB / W mice are a major site for the homeostasis of plasma cells. *European Journal of Immunology* **31**, 2726–2732.

[159] Mumtaz, I. M, Hoyer, B. F, Panne, D, Moser, K, Winter, O, Cheng, Q. Y, Yoshida, T, Burmester, G. R, Radbruch, A, Manz, R. A, & Hiepe, F. (2012) Bone marrow of NZB/W mice is the major site for plasma cells resistant to dexamethasone and cyclophosphamide: implications for the treatment of autoimmunity. *Journal of Autoimmunity* **39**, 180–188.

[160] Hoyer, B. F. (2004) Short-lived Plasmablasts and Long-lived Plasma Cells Contribute to Chronic Humoral Autoimmunity in NZB/W Mice. *Journal of Experimental Medicine* **199**, 1577–1584.

[161] Lee, J, Kuchen, S, Fischer, R, Chang, S, & Lipsky, P. E. (2009) Identification and Characterization of a Human CD5+ Pre-Naive B Cell Population. *The Journal of Immunology* **182**, 4116–4126.

[162] Mauri, C & Bosma, A. (2012) Immune Regulatory Function of B Cells. *Annual Review of Immunology* **30**, 221–241.

[163] Blair, P. A, Norena, L. Y, Flores-Borja, F, Rawlings, D. J, Isenberg, D. A, Ehrenstein, M. R, & Mauri, C. (2010) CD19+CD24hiCD38hi B Cells Exhibit Regulatory Capacity in Healthy Individuals but Are Functionally Impaired in Systemic Lupus Erythematosus Patients. *Immunity* **32**, 129–140.

[164] Nedjic, J, Aichinger, M, Emmerich, J, Mizushima, N, & Klein, L. (2008) Autophagy in thymic epithelium shapes the T-cell repertoire and is essential for tolerance. *Nature* **455**, 396–400.

[165] Klein, L, Kyewski, B, Allen, P. M, & Hogquist, K. A. (2014) Positive and negative selection of the T cell repertoire: what thymocytes see (and don't see). *Nature Reviews Immunology* **14**, 377–391.

[166] Shah, S, Wu, E, Rao, V. K, & Tarrant, T. K. (2014) Autoimmune Lymphoproliferative Syndrome: an Update and Review of the Literature. *Current Allergy and Asthma Reports* **14**, 462.

[167] Hartley, S. B, Crosbie, J, Brink, R, Kantor, A. B, Basten, A, & Goodnow, C. C. (1991) Elimination from peripheral lymphoid tissues of self-reactive B lymphocytes recognizing membrane-bound antigens. *Nature* **353**, 765–769.

[168] Bell, S. E & Goodnow, C. C. (1994) A selective defect in IgM antigen receptor synthesis and transport causes loss of cell surface IgM expression on tolerant B lymphocytes. *The EMBO Journal* **13**, 816–826.

[169] O'Neill, S. K, Veselits, M. L, Zhang, M, Labno, C, Cao, Y, Finnegan, A, Uccellini, M, Alegre, M.-L, Cambier, J. C, & Clark, M. R. (2009) Endocytic sequestration of the B cell antigen receptor and toll-like receptor 9 in anergic cells. *PNAS* **106**, 6262–6267.

[170] Rui, L, Vinuesa, C. G, Blasioli, J, & Goodnow, C. C. (2003) Resistance to CpG DNA-induced autoimmunity through tolerogenic B cell antigen receptor ERK signaling. *Nature Immunology* **4**, 594–600.

[171] Yarkoni, Y, Getahun, A, & Cambier, J. C. (2010) Molecular underpinning of B-cell anergy. *Immunological Reviews* **237**, 249–263.

[172] Omori, S. A, Cato, M. H, Anzelon-Mills, A, Puri, K. D, Shapiro-Shelef, M, Calame, K, & Rickert, R. C. (2006) Regulation of Class-Switch Recombination and Plasma Cell Differentiation by Phosphatidylinositol 3-Kinase Signaling. *Immunity* **25**, 545–557.

[173] Wu, X. n, Ye, Y. x, Niu, J. w, Li, Y, Li, X, You, X, Chen, H, Zhao, L. d, Zeng, X. f, Zhang, F. c, Tang, F. l, He, W, Cao, X. t, Zhang, X, & Lipsky, P. E. (2014) De-

fective PTEN regulation contributes to B cell hyperresponsiveness in systemic lupus erythematosus. *Science Translational Medicine* **6**, 246ra99–246ra99.

[174] Read, S, Malmström, V, & Powrie, F. (2000) Cytotoxic T lymphocyte-associated antigen 4 plays an essential role in the function of CD25(+)CD4(+) regulatory cells that control intestinal inflammation. *The Journal of Experimental Medicine* **192**, 295–302.

[175] Graham, D. S. C, Wong, A. K, McHugh, N. J, Whittaker, J. C, & Vyse, T. J. (2006) Evidence for unique association signals in SLE at the CD28-CTLA4-ICOS locus in a family-based study. *Human Molecular Genetics* **15**, 3195–3205.

[176] Waterhouse, P, Penninger, J. M, Timms, E, Wakeham, A, Shahinian, A, Lee, K. P, Thompson, C. B, Griesser, H, & Mak, T. W. (1995) Lymphoproliferative disorders with early lethality in mice deficient in Ctla-4. *Science* **270**, 985–988.

[177] Krishnan, S, Warke, V. G, Nambiar, M. P, Tsokos, G. C, & Farber, D. L. (2003) The FcR gamma subunit and Syk kinase replace the CD3 zeta-chain and ZAP-70 kinase in the TCR signaling complex of human effector CD4 T cells. *Journal of Immunology* **170**, 4189–4195.

[178] Hedrich, C. M, Crispín, J. C, Rauen, T, Ioannidis, C, Apostolidis, S. A, Lo, M. S, Kyttaris, V. C, & Tsokos, G. C. (2012) cAMP response element modulator α controls IL2 and IL17A expression during CD4 lineage commitment and subset distribution in lupus. *Proceedings of the National Academy of Sciences* **109**, 16606–16611.

[179] Koshy, M, Berger, D, & Crow, M. K. (1996) Increased expression of CD40 ligand on systemic lupus erythematosus lymphocytes. *Journal of Clinical Investigation* **98**, 826–837.

[180] Crispín, J. C, Keenan, B. T, Finnell, M. D, Bermas, B. L, Schur, P, Massarotti, E, Karlson, E. W, Fitzgerald, L. M, Ergin, S, Kyttaris, V. C, Tsokos, G. C, & Costenbader, K. H. (2010) Expression of CD44 variant isoforms CD44v3 and CD44v6 is increased on T cells from patients with systemic lupus erythematosus and is correlated with disease activity. *Arthritis and Rheumatism* **62**, 1431–1437.

[181] Gergely, P, Grossman, C, Niland, B, Puskas, F, Neupane, H, Allam, F, Banki, K, Phillips, P. E, & Perl, A. (2002) Mitochondrial hyperpolarization and ATP depletion in patients with systemic lupus erythematosus. *Arthritis and Rheumatism* **46**, 175–190.

[182] Gergely, P, Niland, B, Gonchoroff, N, Pullmann, R, Phillips, P. E, & Perl, A. (2002) Persistent mitochondrial hyperpolarization, increased reactive oxygen intermediate production, and cytoplasmic alkalinization characterize altered IL-10 signaling in patients with systemic lupus erythematosus. *Journal of Immunology* **169**, 1092–1101.

[183] Lai, Z.-W, Hanczko, R, Bonilla, E, Caza, T. N, Clair, B, Bartos, A, Miklossy, G, Jimah, J, Doherty, E, Tily, H, Francis, L, Garcia, R, Dawood, M, Yu, J, Ramos, I, Coman, I, Faraone, S. V, Phillips, P. E, & Perl, A. (2012) N-acetylcysteine reduces disease activity by blocking mammalian target of rapamycin in T cells from systemic lupus erythematosus patients: A randomized, double-blind, placebo-controlled trial. *Arthritis and Rheumatism* **64**, 2937–2946.

[184] Scheinecker, C, Bonelli, M, & Smolen, J. S. (2010) Pathogenetic aspects of systemic lupus erythematosus with an emphasis on regulatory T cells. *Journal of Autoimmunity* **35**, 269–275.

[185] Shin, M. S, Lee, N, & Kang, I. (2011) Effector T-cell subsets in systemic lupus erythematosus. *Current Opinion in Rheumatology* **23**, 444–448.

[186] Doreau, A, Belot, A, Bastid, J, Riche, B, Trescol-Biemont, M.-C, Ranchin, B, Fabien, N, Cochat, P, Pouteil-Noble, C, Trolliet, P, Durieu, I, Tebib, J, Kassai, B, Ansieau, S, Puisieux, A, Eliaou, J.-F, & Bonnefoy-Bérard, N. (2009) Interleukin 17 acts in synergy with B cell–activating factor to influence B cell biology and the pathophysiology of systemic lupus erythematosus. *Nature Immunology* **10**, 779–786.

[187] Pisitkun, P, Ha, H.-L, Wang, H, Claudio, E, Tivy, C. C, Zhou, H, Mayadas, T. N, Illei, G. G, & Siebenlist, U. (2012) Interleukin-17 Cytokines Are Critical in Development of Fatal Lupus Glomerulonephritis. *Immunity* pp. 1–12.

[188] Linterman, M. A, Rigby, R. J, Wong, R. K, Yu, D, Brink, R, Cannons, J. L, Schwartzberg, P. L, Cook, M. C, Walters, G. D, & Vinuesa, C. G. (2009) Follicular helper T cells are required for systemic autoimmunity. *Journal of Experimental Medicine* **206**, 561–576.

[189] Simpson, N, Gatenby, P. A, Wilson, A, Malik, S, Fulcher, D. A, Tangye, S. G, Manku, H, Vyse, T. J, Roncador, G, Huttley, G. A, Goodnow, C. C, Vinuesa, C. G, & Cook, M. C. (2010) Expansion of circulating T cells resembling follicular helper T cells is a fixed phenotype that identifies a subset of severe systemic lupus erythematosus. *Arthritis and Rheumatism* **62**, 234–244.

[190] Vincent, F. B, Morand, E. F, Schneider, P, & Mackay, F. (2014) The BAFF/APRIL system in SLE pathogenesis. *Nature Reviews Rheumatology* **10**, 365–373.

[191] Mackay, F & Schneider, P. (2009) Cracking the BAFF code. *Nature Reviews Immunology* **9**, 491–502.

[192] Nakagawa, I, Amano, A, Mizushima, N, Yamamoto, A, Yamaguchi, H, Kamimoto, T, Nara, A, Funao, J, Nakata, M, Tsuda, K, Hamada, S, & Yoshimori, T. (2004) Autophagy defends cells against invading group A Streptococcus. *Science* **306**, 1037–1040.

[193] Perrin, A. J, Jiang, X, Birmingham, C. L, So, N. S. Y, & Brumell, J. H. (2004) Recognition of Bacteria in the Cytosol of Mammalian Cells by the Ubiquitin System. *Current Biology* **14**, 806–811.

[194] Sanjuan, M. A, Dillon, C. P, Tait, S. W. G, Moshiach, S, Dorsey, F, Connell, S, Komatsu, M, Tanaka, K, Cleveland, J. L, Withoff, S, & Green, D. R. (2007) Toll-like receptor signalling in macrophages links the autophagy pathway to phagocytosis. *Nature* **450**, 1253–1257.

[195] Martinez, J, Almendinger, J, Oberst, A, Ness, R, Dillon, C. P, Fitzgerald, P, Hengartner, M. O, & Green, D. R. (2011) Microtubule-associated protein 1 light chain 3 alpha (LC3)-associated phagocytosis is required for the efficient clearance of dead cells. *Proceedings of the National Academy of Sciences* **108**, 17396–17401.

[196] Delgado, M. A, Elmaoued, R. A, Davis, A. S, Kyei, G, & Deretic, V. (2008) Toll-like receptors control autophagy. *The EMBO Journal* **27**, 1110–1121.

[197] Watson, R. O, Manzanillo, P. S, & Cox, J. S. (2012) Extracellular M. tuberculosis DNA targets bacteria for autophagy by activating the host DNA-sensing pathway. *Cell* **150**, 803–815.

[198] Cooney, R, Baker, J, Brain, O, Danis, B, Pichulik, T, Allan, P, Ferguson, D. J. P, Campbell, B. J, Jewell, D, & Simmons, A. (2010) NOD2 stimulation induces autophagy in dendritic cells influencing bacterial handling and antigen presentation. *Nature Medicine* **16**, 90–97.

[199] Travassos, L. H, Carneiro, L. A. M, Ramjeet, M, Hussey, S, Kim, Y.-G, Magalhães, J. G, Yuan, L, Soares, F, Chea, E, Bourhis, L. L, Boneca, I. G, Allaoui, A, Jones, N. L, Nuñez, G, Girardin, S. E, & Philpott, D. J. (2009) Nod1 and Nod2 direct autophagy by recruiting ATG16L1 to the plasma membrane at the site of bacterial entry. *Nature Immunology* **11**, 55–62.

[200] Schmid, D, Pypaert, M, & Münz, C. (2007) Antigen-loading compartments for major histocompatibility complex class II molecules continuously receive input from autophagosomes. *Immunity* **26**, 79–92.

[201] Desmet, C. J & Ishii, K. J. (2012) Nucleic acid sensing at the interface between innate and adaptive immunity in vaccination. *Nature Reviews Immunology* **12**, 479–491.

[202] Jounai, N, Takeshita, F, Kobiyama, K, Sawano, A, Miyawaki, A, Xin, K.-Q, Ishii, K. J, Kawai, T, Akira, S, Suzuki, K, & Okuda, K. (2007) The Atg5 Atg12 conjugate associates with innate antiviral immune responses. *Proceedings of the National Academy of Sciences* **104**, 14050–14055.

[203] Tal, M. C, Sasai, M, Lee, H. K, Yordy, B, Shadel, G. S, & Iwasaki, A. (2009) Absence of autophagy results in reactive oxygen species-dependent amplification of RLR signaling. *Proceedings of the National Academy of Sciences* **106**, 2770–2775.

[204] Lee, H. K, Lund, J. M, Ramanathan, B, Mizushima, N, & Iwasaki, A. (2007) Autophagy-dependent viral recognition by plasmacytoid dendritic cells. *Science* **315**, 1398–1401.

[205] Zhou, D, Kang, K. H, & Spector, S. A. (2012) Production of Interferon by Human Immunodeficiency Virus Type 1 in Human Plasmacytoid Dendritic

Cells Is Dependent on Induction of Autophagy. *Journal of Infectious Diseases* **205**, 1258–1267.

[206] Henault, J, Martinez, J, Riggs, J. M, Tian, J, Mehta, P, Clarke, L, Sasai, M, Latz, E, Brinkmann, M. M, Iwasaki, A, Coyle, A. J, Kolbeck, R, Green, D. R, & Sanjuan, M. A. (2012) Noncanonical Autophagy Is Requiredfor Type I Interferon Secretion in Response to DNA-Immune Complexes. *Immunity* **37**, 986–997.

[207] Saitoh, T, Fujita, N, Jang, M. H, Uematsu, S, Yang, B.-G, Satoh, T, Omori, H, Noda, T, Yamamoto, N, Komatsu, M, Tanaka, K, Kawai, T, Tsujimura, T, Takeuchi, O, Yoshimori, T, & Akira, S. (2008) Loss of the autophagy protein Atg16L1 enhances endotoxin-induced IL-1β production. *Nature* **456**, 264–268.

[208] Harris, J, Hartman, M, Roche, C, Zeng, S. G, O'Shea, A, Sharp, F. A, Lambe, E. M, Creagh, E. M, Golenbock, D. T, Tschopp, J, Kornfeld, H, Fitzgerald, K. A, & Lavelle, E. C. (2011) Autophagy controls IL-1beta secretion by targeting pro-IL-1beta for degradation. *The Journal of Biological Chemistry*.

[209] Shi, C.-S, Shenderov, K, Huang, N.-N, Kabat, J, Abu-Asab, M, Fitzgerald, K. A, Sher, A, & Kehrl, J. H. (2012) Activation of autophagy by inflammatory signals limits IL-1β production by targeting ubiquitinated inflammasomes for destruction. *Nature Immunology* **13**, 255–263.

[210] Lupfer, C, Thomas, P. G, Anand, P. K, Vogel, P, Milasta, S, Martinez, J, Huang, G, Green, M, Kundu, M, Chi, H, Xavier, R. J, Green, D. R, Lamkanfi, M, Dinarello, C. A, Doherty, P. C, & Kanneganti, T.-D. (2013) Receptor interacting protein kinase 2–mediated mitophagy regulates inflammasome activation during virus infection. *Nature Immunology* **14**, 480–488.

[211] Nakahira, K, Haspel, J. A, Rathinam, V. A. K, Lee, S.-J, Dolinay, T, Lam, H. C, Englert, J. A, Rabinovitch, M, Cernadas, M, Kim, H. P, Fitzgerald, K. A, Ryter,

S. W, & Choi, A. M. K. (2010) Autophagy proteins regulate innate immune responses by inhibiting the release of mitochondrial DNA mediated by the NALP3 inflammasome. *Nature Immunology* **12**, 222–230.

[212] Joffre, O. P, Segura, E, Savina, A, & Amigorena, S. (2012) Cross□ presentation by dendritic cells. *Nature Reviews Immunology* pp. 1–13.

[213] Dengjel, J, Schoor, O, Fischer, R, Reich, M, Kraus, M, Müller, M, Kreymborg, K, Altenberend, F, Brandenburg, J, Kalbacher, H, Brock, R, Driessen, C, Rammensee, H.-G, & Stevanovic, S. (2005) Autophagy promotes MHC class II presentation of peptides from intracellular source proteins. *Proceedings of the National Academy of Sciences* **102**, 7922–7927.

[214] Lee, H. K, Mattei, L. M, Steinberg, B. E, Alberts, P, Lee, Y. H, Chervonsky, A, Mizushima, N, Grinstein, S, & Iwasaki, A. (2010) In vivo requirement for Atg5 in antigen presentation by dendritic cells. *Immunity* **32**, 227–239.

[215] Aichinger, M, Wu, C, Nedjic, J, & Klein, L. (2013) Macroautophagy substrates are loaded onto MHC class II of medullary thymic epithelial cells for central tolerance. *Journal of Experimental Medicine* **210**, 287–300.

[216] Paludan, C, Schmid, D, Landthaler, M, Vockerodt, M, Kube, D, Tuschl, T, & Münz, C. (2005) Endogenous MHC class II processing of a viral nuclear antigen after autophagy. *Science* **307**, 593–596.

[217] Jagannath, C, Lindsey, D. R, Dhandayuthapani, S, Xu, Y, Hunter, R. L, & Eissa, N. T. (2009) Autophagy enhances the efficacy of BCG vaccine by increasing peptide presentation in mouse dendritic cells. *Nature Medicine* **15**, 267–276.

[218] Ireland, J. M & Unanue, E. R. (2011) Autophagy in antigen-presenting cells results in presentation of citrullinated peptides to CD4 T cells. *Journal of Experimental Medicine* **208**, 2625–32.

[219] Jacquel, A, Obba, S, Boyer, L, Dufies, M, Robert, G, Gounon, P, Lemichez, E, Luciano, F, Solary, E, & Auberger, P. (2012) Autophagy is required for CSF-1-induced macrophagic differentiation and acquisition of phagocytic functions. *Blood* **119**, 4527–4531.

[220] Zhang, Y, Morgan, M. J, Chen, K, Choksi, S, & Liu, Z. g. (2012) Induction of autophagy is essential for monocyte-macrophage differentiation. *Blood* **119**, 2895–2905.

[221] Arsov, I, Adebayo, A, Kucerova-Levisohn, M, Haye, J, MacNeil, M, Papavasiliou, F. N, Yue, Z, & Ortiz, B. D. (2011) A Role for Autophagic Protein Beclin 1 Early in Lymphocyte Development. *The Journal of Immunology* **186**, 2201–2209.

[222] Stephenson, L. M, Miller, B. C, Ng, A, Eisenberg, J, Zhao, Z, Cadwell, K, Graham, D. B, Mizushima, N. N, Xavier, R, Virgin, H. W, & Swat, W. (2009) Identification of Atg5-dependent transcriptional changes and increases in mitochondrial mass in Atg5-deficient T lymphocytes. *Autophagy* **5**, 625–635.

[223] Pua, H. H, Dzhagalov, I, Chuck, M, Mizushima, N, & He, Y.-W. (2007) A critical role for the autophagy gene Atg5 in T cell survival and proliferation. *Journal of Experimental Medicine* **204**, 25–31.

[224] Jia, W & He, Y.-W. (2011) Temporal Regulation of Intracellular Organelle Homeostasis in T Lymphocytes by Autophagy. *The Journal of Immunology* **186**.

[225] Arsov, I, Li, X, Matthews, G, Coradin, J, Hartmann, B, Simon, A. K, Sealfon, S. C, & Yue, Z. (2008) BAC-mediated transgenic expression of fluorescent autophagic protein Beclin 1 reveals a role for Beclin 1 in lymphocyte development. *Cell Death and Differentiation* **15**, 1385–1395.

[226] Jia, W, Pua, H. H, Li, Q. J, & He, Y.-W. (2011) Autophagy Regulates Endoplas-

mic Reticulum Homeostasis and Calcium Mobilization in T Lymphocytes. *The Journal of Immunology* **186**, 1564–1574.

[227] Li, C, Capan, E, Zhao, Y, Zhao, J, Stolz, D, Watkins, S. C, Jin, S, & Lu, B. (2006) Autophagy is induced in CD4+ T cells and important for the growth factor-withdrawal cell death. *Journal of Immunology* **177**, 5163–5168.

[228] Bell, B. D, Leverrier, S, Weist, B. M, Newton, R. H, Arechiga, A. F, Luhrs, K. A, Morrissette, N. S, & Walsh, C. M. (2008) FADD and caspase-8 control the outcome of autophagic signaling in proliferating T cells. *Proceedings of the National Academy of Sciences* **105**, 16677–16682.

[229] Hubbard, V. M, Valdor, R, Patel, B, Singh, R, Cuervo, A. M, & Macian, F. (2010) Macroautophagy Regulates Energy Metabolism during Effector T Cell Activation. *The Journal of Immunology* **185**, 7349–7357.

[230] Kovacs, J. R, Li, C, Yang, Q, Li, G, Garcia, I. G, Ju, S, Roodman, D. G, Windle, J. J, Zhang, X, & Lu, B. (2012) Autophagy promotes T-cell survival through degradation of proteins of the cell death machinery. *Cell Death and Differentiation* **19**, 144–152.

[231] Pua, H. H, Guo, J, Komatsu, M, & He, Y.-W. (2009) Autophagy is essential for mitochondrial clearance in mature T lymphocytes. *Journal of Immunology* **182**, 4046–4055.

[232] Miller, B. C, Zhao, Z, Stephenson, L. M, Cadwell, K, Pua, H. H, Lee, H. K, Mizushima, N. N, Iwasaki, A, He, Y.-W, Swat, W, & Virgin, H. W. (2008) The autophagy gene ATG5 plays an essential role in B lymphocyte development. *Autophagy* **4**, 309–314.

[233] Mortensen, M, Soilleux, E. J, Djordjevic, G, Tripp, R, Lutteropp, M, Sadighi-Akha, E, Stranks, A. J, Glanville, J, Knight, S, W Jacobsen, S. E, Kranc, K. R, &

Simon, A. K. (2011) The autophagy protein Atg7 is essential for hematopoietic stem cell maintenance. *Journal of Experimental Medicine* **208**, 455–467.

[234] Merino, R, Ding, L, Veis, D. J, Korsmeyer, S. J, & Nuñez, G. (1994) Developmental regulation of the Bcl-2 protein and susceptibility to cell death in B lymphocytes. *The EMBO Journal* **13**, 683–691.

[235] Baumgarth, N. (2010) The double life of a B-1 cell: self-reactivity selects for protective effector functions. *Nature Reviews Immunology* **11**, 34–46.

[236] Hayakawa, K. (1999) Positive Selection of Natural Autoreactive B Cells. *Science* **285**, 113–116.

[237] Watanabe, K, Ichinose, S, Hayashizaki, K, & Tsubata, T. (2008) Induction of autophagy by B cell antigen receptor stimulation and its inhibition by costimulation. *Biochemical and Biophysical Research Communications* **374**, 274–281.

[238] Pengo, N, Scolari, M, Oliva, L, Milan, E, Mainoldi, F, Raimondi, A, Fagioli, C, Merlini, A, Mariani, E, Pasqualetto, E, Orfanelli, U, Ponzoni, M, Sitia, R, Casola, S, & Cenci, S. (2013) Plasma cells require autophagy for sustainable immunoglobulin production. *Nature Immunology* **14**, 298–305.

[239] Conway, K. L, Kuballa, P, Khor, B, Zhang, M, Shi, H. N, Virgin, H. W, & Xavier, R. J. (2013) ATG5 regulates plasma cell differentiation. *Autophagy* **9**.

[240] Chaturvedi, A, Dorward, D, & Pierce, S. K. (2008) The B cell receptor governs the subcellular location of Toll-like receptor 9 leading to hyperresponses to DNA-containing antigens. *Immunity* **28**, 799–809.

[241] Leadbetter, E. A, Rifkin, I. R, Hohlbaum, A. M, Beaudette, B. C, Shlomchik, M. J, & Marshak-Rothstein, A. (2002) Chromatin–IgG complexes activate B cells by dual engagement of IgM and Toll-like receptors. *Nature* **416**, 603–607.

[242] Zhou, X. j, Lu, X. l, Lv, J. c, Yang, H. z, Qin, L. x, Zhao, M. h, Su, Y, Li, Z. g, & Zhang, H. (2011) Genetic association of PRDM1-ATG5 intergenic region and autophagy with systemic lupus erythematosus in a Chinese population. *Annals of the Rheumatic Diseases* **70**, 1330–1337.

[243] Kim, S. J, Gregersen, P. K, & Diamond, B. (2013) Regulation of dendritic cell activation by microRNA let-7c and BLIMP1. *Journal of Clinical Investigation* **123**.

[244] Moreau, K, Ravikumar, B, Renna, M, Puri, C, & Rubinsztein, D. C. (2011) Autophagosome Precursor Maturation Requires Homotypic Fusion. *Cell* **146**, 303–317.

[245] de Lartigue, J, Polson, H, Feldman, M, Shokat, K, Tooze, S. A, Urbé, S, & Clague, M. J. (2009) PIKfyve Regulation of Endosome-Linked Pathways. *Traffic* **10**, 883–893.

[246] Singh, S. B, AS, D, GA, T, & V, D. (2006) Human IRGM Induces Autophagy to Eliminate Intracellular Mycobacteria. *Science* **313**, 1438–1441.

[247] Gros, F, Arnold, J, Page, N, Décossas, M, Korganow, A.-S, Martin, T, & Muller, S. (2012) Macroautophagy is deregulated in murine and human lupus T lymphocytes. *Autophagy* **8**, 1054–1053.

[248] Alessandri, C, Barbati, C, Vacirca, D, Piscopo, P, Confaloni, A, Sanchez, M, Maselli, A, Colasanti, T, Conti, F, Truglia, S, Perl, A, Valesini, G, Malorni, W, Ortona, E, & Pierdominici, M. (2012) T lymphocytes from patients with systemic lupus erythematosus are resistant to induction of autophagy. *The FASEB journal* **26**, 4722–4732.

[249] Hampe, J, Franke, A, Rosenstiel, P, Till, A, Teuber, M, Huse, K, Albrecht, M, Mayr, G, De La Vega, F. M, Briggs, J, Günther, S, Prescott, N. J, Onnie,

C. M, Häsler, R, Sipos, B, Fölsch, U. R, Lengauer, T, Platzer, M, Mathew, C. G, Krawczak, M, & Schreiber, S. (2006) A genome-wide association scan of nonsynonymous SNPs identifies a susceptibility variant for Crohn disease in ATG16L1. *Nature Genetics* **39**, 207–211.

[250] Cadwell, K, Liu, J. Y, Brown, S. L, Miyoshi, H, Loh, J, Lennerz, J. K, Kishi, C, Kc, W, Carrero, J. A, Hunt, S, Stone, C. D, Brunt, E. M, Xavier, R. J, Sleckman, B. P, Li, E, Mizushima, N, Stappenbeck, T. S, & Virgin, IV, H. W. (2008) A key role for autophagy and the autophagy gene Atg16l1 in mouse and human intestinal Paneth cells. *Nature* **456**, 259–263.

[251] Lin, N. Y, Beyer, C, Giessl, A, Kireva, T, Scholtysek, C, Uderhardt, S, Munoz, L. E, Dees, C, Distler, A, Wirtz, S, Kronke, G, Spencer, B, Distler, O, Schett, G, & Distler, J. H. W. (2013) Autophagy regulates TNF -mediated joint destruction in experimental arthritis. *Annals of the Rheumatic Diseases* **72**, 761–768.

[252] Connor, A. M, Mahomed, N, Gandhi, R, Keystone, E. C, & Berger, S. A. (2012) TNFa modulates protein degradation pathways in rheumatoid arthritis synovial fibroblasts. *Arthritis Research & Therapy* **14**, R62.

[253] Willemze, A, Trouw, L. A, Toes, R. E. M, & Huizinga, T. W. J. (2012) The influence of ACPA status and characteristics on the course of RA. *Nature Reviews Rheumatology* **8**, 144–152.

[254] Schlosstein, L, Terasaki, P. I, Bluestone, R, & Pearson, C. M. (1973) High association of an HL-A antigen, W27, with ankylosing spondylitis. *New England Journal of Medicine* **288**, 704–706.

[255] McHugh, K & Bowness, P. (2012) The link between HLA-B27 and SpA–new ideas on an old problem. *Rheumatology (Oxford, England)* **51**, 1529–1539.

[256] Turner, M. J, Sowders, D. P, DeLay, M. L, Mohapatra, R, Bai, S, Smith, J. A, Brandewie, J. R, Taurog, J. D, & Colbert, R. A. (2005) HLA-B27 misfolding in transgenic rats is associated with activation of the unfolded protein response. *Journal of Immunology* **175**, 2438–2448.

[257] Ciccia, F, Accardo-Palumbo, A, Rizzo, A, Guggino, G, Raimondo, S, Giardina, A, Cannizzaro, A, Colbert, R. A, Alessandro, R, & Triolo, G. (2013) Evidence that autophagy, but not the unfolded protein response, regulates the expression of IL-23 in the gut of patients with ankylosing spondylitis and subclinical gut inflammation. *Annals of the Rheumatic Diseases*.

[258] Petri, M, Stohl, W, Chatham, W, McCune, W. J, Chevrier, M, Ryel, J, Recta, V, Zhong, J, & Freimuth, W. (2008) Association of plasma B lymphocyte stimulator levels and disease activity in systemic lupus erythematosus. *Arthritis and Rheumatism* **58**, 2453–2459.

[259] Klionsky, D. J, Abeliovich, H, Agostinis, P, Agrawal, D. K, Aliev, G, Askew, D. S, Baba, M, Baehrecke, E. H, Bahr, B. A, Ballabio, A, Bamber, B. A, Bassham, D. C, Bergamini, E, Bi, X, Biard-Piechaczyk, M, Blum, J. S, Bredesen, D. E, Brodsky, J. L, Brumell, J. H, Brunk, U. T, Bursch, W, Camougrand, N, Cebollero, E, Cecconi, F, Chen, Y, Chin, L.-S, Choi, A, Chu, C. T, Chung, J, Clarke, P. G. H, Clark, R. S. B, Clarke, S. G, Clavé, C, Cleveland, J. L, Codogno, P, Colombo, M. I, Coto-Montes, A, Cregg, J. M, Cuervo, A. M, Debnath, J, Demarchi, F, Dennis, P. B, Dennis, P. A, Deretic, V, Devenish, R. J, Di Sano, F, Dice, J. F, Difiglia, M, Dinesh-Kumar, S, Distelhorst, C. W, Djavaheri-Mergny, M, Dorsey, F. C, Dröge, W, Dron, M, Dunn, W. A, Duszenko, M, Eissa, N. T, Elazar, Z, Esclatine, A, Eskelinen, E.-L, Fésüs, L, Finley, K. D, Fuentes, J. M, Fueyo, J, Fujisaki, K, Galliot, B, Gao, F.-B, Gewirtz, D. A, Gibson, S. B, Gohla, A, Goldberg, A. L, Gonzalez, R, González-Estévez, C, Gorski, S, Gottlieb, R. A,

Häussinger, D, He, Y.-W, Heidenreich, K, Hill, J. A, Høyer-Hansen, M, Hu, X, Huang, W.-P, Iwasaki, A, Jäättelä, M, Jackson, W. T, Jiang, X, Jin, S, Johansen, T, Jung, J. U, Kadowaki, M, Kang, C, Kelekar, A, Kessel, D. H, Kiel, J. A. K. W, Kim, H. P, Kimchi, A, Kinsella, T. J, Kiselyov, K, Kitamoto, K, Knecht, E, Komatsu, M, Kominami, E, Kondo, S, Kovács, A. L, Kroemer, G, Kuan, C.-Y, Kumar, R, Kundu, M, Landry, J, Laporte, M, Le, W, Lei, H.-Y, Lenardo, M. J, Levine, B, Lieberman, A, Lim, K.-L, Lin, F.-C, Liou, W, Liu, L. F, Lopez-Berestein, G, López-Otín, C, Lu, B, Macleod, K. F, Malorni, W, Martinet, W, Matsuoka, K, Mautner, J, Meijer, A. J, Meléndez, A, Michels, P, Miotto, G, Mistiaen, W. P, Mizushima, N, Mograbi, B, Monastyrska, I, Moore, M. N, Moreira, P. I, Moriyasu, Y, Motyl, T, Münz, C, Murphy, L. O, Naqvi, N. I, Neufeld, T. P, Nishino, I, Nixon, R. A, Noda, T, Nürnberg, B, Ogawa, M, Oleinick, N. L, Olsen, L. J, Ozpolat, B, Paglin, S, Palmer, G. E, Papassideri, I, Parkes, M, Perlmutter, D. H, Perry, G, Piacentini, M, Pinkas-Kramarski, R, Prescott, M, Proikas-Cezanne, T, Raben, N, Rami, A, Reggiori, F, Rohrer, B, Rubinsztein, D. C, Ryan, K. M, Sadoshima, J, Sakagami, H, Sakai, Y, Sandri, M, Sasakawa, C, Sass, M, Schneider, C, Seglen, P. O, Seleverstov, O, Settleman, J, Shacka, J. J, Shapiro, I. M, Sibirny, A, Silva-Zacarin, E. C. M, Simon, H.-U, Simone, C, Simonsen, A, Smith, M. A, Spanel-Borowski, K, Srinivas, V, Steeves, M, Stenmark, H, Stromhaug, P. E, Subauste, C. S, Sugimoto, S, Sulzer, D, Suzuki, T, Swanson, M. S, Tabas, I, Takeshita, F, Talbot, N. J, Tallóczy, Z, Tanaka, K, Tanaka, K, Tanida, I, Taylor, G. S, Taylor, J. P, Terman, A, Tettamanti, G, Thompson, C. B, Thumm, M, Tolkovsky, A. M, Tooze, S. A, Truant, R, Tumanovska, L. V, Uchiyama, Y, Ueno, T, Uzcátegui, N. L, van der Klei, I, Vaquero, E. C, Vellai, T, Vogel, M. W, Wang, H.-G, Webster, P, Wiley, J. W, Xi, Z, Xiao, G, Yahalom, J, Yang, J.-M, & Yap... (2008) Guidelines for the use and interpretation of assays for monitoring autophagy in higher eukaryotes.

Autophagy **4**, 151–175.

[260] Klionsky, D. J, Abdalla, F. C, Abeliovich, H, Abraham, R. T, Acevedo-Arozena, A, Adeli, K, Agholme, L, Agnello, M, Agostinis, P, Aguirre-Ghiso, J. A, Ahn, H. J, Ait-Mohamed, O, Ait-Si-Ali, S, Akematsu, T, Akira, S, Al-Younes, H. M, Al-Zeer, M. A, Albert, M. L, Albin, R. L, Alegre-Abarrategui, J, Aleo, M. F, Alirezaei, M, Almasan, A, Almonte-Becerril, M, Amano, A, Amaravadi, R, Amarnath, S, Amer, A. O, Andrieu-Abadie, N, Anantharam, V, Ann, D. K, Anoopkumar-Dukie, S, Aoki, H, Apostolova, N, Auberger, P, Baba, M, Backues, S. K, Baehrecke, E. H, Bahr, B. A, Bai, X.-Y, Bailly, Y, Baiocchi, R, Baldini, G, Balduini, W, Ballabio, A, Bamber, B. A, Bampton, E. T. W, Bánhegyi, G, Bartholomew, C. R, Bassham, D. C, Bast, R. C, Batoko, H, Bay, B.-H, Beau, I, Béchet, D. M, Begley, T. J, Behl, C, Behrends, C, Bekri, S, Bellaire, B, Bendall, L. J, Benetti, L, Berliocchi, L, Bernardi, H, Bernassola, F, Besteiro, S, Bhatia-Kissova, I, Bi, X, Biard-Piechaczyk, M, Blum, J. S, Boise, L. H, Bonaldo, P, Boone, D. L, Bornhauser, B. C, Bortoluci, K. R, Bossis, I, Bost, F, Bourquin, J.-P, Boya, P, Boyer-Guittaut, M, Bozhkov, P. V, Brady, N. R, Brancolini, C, Brech, A, Brenman, J. E, Brennand, A, Bresnick, E. H, Brest, P, Bridges, D, Bristol, M. L, Brookes, P. S, Brown, E. J, Brumell, J. H, Brunetti-Pierri, N, Brunk, U. T, Bulman, D. E, Bultman, S. J, Bultynck, G, Burbulla, L. F, Bursch, W, Butchar, J. P, Buzgariu, W, Bydlowski, S. P, Cadwell, K, Cahová, M, Cai, D, Cai, J, Cai, Q, Calabretta, B, Calvo-Garrido, J, Camougrand, N, Campanella, M, Campos-Salinas, J, Candi, E, Cao, L, Caplan, A. B, Carding, S. R, Cardoso, S. M, Carew, J. S, Carlin, C. R, Carmignac, V, Carneiro, L. A. M, Carra, S, Caruso, R. A, Casari, G, Casas, C, Castino, R, Cebollero, E, Cecconi, F, Celli, J, Chaachouay, H, Chae, H.-J, Chai, C.-Y, Chan, D. C, Chan, E. Y, Chang, R. C.-C, Che, C.-M, Chen, C.-C, Chen, G.-C, Chen, G.-Q, Chen, M, Chen, Q, Chen, S. S.-L, Chen, W, Chen, X, Chen, X, Chen, X, Chen, Y.-G, Chen, Y, Chen, Y,

Chen, Y.-J, Chen, Z, Cheng, A, Cheng, C. H. K, Cheng, Y, Cheong, H, Cheong, J.-H, Cherry, S, Chess-Williams, R, Cheung, Z. H, Chevet, E, Chiang, H.-L, Chiarelli, R, Chiba, T, Chin, L.-S, Chiou, S.-H, Chisari, F. V, Cho, C. H, Cho, D.-H, Choi, A. M. K, Choi, D, Choi, K. S, Choi, M. E, Chouaib, S, Choubey, D, Choubey, V, Chu, C. T, Chuang, T.-H, Chueh, S.-H, Chun, T, Chwae, Y.-J, Chye, M.-L, Ciarcia, R, Ciriolo, M. R, Clague, M. J, Clark, R. S. B, Clarke, P. G. H, Clarke, R, Codogno, P, Coller, H. A, Colombo, M. I, Comincini, S, Condello, M, Condorelli, F, Cookson, M. R, Coombs, G. H, Coppens, I, Corbalan, R, Cossart, P, Costelli, P, Costes, S, Coto-Montes, A, Couve, E, Coxon, F. P, Cregg, J. M, Crespo, J. L, Cronjé, M. J, Cuervo, A. M, Cullen, J. J, Czaja, M. J, D'Amelio, M, Darfeuille-Michaud, A, Davids, L. M, Davies, F. E, De Felici, M, de Groot, J. F, de Haan, C. A. M, De Martino, L, De Milito, A, De Tata, V, Debnath, J, Degterev, A, Dehay, B, Delbridge, L. M. D, & Demar... (2012) Guidelines for the use and interpretation of assays for monitoring autophagy. *Autophagy* **8**, 445–544.

[261] de la Calle, C, Joubert, P.-E, Law, H. K. W, Hasan, M, & Albert, M. L. (2011) Simultaneous assessment of autophagy and apoptosis using multispectral imaging cytometry. *Autophagy* **7**, 1045–1051.

[262] Joubert, P. E, Werneke, S. W, de la Calle, C, Guivel-Benhassine, F, Giodini, A, Peduto, L, Levine, B, Schwartz, O, Lenschow, D. J, & Albert, M. L. (2012) Chikungunya virus-induced autophagy delays caspase-dependent cell death. *Journal of Experimental Medicine* **209**, 1029–1047.

[263] Phadwal, K, Alegre-Abarrategui, J, Watson, A. S, Pike, L, Anbalagan, S, Hammond, E. M, Wade-Martins, R, McMichael, A, Klenerman, P, & Simon, A. K. (2012) A novel method for autophagy detection in primary cells: Impaired levels of macroautophagy in immunosenescent T cells. *Autophagy* **8**, 677–689.

[264] Bampton, E. T. W, Goemans, C. G, Niranjan, D, Mizushima, N, & Tolkovsky, A. M. (2005) The dynamics of autophagy visualized in live cells: from autophagosome formation to fusion with endo/lysosomes. *Autophagy* **1**, 23–36.

[265] Chan, L. L.-Y, Shen, D, Wilkinson, A. R, Patton, W, Lai, N, Chan, E, Kuksin, D, Lin, B, & Qiu, J. (2012) A novel image-based cytometry method for autophagy detection in living cells. *Autophagy* **8**, 1371–1382.

[266] Oeste, C. L, Seco, E, Patton, W. F, Boya, P, & Pérez-Sala, D. (2012) Interactions between autophagic and endo-lysosomal markers in endothelial cells. *Histochemistry and Cell Biology* **139**, 659–670.

[267] Lee, J. S & Lee, G. M. (2011) Monitoring of autophagy in Chinese hamster ovary cells using flow cytometry. *METHODS* pp. 1–8.

[268] Lorenz, H. M, Grünke, M, Hieronymus, T, Herrmann, M, Kühnel, A, Manger, B, & Kalden, J. R. (1997) In vitro apoptosis and expression of apoptosis-related molecules in lymphocytes from patients with systemic lupus erythematosus and other autoimmune diseases. *Arthritis and Rheumatism* **40**, 306–317.

[269] van Loosdregt PhD, J, PhD, R. S, PhD, M. R, PhD, B. J. P. M, PhD, M. L. M, & PhD, S. A. M. (2013) Hydroxychloroquine preferentially induces apoptosis of CD45RO+ effector T cells by inhibiting autophagy: A possible mechanism for therapeutic modulation of T cells. *Journal of Allergy and Clinical Immunology* pp. 1–5.

[270] Swerdlow, S, McColl, K, Rong, Y, Lam, M, Gupta, A, & Distelhorst, C. W. (2008) Apoptosis inhibition by Bcl-2 gives way to autophagy in glucocorticoid-treated lymphocytes. *Autophagy* **4**, 612–620.

[271] Chiang, G. G. (2005) Phosphorylation of Mammalian Target of Rapamycin

(mTOR) at Ser-2448 Is Mediated by p70S6 Kinase. *Journal of Biological Chemistry* **280**, 25485–25490.

[272] Ma, X. M & Blenis, J. (2009) Molecular mechanisms of mTOR-mediated translational control. *Nature Reviews Molecular Cell Biology* **10**, 307–318.

[273] Wei, Y, Pattingre, S, Sinha, S, Bassik, M, & Levine, B. (2008) JNK1-Mediated Phosphorylation of Bcl-2 Regulates Starvation-Induced Autophagy. *Molecular Cell* **30**, 678–688.

[274] Goodnow, C. C, Crosbie, J, Jorgensen, H, Brink, R. A, & Basten, A. (1989) Induction of self-tolerance in mature peripheral B lymphocytes. *Nature* **342**, 385–391.

[275] Russell, D. M, Dembić, Z, Morahan, G, Miller, J. F, Bürki, K, & Nemazee, D. (1991) Peripheral deletion of self-reactive B cells. *Nature* **354**, 308–311.

[276] Rathmell, J. C, Cooke, M. P, Ho, W. Y, Grein, J, Townsend, S. E, Davis, M. M, & Goodnow, C. C. (1995) CD95 (Fas)-dependent elimination of self-reactive B cells upon interaction with CD4+ T cells. *Nature* **376**, 181–184.

[277] Liu, Z & Davidson, A. (2011) BAFF and selection of autoreactiveB cells. *Trends in Immunology* **32**, 388–394.

[278] Lens, S. M, den Drijver, B. F, Pötgens, A. J, Tesselaar, K, van Oers, M. H, & van Lier, R. A. (1998) Dissection of pathways leading to antigen receptor-induced and Fas/CD95-induced apoptosis in human B cells. *Journal of Immunology* **160**, 6083–6092.

[279] Patke, A, Mecklenbrauker, I, Erdjument-Bromage, H, Tempst, P, & Tarakhovsky, A. (2006) BAFF controls B cell metabolic fitness through a PKC

- and Akt-dependent mechanism. *Journal of Experimental Medicine* **203**, 2551–2562.

[280] Rubinsztein, S. L. M. G.-A. R. Z. C. P. P. C. T. O. S. D, Garcia-Arencibia, M, Zhao, R, Puri, C, Toh, P. P. C, Sadiq, O, & Rubinsztein, D. C. (2012) Bim Inhibits Autophagy by Recruiting Beclin 1 to Microtubules. *Molecular Cell* **47**, 359–370.

[281] Bhuiyan, M. S, Pattison, J. S, Osinska, H, James, J, Gulick, J, McLendon, P. M, Hill, J. A, Sadoshima, J, & Robbins, J. (2013) Enhanced autophagy ameliorates cardiac proteinopathy. *Journal of Clinical Investigation* **123**, 5284–5297.

[282] Pyo, J.-O, Yoo, S.-M, Ahn, H.-H, Nah, J, Hong, S.-H, Kam, T.-I, Jung, S, & Jung, Y.-K. (2013) Overexpression of Atg5 in mice activates autophagy and extends lifespan. *Nature Communications* **4**, 2300.

[283] Goldfinger, M, Shmuel, M, Benhamron, S, & Tirosh, B. (2010) Protein synthesis in plasma cells is regulated by crosstalk between endoplasmic reticulum stress and mTOR signaling. *European Journal of Immunology* **41**, 491–502.

[284] Narita, M, Young, A. R. J, Arakawa, S, Samarajiwa, S. A, Nakashima, T, Yoshida, S, Hong, S, Berry, L. S, Reichelt, S, Ferreira, M, Tavare, S, Inoki, K, Shimizu, S, & Narita, M. (2011) Spatial Coupling of mTOR and Autophagy Augments Secretory Phenotypes. *Science* **332**, 966–970.

[285] Michaud, M, Martins, I, Sukkurwala, A. Q, Adjemian, S, Ma, Y, Pellegatti, P, Shen, S, Kepp, O, Scoazec, M, Mignot, G, Rello-Varona, S, Tailler, M, Menger, L, Vacchelli, E, Galluzzi, L, Ghiringhelli, F, di Virgilio, F, Zitvogel, L, & Kroemer, G. (2011) Autophagy-Dependent Anticancer Immune Responses Induced by Chemotherapeutic Agents in Mice. *Science* **334**, 1573–1577.

[286] Perry, D, Sang, A, Yin, Y, Zheng, Y.-Y, & Morel, L. (2011) Murine Models of

Systemic Lupus Erythematosus. *Journal of Biomedicine and Biotechnology* **2011**, 1–19.

[287] Andrews, B. S, Eisenberg, R. A, Theofilopoulos, A. N, Izui, S, Wilson, C. B, McConahey, P. J, Murphy, E. D, Roths, J. B, & Dixon, F. J. (1978) Spontaneous murine lupus-like syndromes. Clinical and immunopathological manifestations in several strains. *The Journal of Experimental Medicine* **148**, 1198–1215.

[288] Reininger, L, Winkler, T. H, Kalberer, C. P, Jourdan, M, Melchers, F, & Rolink, A. G. (1996) Intrinsic B cell defects in NZB and NZW mice contribute to systemic lupus erythematosus in (NZB x NZW)F1 mice. *The Journal of experimental medicine* **184**, 853–861.

[289] Reininger, L, Radaszkiewicz, T, Kosco, M, Melchers, F, & Rolink, A. G. (1992) Development of autoimmune disease in SCID mice populated with long-term "in vitro" proliferating (NZB x NZW)F1 pre-B cells. *The Journal of Experimental Medicine* **176**, 1343–1353.

[290] Morel, L. (2010) Genetics of SLE: evidence from mouse models. *Nature Reviews Rheumatology* **6**, 348–357.

[291] Liu, Y, Li, L, Kumar, K. R, Xie, C, Lightfoot, S, Zhou, X. J, Kearney, J. F, Weigert, M, & Mohan, C. (2007) Lupus susceptibility genes may breach tolerance to DNA by impairing receptor editing of nuclear antigen-reactive B cells. *Journal of Immunology* **179**, 1340–1352.

[292] Rolink, A. G, Winkler, T, Melchers, F, & Andersson, J. (2000) Precursor B cell receptor–dependent B cell proliferation and differentiation does not require the bone marrow or fetal liver environment. *The Journal of experimental medicine* **191**, 23–32.

[293] von Boehmer, H & Melchers, F. (2010) Checkpoints in lymphocyte development and autoimmune disease. *Nature Immunology* **11**, 14–20.

[294] Pieper, K, Grimbacher, B, & Eibel, H. (2013) B-cell biology and development. *Journal of Allergy and Clinical Immunology* **131**, 959–971.

[295] Kastan, M. B & Lim, D. S. (2000) The many substrates and functions of ATM. *Nature Reviews Molecular Cell Biology* **1**, 179–186.

[296] Bredemeyer, A. L, Sharma, G. G, Huang, C.-Y, Helmink, B. A, Walker, L. M, Khor, K. C, Nuskey, B, Sullivan, K. E, Pandita, T. K, Bassing, C. H, & Sleckman, B. P. (2006) ATM stabilizes DNA double-strand-break complexes during V(D)J recombination. *Nature* **442**, 466–470.

[297] Alexander, A, Cai, S.-L, Kim, J, Nanez, A, Sahin, M, MacLean, K. H, Inoki, K, Guan, K.-L, Shen, J, Person, M. D, Kusewitt, D, Mills, G. B, Kastan, M. B, & Walker, C. L. (2010) ATM signals to TSC2 in the cytoplasm to regulate mTORC1 in response to ROS. *Proceedings of the National Academy of Sciences* **107**, 4153–4158.

[298] Tsai, W.-B, Chung, Y. M, Takahashi, Y, Xu, Z, & Hu, M. C. T. (2008) Functional interaction between FOXO3a and ATM regulates DNA damage response. *Nature Cell Biology* **10**, 460–467.

[299] Herzog, S, Hug, E, Meixlsperger, S, Paik, J.-H, DePinho, R. A, Reth, M, & Jumaa, H. (2008) SLP-65 regulates immunoglobulin light chain gene recombination through the PI(3)K-PKB-Foxo pathway. *Nature Immunology* **9**, 623–631.

[300] Ochiai, K, Maienschein-Cline, M, Mandal, M, Triggs, J. R, Bertolino, E, Sciammas, R, Dinner, A. R, Clark, M. R, & Singh, H. (2012) A self-reinforcing regulatory network triggered by limiting IL-7 activates pre-BCR signaling and differentiation. *Nature Immunology* **13**, 300–307.

[301] Cerutti, A, Cols, M, & Puga, I. (2013) Marginal zone B cells: virtues of innate-like antibody-producing lymphocytes. *Nature Reviews Immunology* **13**, 118–132.

[302] Pone, E. J, Zhang, J, Mai, T, White, C. A, Li, G, Sakakura, J. K, Patel, P. J, Al-Qahtani, A, Zan, H, Xu, Z, & Casali, P. (2012) BCR-signalling synergizes with TLR-signalling for induction of AID and immunoglobulin class-switching through the non-canonical nF-. *Nature Communications* **3**, 767–12.

[303] Liu, X. D, Ko, S, Xu, Y, Fattah, E. A, Xiang, Q, Jagannath, C, Ishii, T, Komatsu, M, & Eissa, N. T. (2012) Transient Aggregation of Ubiquitinated Proteins Is a Cytosolic Unfolded Protein Response to Inflammation and Endoplasmic Reticulum Stress. *Journal of Biological Chemistry* **287**, 19687–19698.

[304] Wu, T, Qin, X, Kurepa, Z, Kumar, K. R, Liu, K, Kanta, H, Zhou, X. J, Satterthwaite, A. B, Davis, L. S, & Mohan, C. (2007) Shared signaling networks active in B cells isolated from genetically distinct mouse models of lupus. *Journal of Clinical Investigation* **117**, 2186–2196.

[305] Shaffer, A. L, Shapiro-Shelef, M, Iwakoshi, N. N, Lee, A.-H, Qian, S.-B, Zhao, H, Yu, X, Yang, L, Tan, B. K, Rosenwald, A, Hurt, E. M, Petroulakis, E, Sonenberg, N, Yewdell, J. W, Calame, K, Glimcher, L. H, & Staudt, L. M. (2004) XBP1, downstream of Blimp-1, expands the secretory apparatus and other organelles, and increases protein synthesis in plasma cell differentiation. *Immunity* **21**, 81–93.

[306] Shapiro-Shelef, M & Calame, K. (2005) Regulation of plasma-cell development. *Nature Reviews Immunology* **5**, 230–242.

[307] Harding, H. P, Novoa, I, Zhang, Y, Zeng, H, Wek, R, Schapira, M, & Ron, D.

(2000) Regulated translation initiation controls stress-induced gene expression in mammalian cells. *Molecular Cell* **6**, 1099–1108.

[308] Hollien, J. (2006) Decay of Endoplasmic Reticulum-Localized mRNAs During the Unfolded Protein Response. *Science* **313**, 104–107.

[309] Ogata, M, Hino, S. i, Saito, A, Morikawa, K, Kondo, S, Kanemoto, S, Murakami, T, Taniguchi, M, Tanii, I, Yoshinaga, K, Shiosaka, S, Hammarback, J. A, Urano, F, & Imaizumi, K. (2006) Autophagy Is Activated for Cell Survival after Endoplasmic Reticulum Stress. *Molecular and Cellular Biology* **26**, 9220–9231.

[310] Rouschop, K. M. A, van den Beucken, T, Dubois, L, Niessen, H, Bussink, J, Savelkouls, K, Keulers, T, Mujcic, H, Landuyt, W, Voncken, J. W, Lambin, P, van der Kogel, A. J, Koritzinsky, M, & Wouters, B. G. (2010) The unfolded protein response protects human tumor cells during hypoxia through regulation of the autophagy genes MAP1LC3B and ATG5. *Journal of Clinical Investigation* **120**, 127–141.

[311] Hetz, C. (2012) The unfolded protein response: controlling cell fate decisions under ER stress and beyond. *Nature Reviews Molecular Cell Biology* **13**, 89–102.

[312] Vidal, R. L, Figueroa, A, Court, F. A, Thielen, P, Molina, C, Wirth, C, Caballero, B, Kiffin, R, Segura-Aguilar, J, Cuervo, A. M, Glimcher, L. H, & Hetz, C. (2012) Targeting the UPR transcription factor XBP1 protects against Huntington's disease through the regulation of FoxO1 and autophagy. *Human Molecular Genetics* **21**, 2245–2262.

[313] Mortensen, M, Ferguson, D. J. P, Edelmann, M, Kessler, B, Morten, K. J, Komatsu, M, & Simon, A. K. (2010) Loss of autophagy in erythroid cells leads

to defective removal of mitochondria and severe anemia in vivo. *PNAS* **107**, 832–837.

[314] Komatsu, M. (2005) Impairment of starvation-induced and constitutive autophagy in Atg7-deficient mice. *The Journal of Cell Biology* **169**, 425–434.

[315] Kuma, A, Hatano, M, Matsui, M, Yamamoto, A, Nakaya, H, Yoshimori, T, Ohsumi, Y, Tokuhisa, T, & Mizushima, N. (2004) The role of autophagy during the early neonatal starvation period. *Nature* **432**, 1032.

[316] de Boer, J, Williams, A, Skavdis, G, Harker, N, Coles, M, Tolaini, M, Norton, T, Williams, K, Roderick, K, & Potocnik, A. J. (2003) Transgenic mice with hematopoietic and lymphoid specific expression of Cre. *European Journal of Immunology* **33**, 314–325.

[317] Crespo, P, Schuebel, K. E, Ostrom, A. A, Gutkind, J. S, & Bustelo, X. R. (1997) Phosphotyrosine-dependent activation of Rac-1 GDP/GTP exchange by the vav proto-oncogene product. *Nature* **385**, 169–172.

[318] Ogilvy, S, Metcalf, D, Gibson, L, Bath, M. L, Harris, A. W, & Adams, J. M. (1999) Promoter elements of vav drive transgene expression in vivo throughout the hematopoietic compartment. *Blood* **94**, 1855–1863.

[319] Jourdan, M, Caraux, A, De Vos, J, Fiol, G, Larroque, M, Cognot, C, Bret, C, Duperray, C, Hose, D, & Klein, B. (2009) An in vitro model of differentiation of memory B cells into plasmablasts and plasma cells including detailed phenotypic and molecular characterization. *Blood* **114**, 5173–5181.

[320] Wu, Y. T, Tan, H. L, Shui, G, Bauvy, C, Huang, Q, Wenk, M. R, Ong, C. N, Codogno, P, & Shen, H. M. (2010) Dual Role of 3-Methyladenine in Modulation of Autophagy via Different Temporal Patterns of Inhibition on Class I

and III Phosphoinositide 3-Kinase. *Journal of Biological Chemistry* **285**, 10850–10861.

[321] Qu, X, Eskelinen, E.-L, Mizushima, N, Ohsumi, Y, & Levine, B. (2003) Promotion of tumorigenesis by heterozygous disruption of the beclin 1 autophagy gene. *Cell* **112**, 1809–1820.

[322] Yousefi, S, Perozzo, R, Schmid, I, Ziemiecki, A, Schaffner, T, Scapozza, L, Brunner, T, & Simon, H.-U. (2006) Calpain-mediated cleavage of Atg5 switches autophagy to apoptosis. *Nature Cell Biology* **8**, 1124–1132.

[323] Tung, J. W, Mrazek, M. D, Yang, Y, Herzenberg, L. A, & Herzenberg, L. A. (2006) Phenotypically distinct B cell development pathways map to the three B cell lineages in the mouse. *Proceedings of the National Academy of Sciences* **103**, 6293–6298.

[324] Hsu, M.-C, Toellner, K.-M, Vinuesa, C. G, & MacLennan, I. C. M. (2006) B cell clones that sustain long-term plasmablast growth in T-independent extrafollicular antibody responses. *Proceedings of the National Academy of Sciences* **103**, 5905–5910.

8 Appendix

Table 8.1: **Patient characteristics**. ACR - American College of Rheumatologists. HCQ - hydroxychloroquine, Pred **-** prednisolone, MMF - mycophenolate mofetil, MTX - methotrexate

Patient	**Sex**	**Age**	**Diagnostic Clinical Features (ACR)**	**Antibodies**	**C3/4**	**SLEDAI**	**Medication**
1	F	33	Arthritis, Immunologic, Pleurisy, ANA	Anti-dsDNA	Low	10	Aza, Pred
2	F	63	Malar rash, Oral ulcers, ANA Discoid		Normal	6	HCQ
3	F	23	Photosensitivity, ANA, Immunologic, Lymphopenia	Anti-dsDNA	Normal	4	MMF, HCQ
4	F	25	Renal, ANA, Immunologic, Haematologic	Anti-dsDNA	Normal	6	HCQ, Pred

5	F	55	Arthritis, ANA, Renal, Haematologic	Anti-Ro	Normal	4	Pred
6	F	45	Renal, ANA, Immunologic, Haematologic	Anti-Sm, anti-RNP	Normal	8	MMF, Pred
7	F	26	Arthritis, Mouth ulcers, ANA, Immunologic	Anti-dsDNA	Normal	10	HCQ
8	F	54	Haematologic, ANA, Immunologic, Arthrtis	Anti-dsDNA	Normal	5	HCQ, Pred
9	F	28	Arthritis, Mouth ulcers, ANA, Immunologic	Anti-cardiolipin	Normal	6	HCQ, Pred
10	F	43	Arthritis, Mouth ulcers, ANA, Arthritis		Normal	6	HCQ
11	F	34	Renal, Photo-sensitivity, ANA, Malar rash		Normal	0	MMF, HCQ

12	F	31	Arthritis, Mouth ulcers, Immunologic, ANA	Anti-dsDNA, anti-Ro	Low	12	MMF, Pred
13	F	42	Malar rash, Haematologic, Arthritis, Immunologic, Photosensitivity	Anti-Ro, anti-RNP	Normal	3	MMF, HCQ
14	F	39	Haematologic, Arthritis, ANA, Immunologic	Anti-RNP, anti-cardiolipin	Normal	1	MTX, HCQ
15	F	28	Immunologic, ANA, Renal, Cerebral	Anti-dsDNA	Normal	4	MMF, HCQ
16	F	46	Photosensitivity, Mouth ulcers, Immunologic, ANA	ANA, Ro	Low	10	MMF, Pred
17	F	38	Photosensitivity, Renal, Arthritis, ANA, Immunologic	Anti-dsDNA, anti-Ro, anti-RNP	Low	8	Pred, HCQ
18	F	47	Renal, ANA, Immunologic, Haematologic	Anti-Ro, anti-dsDNA	Low	8	Aza, Pred, HCQ

19	F	69	Malar rash, ANA, Immunologic, Haematologic	Anti-Ro/La, anti-dsDNA	Low	8	Pred, HCQ
20	F	62	ANA, Arthritis, Photosensitivity, Renal		Normal	7	Aza, Pred, HCQ
21	F	22	Arthritis, Malar rash, Pleuritis, ANA, Immunologic, Haematologic	Anti-dsDNA	Low	13	MMF, HCQ
22	F	36	Immunologic, ANA, Malar rash, Mouth ulcers	Anti-dsDNA, Ro, RNP	Normal	6	MMF, MTX, Pred
23	F	27	Renal, ANA, Immunologic, Arthritis, Photosensitivity	Anti-RNP, anti-Ro, anti-Sm, anti-dsDNA	Low	12	MMF, Pred
24	F	41	Renal, ANA, Immunologic, Mouth ulcers	Anti-dsDNA	Low	12	Aza, Pred, HCQ

25	M	32	Arthritis, Discoid rash, Malar rash, ANA	Anti-Ro	Low	11	Pred
26	F	27	Arthritis, Photosensitivity, ANA, Immunologic	Anti-dsDNA, anti-Ro	Normal	8	Pred
27	F	29	ANA, Mouth ulcers, Malar rash, Renal, Haematologic, Neurologic	Anti-dsDNA, anti-Ro, anti-Sm	Low	14	Pred, MMF
28	F	54	ANA, Arthritis, Photosensitivity, Renal, Immunologic	Anti-RNP, anti-Sm	Low	8	HCQ
29	F	44	ANA, Cerebral, Arthritis, Photosensitivity		N	0	Aza, Pred, HCQ
30	M	23	ANA, Malar rash, Immunologic, Renal	Anti-dsDNA, anti-Ro	Low	8	Pred, MMF

31	F	51	ANA, Immunologic, Renal, Pericarditis, Malar rash	Anti-dsDNA, anti-Ro/La	Low	6	MMF, Pred, HCQ
32	M	23	ANA, Malar rash, Renal, Photosensitivity, Immunologic	Anti-dsDNA	Low	12	MMF, Pred, HCQ
33	F	33	Malar rash, Photosensitivity, Arthritis, ANA, Immunologic	Anti-dsDNA, anti-Ro	Low	10	HCQ
34	F	41	ANA, Arthritis, Immunologic, Photosensitivity	Anti-dsDNA, anti-Ro, anti-Sm	Low	8	MMF, HCQ
35	F	43	Renal, Mouth ulcers, Immunologic, Malar rash	Anti-Ro, anti-RNP	Normal	8	MMF, Pred, HCQ
36	M	24	Malar rash, Arthritis, ANA, Immunologic	Anti-dsDNA	Normal	6	Nil

37	F	29	ANA, Haematologic, Immunologic, Arthritis	Anti-dsDNA, anti-Ro, anti-RNP	Low	6	Pred, Mepacrine
38	F	30	ANA, Arthritis, Photosensitivity, Malar rash		Normal	0	HCQ
39	F	30	Arthritis, Malar rash, Mouth ulcers, Immunologic	Anti-dsDNA, anti-Ro	Low	12	HCQ
40	F	36	ANA, Mouth ulcers, Photosensitivity, Arthritis		Normal	4	HCQ
41	F	24	ANA, Mouth ulcers, Malar rash, Immunologic	Anti-dsDNA, anti-Ro	Low	8	HCQ, Pred
42	M	52	ANA, Photosensivity, Arthritis, Mouth ulcers		Normal	0	HCQ

43	F	29	ANA, Discoid, Mouth ulcers, Arthritis, Immunologic	Anti-dsDNA	Low	9	HCQ